Department of Experimental and Health Sciences
Faculty of Health and Life Sciences
Universitat Pompeu Fabra
Doctoral Thesis
2015

Characterization of Endothelial to Mesenchymal Transition induced By Notch

Dissertation presented by
Àlex Frías Hernández
For the degree of Doctor in Biomedical Research

Work carried out under the supervision of Drs. Víctor Manuel Díaz Cortés and Antonio García de Herreros in the Epithelial to Mesenchymal Transition and Tumor Progression Group in the Cancer Research Program in the Institud Hospital del Mar d'Investigacions Mèdiques (IMIM)

Barcelona, 2015

Dr. Víctor M.Díaz Cortés, (thesis co-director)

Dr. Antonio García de Herreros (thesis co-director)

Àlex Frías Hernandez (PhD student)

A la meva família

i a la Sareta

ABSTRACT

Notch activation in aortic endothelial cells (ECs) takes place at embryonic stages during cardiac valve formation and induces an endothelial-to-mesenchymal transition (EndMT). Using aortic ECs, we show here that active Notch expression promotes EndMT resulting in down-regulation of VE-cadherin and up-regulation of mesenchymal genes such as Fibronectin and Snail1/2. In these cells, TGF-β1 exacerbates Notch effects increasing Snail1 and Fibronectin activation. When Notch-downstream pathways were analyzed, we detected an increase in GSK-3β phosphorylation and inactivation what facilitates Snail1 nuclear retention and protein stabilization. However, the total activity of Akt was down-regulated. The discrepancy between Akt activity and GSK-3β phosphorylation is explained because Notch induces a switch in the Akt isoforms since it decreases Akt1, the predominant isoform expressed in ECs, and up-regulates Akt2 transcription. Mechanistically, Akt2 induction requires the stimulation of TCF-4/β-catenin transcriptional complex that activates the *Akt2* promoter. Active phosphorylated Akt2 translocates to the nucleus in Notch-expressing cells resulting in GSK-3β inactivation in this compartment. In the nucleus Akt2, but not Akt1 co-localizes with Lamin B in the nuclear envelope. Besides promoting GSK-3β inactivation, Notch down-regulates FoxO1, another Akt2 nuclear substrate. As a consequence, Notch protects ECs against oxidative stress-induced apoptosis through an Akt2 and Snail1-dependent mechanism.

L'activació de Notch en cèl·lules endotelials de la aorta (ECs), té lloc durant la formació de la vàlvula cardíaca i indueix la transició endoteli-mesènquima (EndMT). Utilitzant ECs, mostrem que l'activació de Notch promou la EndMT degut a la baixada de VE-Cadherina i l'augment de gens mesenquimals com Fibronectina i Snail1/2. En aquestes cèl·lules, TGF-β1 incrementa els afectes de Notch augmentant l'activació de Snail1 i Fibronectina. Quan s'investiguen les vies de senyalització "downstream" de Notch, vam detectar un augment en la forma inactiva de GSK-3β que facilita la retenció nuclear de Snail1 augmentant així la seva estabilitat. En estudiar la activació d'Akt, la principal quinasa que fosforila/inactiva GSK-3β, vam observar que baixava en les cèl·lules Notch. Aquesta discrepància entre els nivells de GSK-3β fosforilat i l'activitat d'Akt s'explica per la pujada especifica de la isoforma Akt2 vers la baixada de la isoforma predominant en les ECs Akt1. L'augment transcripcional d'Akt2 requereix l'estimulació del complex transcripcional TCF-4/β-catenina que activa el promotor d'Akt2. L'Akt2 actiu es transloca al nucli i inactiva GSK-3β nuclear. En aquest compartiment, Akt2 però no Akt1 co-localitza amb la Lamina B en la membrana nuclear. A part d'inactivar GSK-3β, Notch disminueix FoxO1, un altre substrat nuclear d'Akt2 i com a conseqüència, Notch protegeix les ECs de la apoptosis per estrès oxidatiu a través d'un mecanisme depenent d'Akt2 i Snail1.

TABLE OF CONTENTS

FIGURE INDEX

Introduction figures index

Results figures index

TABLE INDEX

Abbreviations

Aa: amino acids

ADAM: A disinterring and metalloproteinase

Ank: Ankyrin

APC: Adenomatous polyposis coli

ATM: Ataxia telangiectasia mutated

AV: Atrioventricular

Bcl-2: B-cell lymphoma 2

bHLH: Basic helix loop helix

β-TrCP1: Beta-transducing repeat containing E3 ubiquitin protein 1

CAF: Cancer associated fibroblast

CHX: Cycloheximide

CK1: Casein kinase 1

CoREST: Rest co-repressor 1

CRM-1: Chromosomal Maintenance 1

CSL: CBF1, Suppressor of Hairless, Lag-1

CtBP1: C-terminal binding protein 1

DLL1/3/4: Delta like 1/3/4

DSL: Delta/Serrate/LAG-2

E-Cadherin: Epithelial Cadherin

EGF: Epidermal growth factor

EMT: Epithelial to mesenchymal transition

EndMT: Endothelial to mesenchymal transition

ERK: Extracellular signal-regulated kinases

Fbxl: F-box and leucine-rich repeat protein

Fbxo: F-box protein

FoxO: Forkhead box O1

Fz: Frizzled

GSK-3β: Glycogen synthase kinase 3 beta

HDAC1/2: Histone deacetylase 1/2

HES1/2: Hairy and enhancer of split-1/2

HIF-1α: Hypoxia-inducible factor 1-alpha

HM: Homo domain

H_2O_2: Hydrogen Peroxide

HRE: Hormone response element

IGF-1: Insulin growth factor 1

JAG1/2: Jagged1/2

Lag-1: Lymphocyte activation gene-1

Lef-1: Lymphoid enhancer-binding factor-1

LOX-L: Lysyl oxidase-like

LRP5/6: Low-density lipoprotein receptor-related protein 5 /6

MAML: Mastermind-like

MDM2: Mouse double minute 2 homologue

mTORC2: Mammalian target of rapamycin complex 2

NECD: Notch extracellular domain

NES: Nuclear export sequence

NF-κB: nuclear factor kappa-light-chain-enhancer of activated B cells

NICD: Notch intracellular domain

NLS: Nuclear localization sequence

OT: Outflow tract

PARP: Poly-(ADP-ribose) polymerase

PDK1: Pyruvate dehydrogenase kinase, isozyme 1

PEST: Region rich in proline (P), glutamine (E), serine (S) and threonine (T) residues.

PH: Pleckstrin Homology

PI: Propidium Iodide

PIP_3: Phosphatidylinositol (3,4,5)- trisphosphate

PI3K: Phosphoinositide 3-kinase

PKB : Protein Kinase B

PRC2: Polycomb repressor complex 2

p90-RSK: 90 kDa ribosomal protein S6 kinase 1

RAM: RBP-J-associated module TGF-β: Transforming growth factor beta

RBPJ: Recombinant binding protein suppressor of hairless

RD: Regulatory domain

SMAD: Sma and Mad Related Family

SNAG: Snail/Gfi

Su(H): Supressor of hairless

TACE: Tumor necrosis factor α converting enzyme

TAD: Transactivation domain

TCF-4: Trancription factor 4

TF: Transcriptional factor

TM: Transmembrane

TRADD: TNFRSF1A-Associated Via Death Domain

TRAIL: TNF-related apoptosis-inducing ligand

VE-Cadherin: Vascular Endothelial Cadherin

VEGF: Vascular endothelial growth factor

Zeb1/2: Zinc Finger E-Box Binding Homeobox 1/2

ZnF: Zing Finger

INTRODUCTION

I.1 General view of Epithelial to Mesenchymal Transition (EMT)

EMT is a reversible process by which epithelial cells are transformed into a mesenchymal phenotype. This transformation starts losing the cell-cell adhesion junctions such as adherent junctions and desmosomes. Thus, they change their polarity resulting in a spindle-shape phenotype, increase in motility and become more resistant to cell death. EMT is critical in order to build from a single cell a complex organism [1].

During embryonic development there are three phases of EMT called primary, secondary and tertiary EMT that are summarized in Figure I.1. Primary EMT occurs during gastrulation, which is the process where ectoderm, mesoderm and endoderm are formed. Other example of primary EMT is the delamination of the neural crest in vertebrates. As shown in figure I.1.A there is a group of cells termed neural crest cells characterized by their high motility that allows them to populate distant tissues that requires an EMT[2].

After primary EMT, cells condensed into transient epithelial structures by mesenchymal to epithelial transition (MET), forming the notochord, the somites, the somatopleure, the splanchnopleure and the precursor urogenital system. All except notochord will undergo secondary EMT leading to the generation of mesenchymal cells that differentiate into more specific cell types [2].

An example of tertiary EMT is the endothelial to mesenchymal transition (EndMT). It has been reported that EndMT is essential for cardiac valve formation. It arises during the formation of the cushion mesenchyme in the heart from the atrioventricular (AV) canal or the outflow tract (OT). The cushion mesenchyme is the precursor of the cardiac valves [2].

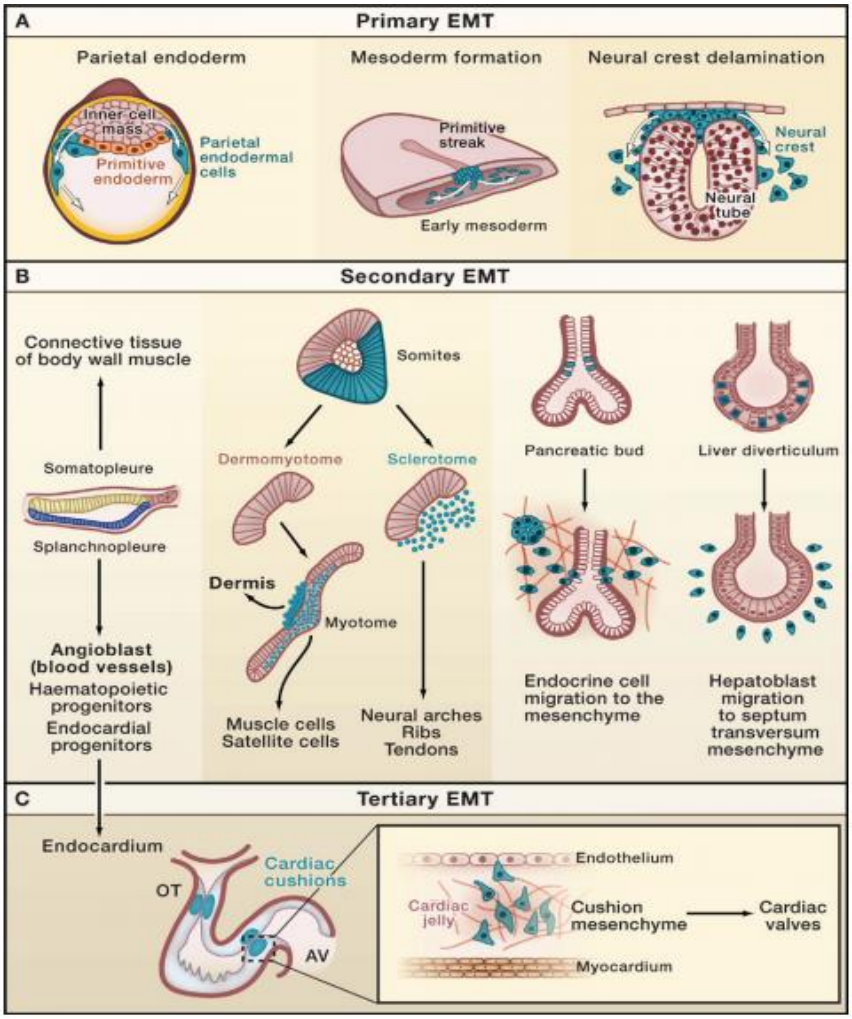

Figure I.1. Three EMT subtypes during embryonic development. (A) Primary EMT in early embryonic development. It forms the parental endoderm, the mesoderm and the neural crest delamination. (B) After first EMT, a transient epithelial state undergoes de secondary EMT in the formation of differentiated tissues. (C) Tertiary EMT, also called EndMT. A subset of endothelial cells suffers a transition from a endothelium to a mesenchyme tissue in order to form the cardiac valve during embryogenesis.(Adapted from [2]).

I.2 EndMT

As explained above, Endothelial to mesenchymal transition is a subtype of EMT. It was first identified in studies of heart development. This process occurs when a subset of endothelial cells undergoes phenotypic changes, loses their endothelial characteristics and gains mesenchymal properties (Figure I.2). The generation of mesenchymal cells from endothelium is a crucial step in endothelial cell differentiation to several lineages, including fibroblasts, myofibroblasts, pericytes, osteoblasts, chondrocytes and adipocytes[3]. EndMT may be initiated by different cell signals such as TGF-β, derived from fibroblasts, or metalloproteinases (MMPs) secreted from immune cells. Once started, endothelial cells acquire first an intermediate transitory phenotype with both mesenchymal and endothelial characteristics and then progress to complete loss of endothelial characteristics (Fig.I.2) [4].

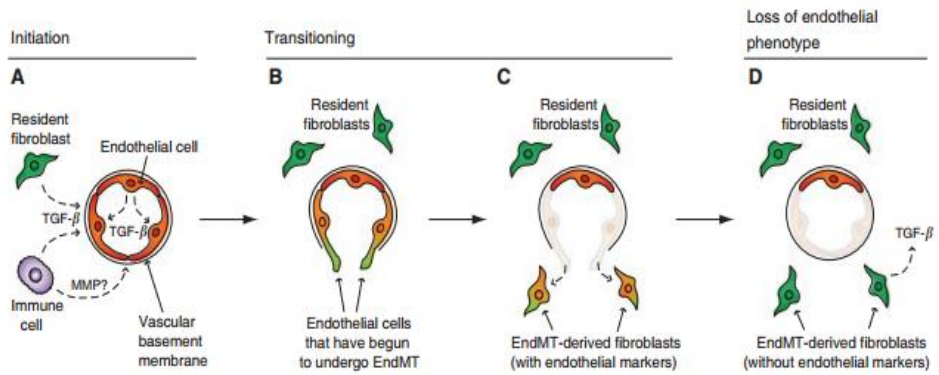

Figure I.2. Progression of EndMT. (A) After signals from surrounding cells such as TGF-β, the EndMT may be initiated. (B-C) Endothelial cells acquire mesenchymal properties and start the transition gaining a migratory phenotype. (D) Endothelial cells completely lose their characteristics and derive to a fibroblast-like cell with some mesenchymal markers [4].

Although EndMT has been associated with many physiological processes such as cardiac valve formation or angiogenesis, in the last years it has been related to important diseases such as atherosclerosis, cardiac fibrotic disorders and tumors[5]. In order to better understand how EndMT works, it would be useful to compare it with EMT. As it is shown in table I.1., EndMT and EMT have some similarities on their final characteristics although probably both transitions are regulated by different mechanisms [4] (see Table I.1.).

Table I.1. Characteristics and markers of epithelial, endothelial and mesenchymal cells [4]**.**

	Epithelial cell	**Endothelial cell**	**Mesenchymal cell**
Cell-cell junctions	Adherens junctions E-Cadherin Tight junctions Desmosomes	Adherens junctions VE-Cadherin Limited tight junctions	None (or focal)
Organized cell layer	YES	YES	NO
Apico-basolateral polarity	YES	YES	NO
Basement membrane	YES	YES	NO, but makes intersticial matrix
Migratory	NO	NO	YES
Markers	E-Cadherin	VE-Cadherin	Fibronectin, Lef1, α-SMA

I.3 Physiology and pathology of EndMT

I.3.1 Cardiac valve formation

The initial stages of cardiac morphogenesis are regulated by this specialized type of EMT, the EndMT. At embryonic day 8.5 (E8.5), the mouse heart tube is formed by an outer myocardial layer lined by a monolayer of specialized endothelium, the endocardium. They are separated by a thick extracellular matrix, called cardiac jelly, first secreted by the myocardial cells[6]. At E9.5, in response to myocardial signals, a subset of endothelial cells, specifically called endocardial cells, which cover the atrioventricular (AV) canal and the outflow tract (OT) regions, undergoes the tertiary EMT in embryogenesis, the EndMT [6]. In this process endocardial cells lose cell to cell contacts and acquire more motility and invade the cardiac jelly, where they subsequently proliferate and complete their differentiation into mesenchymal cells (Figure I.3)[7].

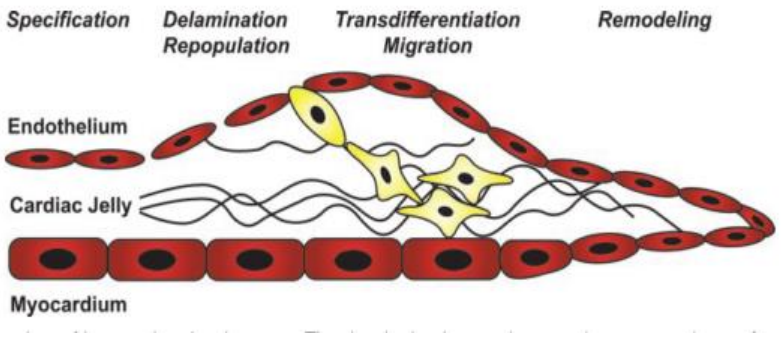

Figure I.3. Scheme of EndMT. Endothelial cells start to lose their contacts and migrate through the cardiac jelly [7].

As the cardiac chambers start to form, the cardiac jelly gets thicker in the AV and OT regions, where endothelium-derived mesenchymal cells invade the adjacent cardiac jelly to form the endocardial cushion tissue.

I.3.2 Angiogenesis

Angiogenesis is the process involved in the generation of new blood vessels from the pre-existed ones. It is normal in embryogenesis, wound healing, tissue growth and also it has a role in tumor progression [8].

Regarding angiogenesis in tumor development, endothelial cells from pre-existing blood vessels move away from this static cell layer and migrate into the surrounding tissue towards the tumor requiring vascularization [9]. It is hypothesized that EndMT must take place during the angiogenic sprouting: a process that allows the so-called “tip cells”, which lead an emerging vascular plexus, to migrate into adjacent tissues. Tip cells lead the newly forming blood vessel towards the tumor. These cells have a migratory and invasive phenotype that seems to be consistent with EndMT and thus it is likely that EndMT occurs during angiogenesis [4].

I.3.3 Cardiac Fibrosis

Other evidence of that post-natal EndMT occurs is in fibrotic disorders that are accompanied with an excess of extracellular matrix and inappropriate proliferation of fibroblasts. It has been detected fibrosis in many organs such as in kidney, lung and heart, being the last organ the most usual. Cardiac fibrosis is a common result of heart failure [3].

It has been shown that approximately 27-35% of all fibroblasts in fibrotic heart tissue were found to arise through EndMT [10]. Therefore, anti-fibrotic therapies might be useful in improving cardiac function of the diseased heart. However, the development of such therapies has been limited by an incomplete understanding of the mechanisms of fibroblasts generation in the heart.

I.3.4 Tumor progression

In the same way that EMT, the EndMT has been related to tumor progression. EndMT accounts for up to 40% of cancer-associated fibroblasts (CAFs) [4]. CAFs play an important role in tumor progression and alter the microenvironment in several ways. In particular, CAFs deposit various extracellular matrix molecules and secrete paracrine factors that directly affect the behavior of many different cell types within the tumor. Furthermore, CAFs release potentially oncogenic signals, such as transforming growth factor-β (TGF-β), and are a principle source of host-derived vascular endothelial growth factor (VEGF), which promotes angiogenesis [11].

I.4 Signalling during EndMT

I.4.1 Notch pathway

Notch is a very conserved signaling pathway in the animal kingdom. It consists of four types I transmembrane receptors (Notch 1 to Notch 4) that regulate different cell fates through cell to cell communication. Notch receptors are composed of three parts, the extracellular, the transmembrane and the intracellular domain [12]. The extracellular domain is formed by 29-36 multiple epidermal growth factor (EGF)-like repeats and another region with three cysteine rich LIN (Lin-12/Notch) repeats.It also contains a region which is the link between the extracellular and intracellular domain. a part is very important in order to prevent early activation of the pathway [13]. The Notch Intracellular Domain (NICD) is the important part for the signaling. It is composed by a RBP-J-kappa-associated module (RAM) domain and six ankyrin (Ank) repeats which mediate and facilitate the interaction between cytosolic and nuclear proteins, and the C-terminal PEST sequence that is rich in proline (P), glutamic acid (E), serine (S), and threonine (T) is essential for its regulation. It also contains nuclear localization signals and the Trans-Activation Domain (TAD) which is necessary for activation transcription (Figure I.4.) [14].

In order to activate this signaling pathway, Notch receptors need to interact with their ligands. In mammals, there are five ligands: three Delta-like (DLL1, DLL3, DLL4) and two Jagged (JAG1 and JAG2). Jagged1 and Jagged2 have almost twice the number of EGF repeats than Delta-like ligands, some of which contain conserved insertions of unknown function [15][16]. The intracellular region of the ligands contain multiple lysine residues and a C-terminal PDZ (PSD-95/Dlg/ZO-1) motif which are required for ligand signaling activity and interactions with the cytoskeleton, respectively [17].

Notch1 and Notch4 and Jagged1, Dll1, and Dll4 are predominantly expressed in vascular endothelial cells and are important for many aspects of vascular biology [15]. Notch signaling pathway has been reported in several contexts and in different cell types. Among others, one of the most studied role of Notch function is during vascular and heart development, more concretely, during the EndMT [18]. In fact, alterations on this pathway have been reported to occur in some cardiovascular defects in humans [19]. Actually, in humans, mutations in Notch signaling components are associated with several congenital disorders involving malformed valves, aortic arch, and defective chamber septation [18].

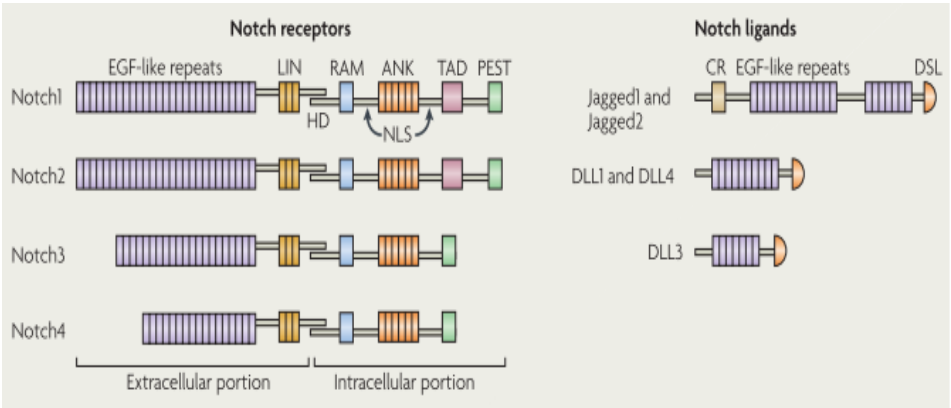

Figure I.4.Protein domains of Notch1-4 receptors and their ligands Delta-like (DLL1,DLL3 and DLL4) and Jagged (JAG1 and JAG2). (Left panel) Scheme of four Notch receptors. Extracellular portion is referred to the Notch extracellular domain (NECD) and the Intracellular portion to Notch intracellular domain (NICD). (Right panel) Jagged-1 and Jagged-2 ligands and the three Delta-like ligands (DLL-1,3 and 4) [14]**.**

Activation of Notch signaling through cell-cell interactions (trans-interactions) has been well characterized; however, Notch ligands also regulate the Notch pathway by binding to Notch receptors within the same cell (cis-interactions) [20], [21]. In general, trans-interactions between Notch ligands and receptors activate Notch signaling, whereas cis-interactions are believed to inhibit Notch signaling [22].

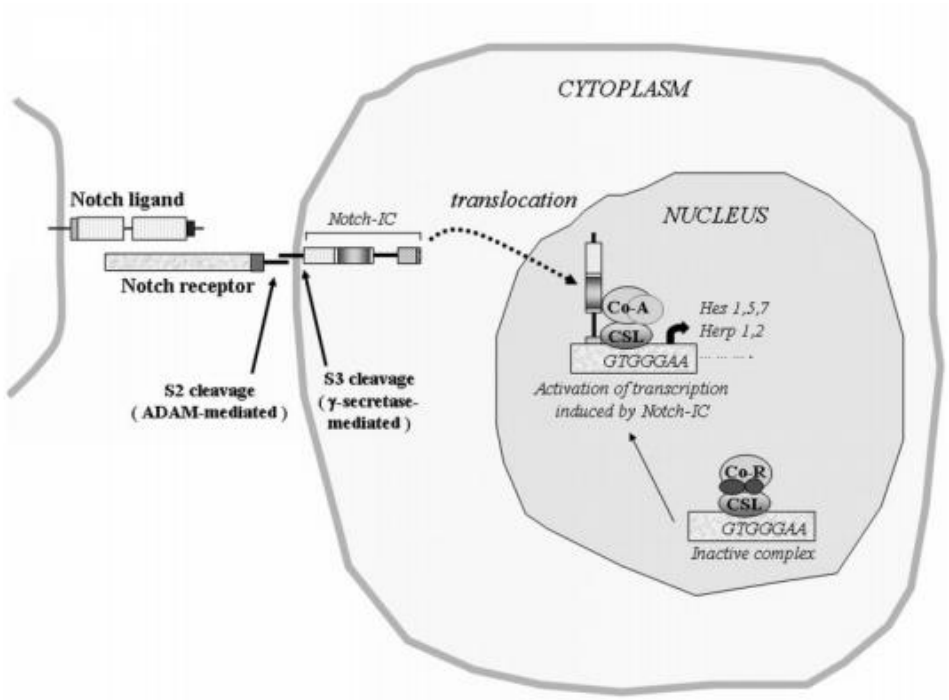

Figure I.5. Schematic view of Notch signaling pathway. Notch receptor binding with Notch ligand undergoes two proteolytic events; first, by ADAM metalloprotease, and then by γ-secretase. The Notch intracellular domain (NICD) is translocated to the nucleus and together with CSL complex and co-activator (p300 and MAML) induce the transcription of its target genes such as Hes-1, Hes-2 among others. Adapted from [23].

Upon ligand binding, the Notch extracellular domain (NECD) is cleaved away from the TM (trans-membrane)-NICD domain by TACE (TNF-α ADAM metalloprotease converting enzyme). In the signal-receiving cell, γ-secretase releases the NICD from the TM, which allows nuclear translocation, association with the CSL (CBF1/Su(H)/Lag-1) transcription factor complex and Mastermind (MAML), and subsequent activation of the canonical Notch target genes: Myc, p21, and the HES-family members (Hes1 and Hes2) (figure I.5) [24].

Recently, it has been shown that activation of the pathway can also be attained in a 'non-canonical', ligand-independent manner, as the receptor traffics through endocytic compartments. Indeed, endocytosis has emerged as another important regulator of Notch signals, affecting its activity at multiple stages of the endocytic pathway [25]. In any case this non-canonical activation generates the same NICD than the canonical one.

I.4.2 Wnt/β-catenin

Wnt signaling pathway has been related to cancer progression, but also has a role in embryonic development [26]. During embryogenesis, Wnt is involved in body axis patterning, cell-fate specification, cell proliferation, and cell migration [27].

At least nineteen Wnt proteins initiate the Wnt/β-catenin cascade. Wnt proteins are secreted glycoproteins that interact with the N-terminal extra-cellular cysteine-rich domain of the Frizzled (Fz) receptor family which there are ten in humans. The Fz protein is a seven-transmembrane-span protein with topological homology to G-protein coupled receptors. In addition to the interaction between Wnt and Fz,

LRP5/6 co-receptors are also required for mediating Wnt signaling (see figure I.6) [27].

After Wnt protein binding to the receptors LRP5/6 and Fz, the APC/Axin/GSK-3β complex and Dishevelled protein are recruited from the cytoplasm to the membrane. This recruitment in the membrane impairs the degradation of β-catenin by the E3 β-TrCP1 and allows β-catenin to be stabilized in the cytoplasm [28][29]. This accumulation facilitates β-catenin translocation into the nucleus where it complexes with Lef/TCF family members and mediate the transcription of its target genes (Figure I.6) [27][30].

Canonical Wnt/β-catenin signaling pathway is essential during cardiogenesis in several animal models [31]. For example, the loss of canonical Wnt signaling in the myocardium results in tricuspid atresia with hypoplastic right ventricle associated with the loss of AV myocardium [32]. Moreover it has been shown that Wnt/β-catenin is important for cardiac tissue repair after myocardial infarction (MI) through EndMT. This process contributes to a generation of biopotential mesenchymal cells that also might take place in angiogenesis and fibrosis, arising new blood vessels and scar tissue, respectively [33].

As mentioned above Wnt/β-catenin promotes EMT inducing transcription activation of mesenchymal markers such as Twist1 and Fibronectin [34]–[36]. Furthermore, the up-regulation of Wnt/β-catenin signaling, inhibits Snail phosphorylation and consequently increases Snail protein levels and activity while driving an in vivo epithelial-mesenchymal transition down-regulating E-Cadherin [37].

Wnt/β-catenin presents a crosstalk during signaling in a large number of cell types during development. They can interact in a synergic or antagonistic manner, depending on the context. For example, Notch

and Wnt/ β-catenin synergistically act to induce arterial endothelial cells gene expression through RBP-J dependent manner [38].

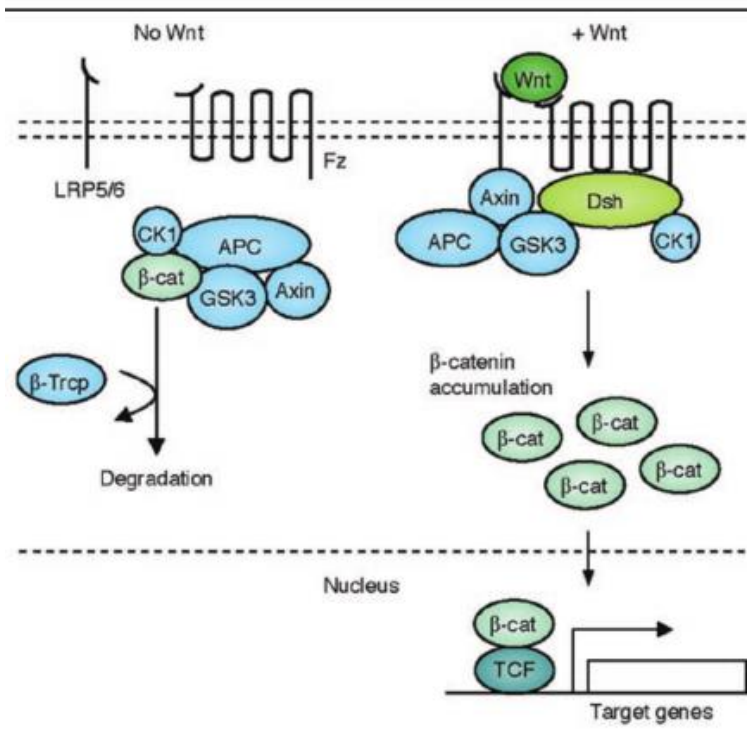

Figure I.6. The Wnt/β-catenin pathway. After Wnt protein interaction with the LRP5/6 and Frizzled (Fz) transmembrane protein, the complex formed by APC/Axin/GSK-3β is translocated to the membrane. Then β-catenin is not degraded and it goes to the nucleus and together with the Lef/TCF family members transcriptionally activates it targets genes [27].

I.4.3 TGF-β

Transforming growth factor-β (TGF-β) is a multifunctional cytokine involved in the regulation of proliferation, differentiation, migration, and survival of many different cell types. It has been widely studied during

embryogenesis and cancer progression. It is known to induce EMT/EndMT through Smad proteins cascade [39].

TGF-β signals via two distinct receptor serine/threonine kinases, the type I and type II receptors. When the ligand interact with the type II receptor, it transphosphorylates and activates the type I receptor, which then phosphorylates cytoplasmic Smad (Smad2 and Smad3) transcriptional factors. Activated Smad2/3 forms complexes with Smad4. They are translocated to the nucleus and bind to specific transcriptional factors and regulate expression of genes that play critical roles in the control of cell proliferation, differentiation (including EMT and EndMT), apoptosis and cell migration (Figure I.7) [40].

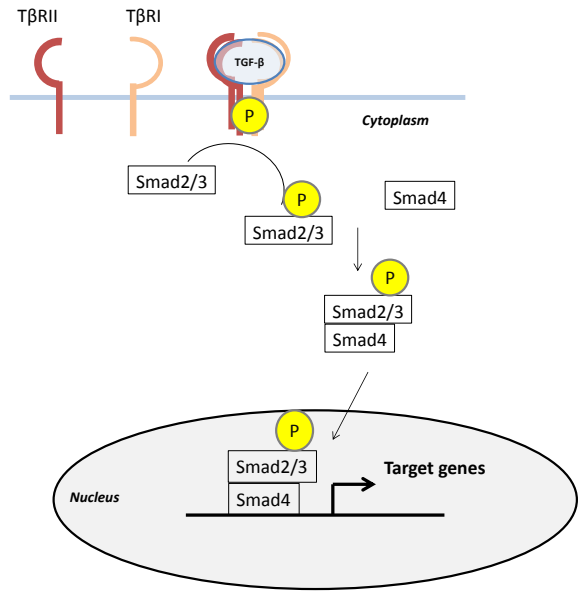

Figure I.7. TGF-β signaling pathway: Upon TGF-β binding with its receptors, Smad2/3 gets activated by phosphorylation. Once activated, it interacts with Smad4. After the interaction they translocate to the nucleus and bind to DNA activating its target genes [41].

In fact, it is very well stablished that TGF-β induces mesenchymal markers such Snail1, a key transcriptional factor during EMT/EndMT. In the context of EndMT, TGF-β is required for cardiac valve formation during embryogenesis, cardiac fibrosis and in regeneration of new blood vessels [42][39][43].

I.5 EMT Transcriptional factors (EMT-TFs)

All the pathways described above have something in common in order to induce EMT or EndMT: epithelial or endothelial markers must be down-regulated. It is well known that transcriptional factors are involved in the down-regulation of epithelial genes such as E-Cadherin by binding to its promoter and repressing it. This requires direct association of repressors to E-Box elements located on the promoter of target genes. The consensus sequence of the E-Box is usually CACCTG or CAGGTG; however, there exist other E-boxes of similar sequences called non-canonical E-boxes (CACGTG and CAGCTG) [44][45].

Regarding the EMT, the first identified repressors were the Zinc fingers domain transcriptional factors Snail1 and Snail2 [46]–[48] and the transcriptional repressors Zeb1 and Zeb2 [49][50]. All of them are capable to bind to E-Cadherin promoter and repress it. Other potent repressors are the family of transcription factors basic helix-loop-helix such as Twist. They down-regulate E-Cadherin although requiring other similar transcriptional repressors [51].

Both E-Cadherin and VE-Cadherin promoters contains functional E-boxes, suggesting that they are repressed by transcriptional factors [52]. Probably all the transcriptional factors described in EMT have a similar role during EndMT.

I.5.1 The ZFH family

The Zinc Finger homeodomain (ZFH) family of transcription factors is formed by two members: Zeb1 and Zeb2 (also known as Sip1). These proteins have two Zinc finger domains, one at the N-terminal and the other one at the C-terminal part. In the middle of the protein they have a homeodomain [53]. Zeb1/2 are involved in the down-regulaion of epithelial genes and in the upregulation of mesenchymal genes and are transcriptionally activated by different signaling pathways such as TGF-β, TNF-α and Wnt [53][54].

It is common to find a crosstalk between EMT transcriptional factors. For example, Snail1 and Twist can regulate Zeb1 protein stability by inducing ETS-1, β-Catenin, NF-κB and also down-regulating micro-RNA (miRNA)-200 [55]. Zeb1 induction happens later than Snail1, allowing a sustained down-modulation of E-Cadherin. On the other hand, Zeb2 can also be stimulated by Snail1 in an indirect manner through the alternative processing of ZEB2 mRNA [56].

I.5.2 The bHLH family

The basic helix-loop-helix (bHLH) transcriptional factors Twist1 and Twist2 are the most studied bHLH proteins during EMT. Both, Twist1/2, share a similar structure organization formed by two parallel α-helix joined by a loop required for dimerization. They bind DNA as homo- or heterodimers using consensus E-boxes. Both can activate or repress genes through its Twist-box domain in the C-terminal part. For instance Twist1 recruits Mi-2/NuRD complex to repress E-Cadherin expression and promote EMT [57].

Twist proteins are up-regulated upon TGF-β, Wnt and hypoxia among others stimuli. Twist1 transcriptional increase by hypoxia requires an hypoxia-inducible factor-responsible element (HRE) which is bound by HIF-1α in hypoxia conditions [58]. Regarding the up-regulation upon TGF-β, the expression of Twist was analyzed in NMuMG cells. An up-regulation of the Twist protein was observed 1 h after addition of the cytokine. However, increases in Twist1 mRNA levels were detected after 24 h, with a maximal activation observed at 72 h. Both the early stimulation in Twist protein levels and the late activation of mRNA expression were dependent on Snail1 expression [55].

I.5.3 The Snail family

The Snail group of proteins consists of three members, Snail1, Snail2 (also known as Slug) and Snail3 (Smuc). Snail1 was the first factor to be described as an E-Cadherin repressor [46][47]. It has been widely studied its role during neural crest formation, gastrulation, cancer progression, cell survival and cell movement [59].

Snail1 has in the N-terminal part of the protein the SNAG domain formed by 9 amino acids that is required for transcriptional repression. Moreover the N-terminal part has a phospho-serine rich domain (P-S rich, aa 90-120) that contains various phosphorylation motifs (figure I.8)[60]. In the middle of the protein has a nuclear export sequence (NES) that binds to CRM1 (Exportin-1, aa 139-148)[60]. At the C-terminal part we find four zinc fingers (ZnF); the canonical three ZnFs of the C_2H_2 type and the fourth, an atypical ZnF; all important for binding to E-boxes[50] [51].

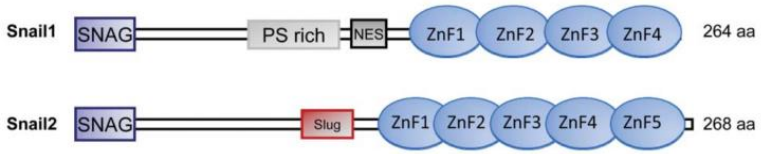

Figure I.8. Snail domains. Snail1 protein consists in four main domains. SNAG for gene repression. P-S rich motif where undergoes some different phosphorylation events. NES regulates nuclear to cytoplasm export and the zinc finger domain which binds to DNA. Snail2 contains one ZnF more in the C-terminal part and a Slug domain. Adapted from [60].

The SNAG domain (Figure I.8) is important for the recruitment of different chromatin modifier complexes such as HDAC1/2 through the Sin3A co-repressor. Overexpressing Snail1 correlates with a global deacetylation of histones 3 and 4 [63]. This domain is also necessary for the recruitment of Polycomb repressive complex 2 (PRC2) to the E-Cadherin promoter and trymethylation of lysine 27 on H3 [64]. Also, this specific domain recruits other complexes such as LSD1 (lysine specific demethylase 1) together with CoREST (repressor element-1 silencing transcription) forming a ternary complex that helps to repress some epithelial genes [65]. Moreover it has been demonstrated that other specific proteins such as lysil-oxidase-like (LOXL) 2 and 3 interact with Snail1 through the SNAG domain. This cooperation is also necessary to the repression of E-Cadherin [66] and for the regulation of the heterochromatin during EMT [67].

Snail1 nuclear/cytoplasmic localization is finely regulated. The nuclear export sequence (NES) (figure I.8) is the domain responsible for the binding to CRM1, thus controlling the nuclear export of the protein [68]. Furthermore, nuclear localization depends on the C-terminal part that contains a nuclear localization signal (NLS) composed by non-

consecutive basic residues at defined positions in at least three sequential ZnFs [69][70]. Phosphorylation of P-S rich domain also regulates nuclear export [68]. In fact, phosphorylation by GSK-3β affects Snail1 conformation and makes the NES more accessible to CRM1, leading to its translocation to the cytoplasm [60].

Snail1 has not only been reported to act as E-Cadherin repressor but also for other epithelial markers such as desmoplakin, cytokeratin 18, occludin, claudins, Vitamin D receptor and among others [71][72][73]. It is also important in the up-regulation of extracellular matrix modifiers such as Matrix Metalloprotease 9 (MMP-9), favoring invasion [74]. Moreover, Snail1 has been found to interact with p65 subunit of NF-κB and PARP1 in the Fibronectin promoter inducing gene transcription [75]. The role of Snail1 as an activator it has been seen in the up-regulation of other mesenchymal genes such as Lef-1 and Zeb1 [73] and also with co-operation with Twist in the up-regulation and maintenance of N-Cadherin [76][77].

Snail1 is up-regulated by many different stimuli and signaling pathways at protein and RNA level. For example, it has been described Snail1 transcription to be induced by TGF-β through a Smad cascade [78]. Moreover it has also been described that NF-κB induces Snail1 transcription in a positive feedback loop [79][80].

Snail1 is a very unstable protein and is highly post transcriptionally regulated. As previously explained, GSK3-β regulates the exit of Snail1 from the nucleus and the further ubiquitination by β-TrCP1 in the cytoplasm [37]. Snail1 nuclear localization is also controlled by Lats2 and p21-activated kinase, PAK1 [81][60]. Both phosphorylate the C-terminal part of Snail1 in the nucleus increasing its stability. Moreover, it has been described other phosphorylation at N-Terminal part, at serine 100, by ATM; important for its stabilization and radio sensitivity

of the cell [82]. Recently it has been also described another kinase doing the same function in the N-terminal; ERK2 that specifically phosphorylates at serine 82 and serine 104 retaining Snail1 in the nucleus [83]. Snail1 can be ubiquitinated and degraded not only by β-TrCP1, but also by Fbxl14 and Fbxl5 independently of GSK-3β phosphorylation and by Fbxo11 requiring a previous PDK1 phosphorylation at serine 11 [84] [85][86].

Regarding the other member of the family, Snail2 (Slug) has been less studied, but also induces EMT through the repression of E-cadherin. When compared to Snail2, Snail1 is a more efficient repressor since it presents better affinity for E-box sequences [48].

As it is shown in the figure I.7, Snail2 contains a specific domain called SLUG domain. This domain interacts with CtBP1 for gene repression and also recruits proteins such as HDAC1. Snail2 transcription is regulated by different signaling pathways such as Wnt, Notch, TGF-β, estrogens, ERK and TNF-α[87]. Slug also has been reported to be ubiquitinated and degraded by different ubiquitin ligases: MDM2, Fbxl14 and β-TrCP1, in this case after GSK-3β phosphorylation in a non-canonical motif [87][84][88]. Most recently, it has been described another ubiquitin ligase involved in its degradation upon GSK-3β phosphorylation, which is the carboxyl terminus of Hsc70-interacting protein (CHIP) [89].

Snail transcriptional factors are very important for EMT and their post-transcriptional regulation play a key role during this process. In fact, GSK-3β seems to be one of the main kinases involved in Snail1 regulation since it induces Snail1 export from the nucleus and its degradation by β-TrCP1 and Fbxl14. Besides Wnt signaling pathway, GSK-3β is inhibited by phosphorylation: the Serine/Threonine kinase PKB/Akt is the main kinase involved in GSK-3β phosphorylation at

Serine 9 promoting its inactivation [90]. In addition, it has been suggested that ERK associates with GSK-3β through a docking motif (^{291}FKFP) of GSK-3β and phosphorylates it at threonine 43, which primes GSK-3β for its subsequent phosphorylation at serine 9 by p90RSK [91], resulting in GSK-3β inactivation.

I.6 Serine/threonine kinase Akt

Akt is a well-known protein of the AGC kinases subfamily and the homolog of v-Akt (protein from isolated Akt8 virus from a mouse T-lymphocyte) [92]. The AGC group is named after the protein kinase A, G, and C families (PKA, PKC, PKG). Akt, also known as PKB, is a main regulator in many different processes not only in normal but also in tumoral cells. It has been described functions of Akt in proliferation, growth, metabolism differentiation, migration, angiogenesis and survival. It has also a relevant role in tumor progression and it has been implicated in EMT [93][94].

In mammals, Akt family has three isoforms: Akt1/PKBα, Akt2/PKBβ and Akt3/PKBγ (Figure I.9). All three isoforms share a high conserved structure, with more than 80% of homology. They have three principal domains. In the N-terminal part of the protein there is the pleckstrin homology domain (PH). This domain is essential for binding to phosphatidylinositol-(3,4,5)-trisphosphate (PIP_3) in the cytoplasmic membrane (PIP_3, is the product of phosphoinositide 3-kinase (PI3K) phosphorylation of phosphatidylinositol-(4,5)-bisphosphate, PIP_2).The central part of the protein contains the catalytic domain, where is localized the threonine 308 (for AKT1) residue important for its activation. Finally,

the regulatory domain (RD), also known as hydrophobic motif (HM) is located in the C-terminal part of the protein. In this domain there is the second residue (serine 473 for Akt1) involved on its activation (figure I.9).

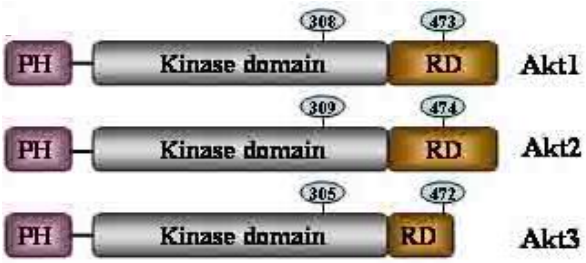

Figure I.9. Akt isoforms: Akt domains and their phosphorylation residues for each isoform. The three proteins have more than 80% of identity

Akt1 and Akt2 are present in all tissues although Akt1 is more abundant than Akt2 (approximately threefold) [93]. On the other hand Akt3 has been reported only to be expressed in some specific tissues such as in the brain. Regarding the different function of each isoform, it has been shown in deficient mice for each specific isoform that Akt1 -/- mice show early death or delay in growth [95]; the Akt2 -/- mice show insulin-resistance similarly to diabetes type II [96], and Akt3 -/- mice present a 25% reduction of the size brain [97]. Moreover, depleting all Akt isoforms causes embryonic death at E12.

I.6.1 Akt activation

As mentioned above, besides binding to PIP_3, Akt need to be phosphorylated in two residues in order to be active. Depending on the isoform, the position of the residues changes (Figure I.9). The phosphorylation of Akt requires previous activation of PI3K, insulin, IGF-1, TGF-β, or others stimuli. Once PI3K is activated, it phosphorylates PIP_2 forming PIP_3. Then, Akt is recruited to the cytoplasmic membrane through the PH domain. After this, Akt can be activated by PDK1 in threonine 308 (for Akt1) and in Serine 473 (for

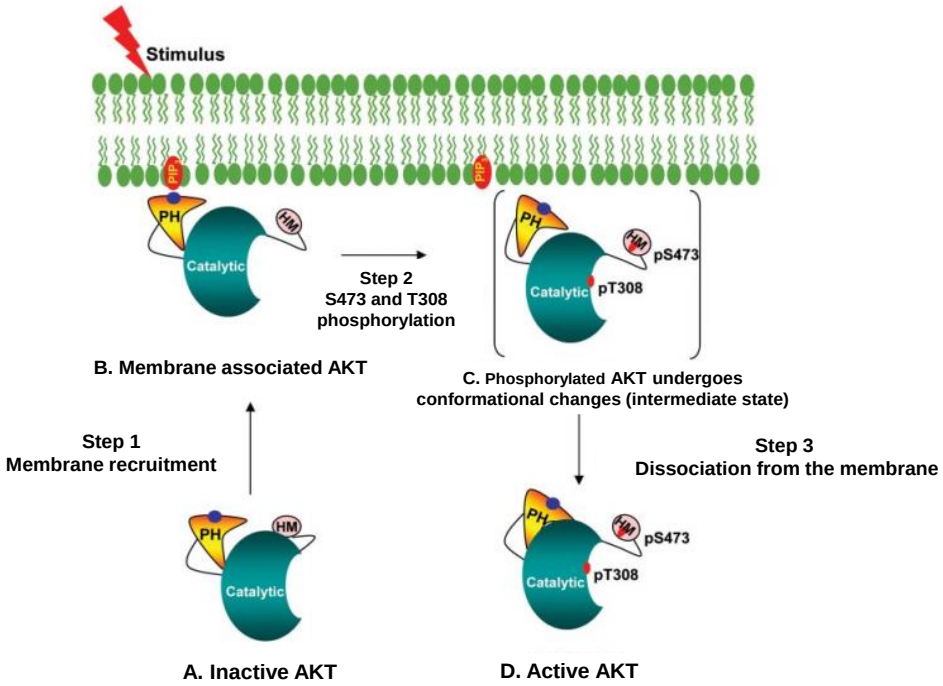

Figure I.10. Activation of Akt. Schematic view of how inactive Akt (A) is recruited to the plasma membrane (B) where is phosphorylated at S473 and T308 and undergoes changes in its structure (C) and is dissociated from the membrane and remain activated in the cytoplasm (D). Adapted from [98].

Akt1) by different kinases being the most accepted, mTORC2. Akt must be phosphorylated in both residues to be fully active. Once Akt is active, it is translocated to the cytosol or the nucleus in order to act on its substrates (figure I.10) [98].

I.6.2 Akt functions

Activated Akt phosphorylates numerous substrates associated with cell proliferation, survival, intermediary metabolism, angiogenesis and cell growth [99]. Although PI3K/Akt has been demonstrated to be relevant during embryogenesis, dysregulation of Akt leads to different diseases such as cancer, diabetes, cardiovascular and neurological disorders (Alzheimer). The consensus sequence for Akt phosphorylation, RXRXXS/T, is found in most but not all these substrates [100].

It has been reported that EMT is induced by Akt activation. This induction causes typical cellular changes allowing the transformation to a more mesenchymal phenotype [94]. The first substrate described for Akt was GSK-3β [90]. As previously mentioned, GSK-3β is supposed to be a key kinase relevant in the post-transcriptional regulation of Snail1 protein, thus important during EMT [101]. Akt also induces production of metalloproteases, promoting cell invasion [102].

As mentioned above, Akt also regulates cell death at different levels. Apoptosis is a special type of cell death different from necrosis, with a number of events that occur systematically and sequentially. The understanding of apoptosis has provided the basis for novel targeted therapies that can induce death in cancer cells or sensitize them to established cytotoxic agents and radiation therapy [103].

Apoptosis can occur when a cell is damaged beyond repair, infected with a virus, undergoing stress conditions such as

starvation, grown with low oxygen or under oxidative stress. Each pathway activates its own initiator caspase (8, 9 or 10) which in turn will activate the executioner caspase-3. The execution pathway results in characteristic cytomorphological features including cell shrinkage, chromatin condensation, formation of cytoplasmic blebs and apoptotic bodies and finally phagocytosis of the apoptotic bodies by adjacent parenchymal cells, neoplastic cells or macrophages [104].

One of the main substrates of Akt involved in apoptosis is the family of FoxO proteins. In mammals, there are four FoxO genes, FoxO1, 3, 4, and 6 [105]. These proteins are transcriptional factors that promote apoptosis [106]. The phosphorylation of FoxO by Akt induces their translocation from the nucleus to the cytoplasm where it is degraded. This exclusion from the nucleus leads to the down-regulation of FoxO target genes such as the Fas ligand, TRAIL (TNF-related apoptosis-inducing ligand) and TRADD (TNF receptor type 1 associated death domain), and intracellular components for apoptosis like Bim (bcl-2 interacting mediator of cell death), a pro-apoptotic Bcl-2 family member, and Bcl-6 [107].

Akt also plays a critical role in cell growth by directly phosphorylating mTOR in a rapamycin-sensitive complex containing raptor [108]. More importantly, Akt phosphorylates and inactivates tuberin (TSC2), an inhibitor of mTOR within the mTOR-raptor complex [109]. Inhibition of mTOR stops the protein synthesis machinery due to inactivation of its effector, p70 S6 kinase and activation of the eukaryotic initiation factor 4E binding protein 1 (4E-EP1), an inhibitor of translation [109], [110].

As it has been published that Notch can induce EndMT, we started to investigate in detail the role of Snail1 during this process. Moreover, we wondered how Snail1 can be stabilized analyzing the most important kinases that has been reported to regulate it. As it has been

explained above, Snail1 can block apoptosis during EMT. We questioned if Snail1 also have this function during EndMT and how it acts and its relevance.

OBJECTIVES

The general objective of this thesis is to describe the Endothelial to mesenchymal transition (EndMT) induced by Notch and the role of Snail1 during this process. To this aim we focused on:

I. The characterization of the downstream effects of Notch in endothelial cells
II. To investigate the role of Snail1 and the kinases involved on its stability
III. The role of Akt and Snail1 in apoptosis protection induced by Notch

.

RESULTS

R.1 Notch induces EndMT through Snail1

Although Snail1 is up-regulated and represses E-cadherin during EMT, its role during EndMT is less known. We wonder if Snail1 is involved in the EndMT induced by Notch.

In order to better study this process, Pig Aortic Endothelial (PAE) cell line stably transfected with Notch Intracellular Domain (NICD) were used. Two cell populations with different expression level of NICD-Myc, PAE-NICD1 and PAE-NICD2, were generated. Control cells (PAE-TCL) were stably transfected with GFP. Control cell grew on plastic and became contact inhibited on confluence. They presented a more organized and elongated shape forming compacted colonies (figure R.1.A). PAE-NICD1 and PAE-NICD2 cells, however, lost contact inhibition, exhibited a less endothelial-like and more elongated morphology, and they presented an scatter-like phenotype[18]. These phenotypic changes were associated to a down-regulation of the endothelial marker VE-Cadherin and the up-regulation of mesenchymal markers, such as Snail1, Snail2 (Slug), Fibronectin, α-SMA and N-Cadherin (figure R.1.B).

This morphological and protein analysis suggests that Notch signaling induces in a dose dependent manner a transition from an endothelial cell to a more mesenchymal phenotype. This cellular model was further study to better understand how EndMT works.

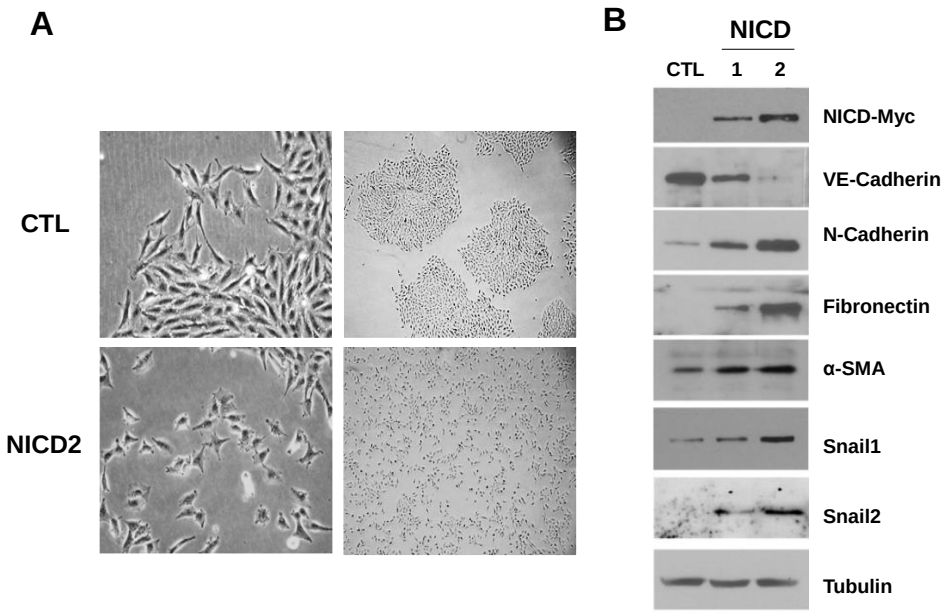

Figure R.1. Notch induces EndMT. (A) PAE-CTL and PAE-NICD2 cells under light microscopy. Left (10x); right (4x). (B)Total extracts using 2% SDS buffer of the three different subpopulations of cells were analyzed by western blot with indicated antibodies.

As shown, the repression of VE-Cadherin was detected upon Notch expression. In order to be sure that Snail1 was affecting VE-Cadherin, we silenced Snail1 using an specific siRNA. After siRNA transfection, we isolated the mRNA and performed a semi-quantitative RT-PCR against VE-Cadherin and Snail1. HPRT gene was used as a loading control. Levels of VE-Cadherin were slightly up-regulated when Snail1 was silenced in both PAE-CTL and PAE-NICD2 (figure R.2). In addition, Notch induced Snail1 mRNA confirming the up-regulation of Snail1 in the previous experiment.

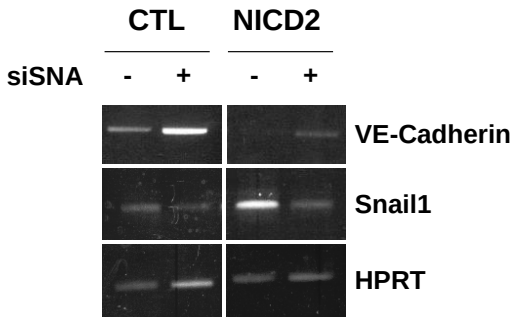

Figure R.2. Snail1 induced by Notch represses VE-Cadherin transcription. PAE-CTL and PAE-NICD2 were transfected for 72 hours with specific Snail1 siRNA. After mRNA Phenol-Chloroform extraction, semi-quantitative RT-PCR was performed using specific primers for indicated genes. HPRT was used as a control.

We also investigated the cooperation between Notch and other classical EMT inducer, TGF-β1. CTL cells treated with TGF-β1 for 24 hours did not up-regulate Snail1, Fibronectin or Lef-1 neither they down-regulated VE-Cadherin levels (figure R.3). However, TGF-β1 cooperated with Notch in the stimulation of Snail1, Fibronectin and Lef-1 but not in the VE-Cadherin repression (figure R.3). Interestingly, when Snail1 mRNA was analyzed, we observed a clear increase induced by TGF-β (Figure R.4). Similar results were obtained with Fibronectin. Both Fibronectin protein and mRNA were only strongly activated upon TGF-β1 when Notch was expressed (figure R.3.A; figure R.4). These results suggest that Notch transcriptionally activates Snail1 and Fibronectin and also that Notch and TGF-β1 pathways cooperate during EndMT.

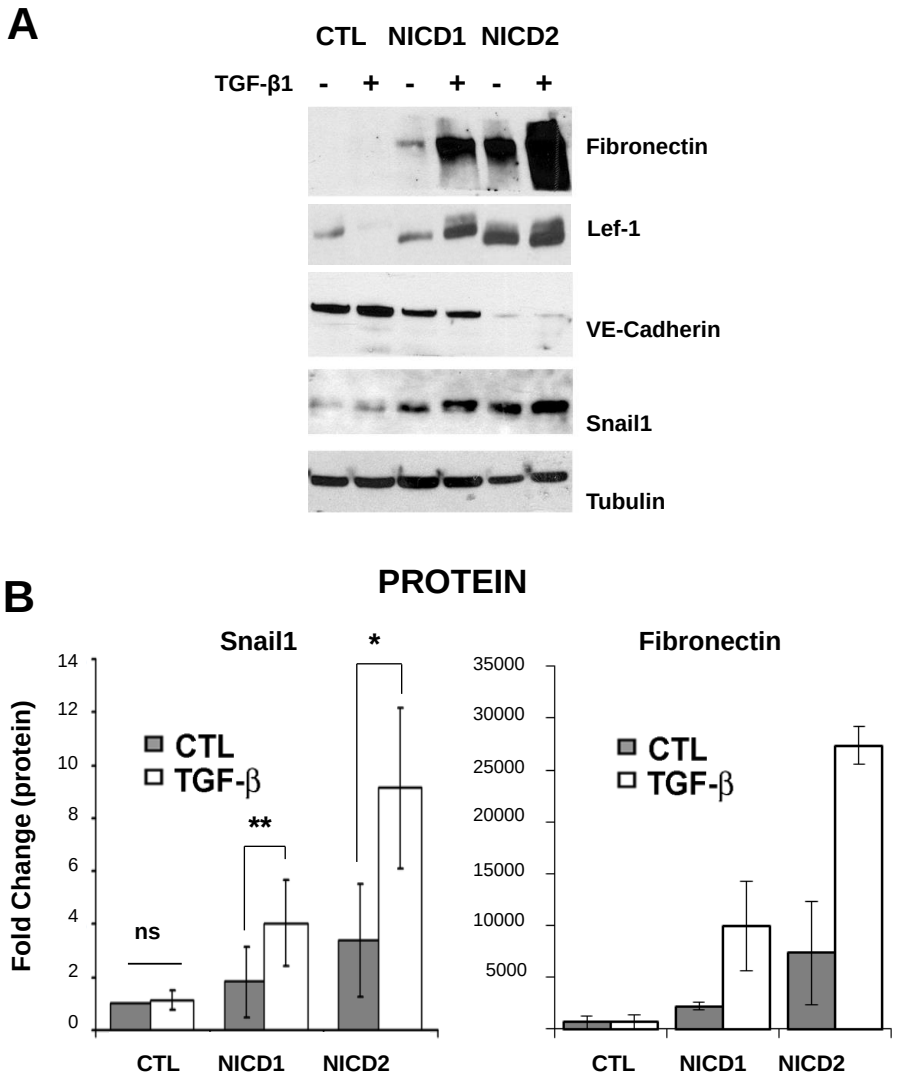

Figure R.3. Notch and TGF-β cooperate in EndMT induction. (A) Cells were treated with 5 ng/ml of TGF-β1 during 24 hours and analyzed with indicated antibodies by Western Blot (representative result) (B) The average ±SD (n=4) of the quantification of Snail1 and Fibronectin using ImageJ software of four different experiments. P-values were calculated using unpaired, two-tailed student's t-test (**P<0.01; *P<0.05 or not significance, "ns").

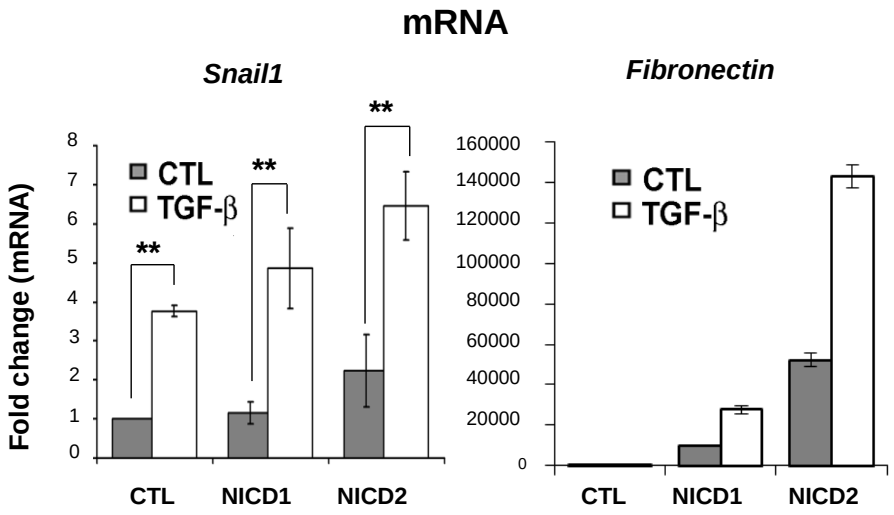

Figure R.4. TGF-β1 induces *Snail1* mRNA but only *Fibronectin* in cooperation with Notch. mRNA isolated with Phenol-Chloroform was isolated and analyzed by RT-qPCR using specific primers for Pig. P-values were calculated using unpaired, two-tailed student's t-test (**P<0.01).

Other important result observed was the different increase of Snail1 mRNA and protein after TGF-β1 in control cells (Figure R.3 and R.4). While in control cells Snail1 mRNA increases upon TGF-β1, at protein level does not augment. However, in Notch expressing cells, a synergistic effect is observed at protein level. This result is suggesting that Snail1 is undergoing a post-transcriptional modification promoting its stability.

Taking all these results together, it suggests that Notch and TGF-β1 cooperate in the up-regulation of mesenchymal markers, such as Snail1, Fibronectin and Lef-1 during EndMT. On one hand, TGF-β1 increases mRNA of Snail1 and, on the other hand, Notch helps to maintain high protein expression of Snail1.

R.2 Notch stabilizes Snail1 protein through inactivation of GSK-3β

Since Snail1 protein is very unstable, we examined if Snail1 up-regulation upon Notch expression was associated to protein stability.

We transfected PAE cells with pcDNA3-Snail1-HA for 24 hours and then they were treated with CHX, to block the translation from mRNA to a protein, for the indicated times. As it is shown in figure R.5.A, the relative half-life of Snail1-HA was increased in NICD1 or NICD2 cells with respect to the control.

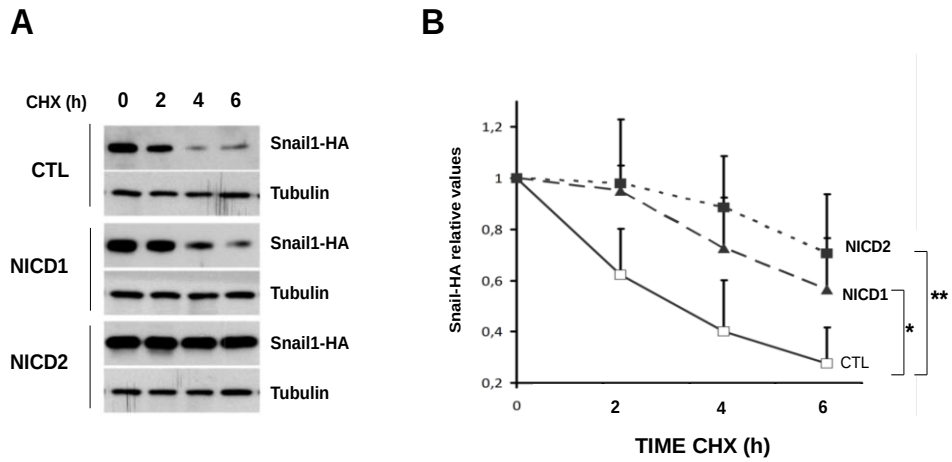

Figure R.5. Notch stabilizes Snail1 in endothelial cells. (A) Notch stably expressing PAE clones transiently transfected with Snail1-HA were treated with CHX (20 µg/ml) for the indicated times. Total extracts were analyzed by western blot. (B) Western blot bands quantification of four different experiments using ImageJ software and normalized with respect to Tubulin. P-values were calculated using unpaired, two-tailed student's t-test (**P<0.01; *P<0.05).

This same experiment was done four times and quantified. Expression of Snail1-HA was normalized by Tubulin. The statistical analysis of Snail1 expression, showed significance differences between control and Notch expressing cells (figure R.5.B).

Stabilization of Snail1 by Notch does not only occur in endothelial cells, but it was also observed in HEK-293T and RWP-1 cells (figure R.6). For instance, in HEK-293T cells we observed a greater stabilization of Snail1 upon Notch expression (Figure R.6.A). Figure R.6.B shows the quantification of two independent experiments. Otherwise, in RWP-1 cells the overexpression of Notch increased the basal levels of Snail1-HA indicating a post-transcriptional mechanism (figure R.6.C).

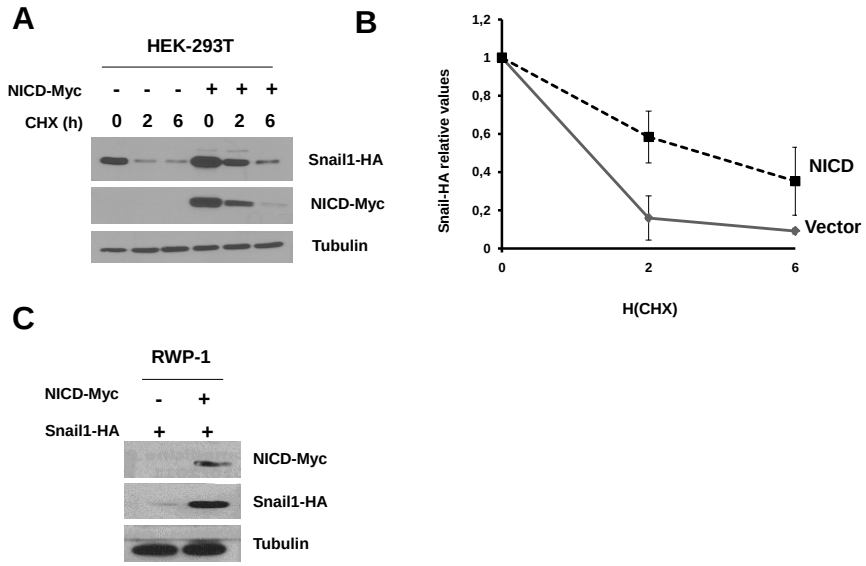

Figure R.6. Notch stabilizes Snail1 in epithelial cells. (D) HEK-293T cells, transient transfected with NICD-Myc and Snail1-HA, were treated with CHX for the indicated times. (B) Quantification of western blot bands of two experiments using ImageJ software and normalized with respect to Tubulin. The graph shows the average ± SD. (C) Analysis of Snail1-HA overexpressing NICD-Myc in RWP-1 cells

We verified that Snail1 stabilization was associated to a lower ubiquitination in Notch cells. Control and NICD2 cells were co-transfected with pcDNA3-Snail1-HA and HIS-tagged Ubiquitin. Nickel nitriloacetic acid (Ni-NTA) agarose beads were used to capture all ubiquitinated Snail1-HA after inhibition of the proteasome using MG-132 to preserve the ubiquitin chains. As expected, the amount of Snail1, labeled as Snail1-HA-$(Ub)_n$ was highly decreased in Notch expressing cells (figure R.7).

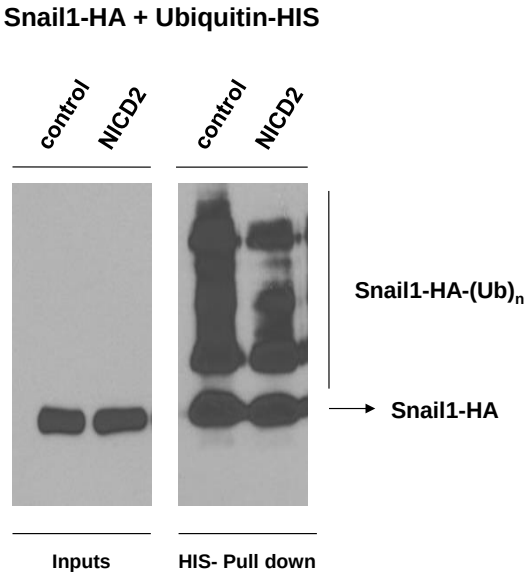

Figure R.7. Notch reduces Snail1 ubiquitination. PAE-CTL and PAE-NICD2 were transient transfected with Snail1-HA and Ub-HIS for 24 hours and treated with MG-132 for 6 hours before lysis. Ni-NTA beads were used to pull down ubiquitinated proteins. Anti-HA antibody was used to specific recognize ubiquitinated Snail1.

These results suggest that Notch expression blocks Snail1 ubiquitination and induces protein stabilization.

As mentioned in the introduction, Snail1 is a very unstable protein, very sensitive to proteasome degradation. At least three E3 ubiquitin ligases are involved in Snail1 ubiquitin degradation. These E3-ligases are Fbxl14, Fbxl5 and β-TrCP1 (also known as Fbxw1) [37], [84], [85].

Then, we analyzed the capability of different Snail1 E3 ubiquitin ligases to promote Snail1 degradation in control or NICD-expressing cells using HEK-293-T cells.

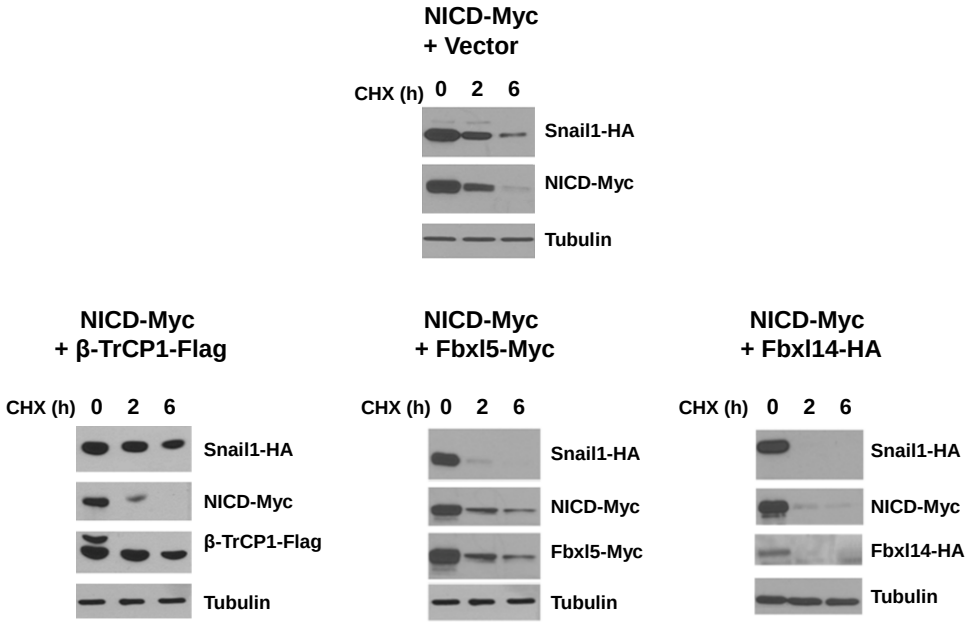

Figure R.8. Notch Blocks Snail1 degradation by β-TrCP1. (A) HEK-293-T cells were transiently transfected with Snail1-HA and NICD-Myc together with an empty vector or β-TrCP1-Flag, Fbxl14-HA or Fbxl5-Myc as indicated. After 24 hours of transfection, CHX (20μg/ml) was added for the indicated times. Ectopic Snail1 protein was analyzed by western blot. Tubulin was used as a loading control.

After 24 hours of transfection, cells were treated with CHX for the indicated times, and we determined the levels of exogenous Snail1-HA. Transfection of E3 ligases Fbxl14 or Fbxl5 induced Snail1 down-regulation in Notch expressing HEK-293-T cells; however, ectopic β-TrCP1 was not effective, indicating that the action of β-TrCP1 ligase was impaired after Notch expression. Therefore, Notch blocked the degradation by β-TrCP1 but not the function of Fbxl5 or Fbxl14 (figure R.8) suggesting that Notch increases Snail1 protein stability through a mechanism that specifically impairs its degradation by β-TrCP1.

As mentioned, β-TrCP1-dependent degradation of Snail1 requires its previous phosphorylation by GSK-3β. The levels of this protein kinase and β-TrCP1 were not decreased by Notch (figure R.9.A). However, phosphorylation at serine 9 of GSK-3β was clearly increased in both NICD1 and NICD2 cells when compared with control cells (figure R.9.A). This phosphorylation at serine 9 of GSK-3β is indicative of inactivation.

We also wanted to investigate the expression of pGSK-3β by immunofluorescence. As expected, in NICD2 cells the amount of the inactive GSK-3β was highly increased. Surprisingly, the staining of pGSK-3β reveals an accumulation of the phosphorylation protein in the nucleus (figure R.9.B).

With this result we conclude that in PAE cells Notch stabilizes Snail1 protein through inactivation of GSK-3β. This inactivation does not permit Snail1 phosphorylation and posterior degradation by β-TrCP1.

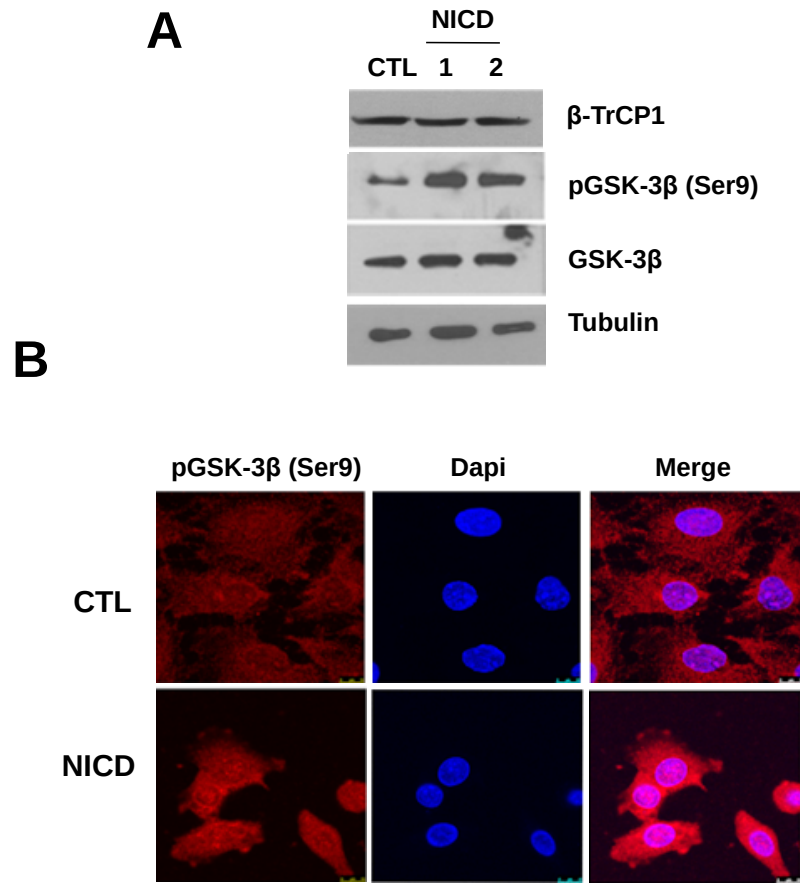

Figure R.9. Notch inactivates GSK-3β. (A) Indicated proteins of total extracts were analyzed by western blot in PAE cells. (B) Immunofluorescence by confocal microscopy was used for pGSK-3β (red) localization. Dapi was used as a nuclei staining.

R.3 Notch inactivates GSK-3β through Akt2 up-regulation

According with our results that GSK-3β is phosphorylated and inactivated in endothelial cells when Notch is expressed, we started to investigate the pathways involved in GSK-3β phosphorylation. The main kinase involved in this modification is the serine/threonine kinase Akt. As mentioned in the introduction, Akt needs to be phosphorylated at serine 473 and threonine 308 to be active.

In order to study this pathway, total extracts of PAE cells were analyzed. Unexpectedly, although pGSK-3β (Ser 9) was up-regulated in Notch cells, total levels of pAkt (Ser 473) were decreased (figure R.10.A).

Akt family of proteins consists of three isoforms. Akt1 and Akt2 are ubiquitously expressed whereas Akt3 less abundant and is more detected in specific tissues. Upon Notch induction Akt1 was down-regulated whereas Akt2 was increased (figure R.10.A). RNA analysis by RT-qPCR, showed an inverse transcriptional modulation of both *Akt1* and *Akt2* gene expression by Notch (figure R.10.B). The levels of Akt1 and Akt2 were explored by immunofluorescence; as expected, we observed a switch between both isoforms upon Notch induction (figure R.10.C).

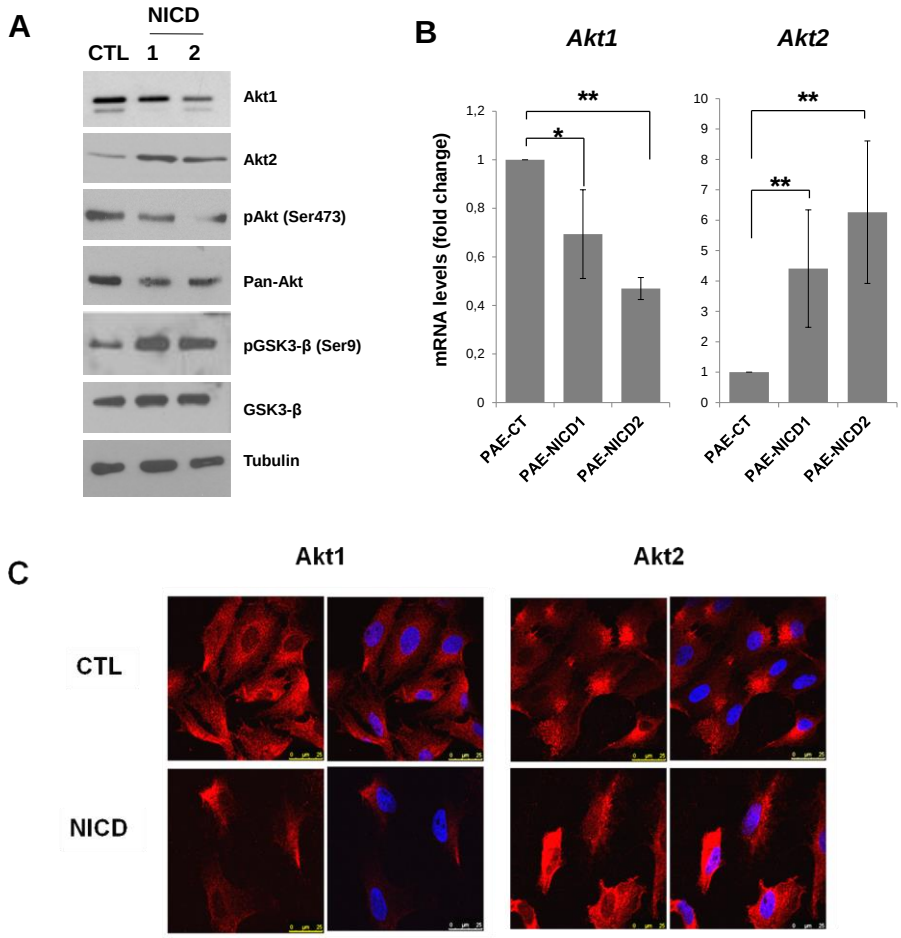

Figure R.10. Akt isoforms are modulated by Notch expression. (A) Proteins involved in Akt pathway were analyzed in total extracts from PAE cells. Tubulin was used as a loading control (B mRNA levels of Akt1 and Akt2 were analyzed by RT-qPCR using specific primer sequences. The average (n=4) ±SD is shown. (C) Total immunofluorescence of Akt1 (left panel) and Akt2 (right panel). Dapi was used as a nuclei staining. P-values were calculated using unpaired, two-tailed student's t-test (**P<0.01; *P<0.05).

Akt2 isoform has been associated with a more mesenchymal phenotype whereas Akt1 is more related to more epithelial characteristics [92][110][111]. The increase in the ratio Akt2/Akt1 in

Notch expressing cells that we observed was in agreement with the hypothesis that Akt2 could have also a role during EndMT induced by Notch.

We also explored other pathways involved in GSK-3β inactivation. It has been described that Erk can phosphorylate GSK-3β at threonine 43 favoring a posterior phosphorylation at serine 9 [91]. As shown in figure R.11, Erk is activated in Notch expressing cells.

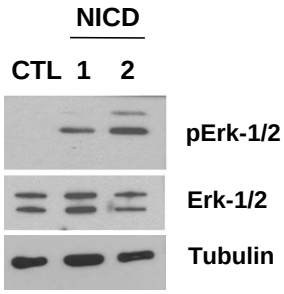

Figure R.11. Notch activates ERK pathway. Total extracts of PAE cells were analyzed by western blot. Tubulin was used as a loading control

The immunofluorescences previously shown of pGSK-3β, suggest a possible inactivation of the kinase in the nucleus (figure R.9.B). We wanted to investigate if this nuclear staining was related to a specific inactivation, probably induced by Akt or Erk, in the nucleus. To achieve this aim, protein levels of both different kinases were analyzed in the cytoplasmic and nuclear compartments.

As shown in figure R.12.A the up-regulation of pGSK-3β in the nucleus correlates with an up-regulation of Akt2 and also pErk2 (lower band). Moreover, it is also observed a decrease of Akt1 in the nucleus in Notch expressing cells. Concomitantly Snail1 is up-regulated in Notch cells and increased in the nucleus, suggesting that Snail1 is retained in this compartment. Supporting this, a clear nuclear accumulation of Snail1 in the nucleus was observed by immunofluorescence analysis (figure R.12.B).

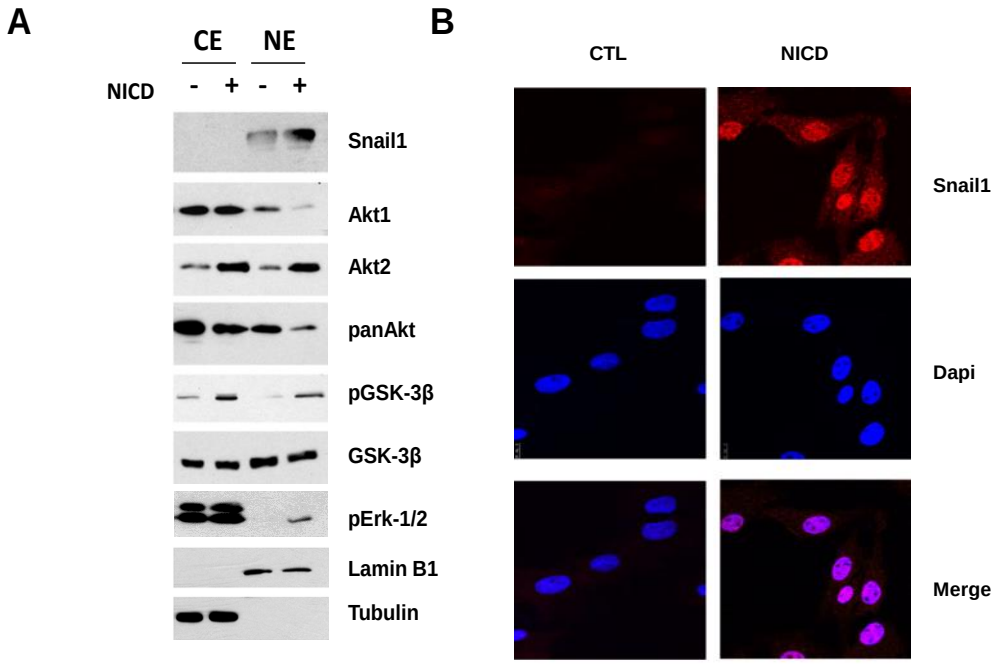

Figure R.12. Notch induces Snail1 nuclear retention and nuclear inactivation of GSK-3β. (A) Cytoplasmic (CE) and nuclear (NE) extracts were separated. Lamin B1 and Tubulin were used as controls of nuclear and cytoplasmic fractions, respectively. (B) Immunofluorescence of endogenous Snail1 in PAE-CTL and NICD2 using confocal microscopy. Dapi was used to detect the nucleus.

To elucidate the pathway involved in GSK-3β inactivation, we took advantage of allosteric inhibitors that block the phosphorylation of both Akt and Erk kinases (MK-2206 for Akt and UO126 for Erk) [113][114], thus their activation. We treated control and NICD2 cells with both inhibitors separately and together during 24 hours and analyzed Snail1 and pGSK-3β. As expected, upon Notch expression Snail1 and pGSK-3β were clearly up-regulated. Levels of pAkt (Ser 473) and pErk-1/2 were sensitive to MK-2206 and UO126, respectively (figure R.13). Interestingly, when Notch cells were treated with MK-2206 and UO126, Snail1 expression was strongly reduced. However, only in cells treated with Akt inhibitor we observed a decrease of GSK-3β phosphorylation (figure R.13). Furthermore, when both inhibitors were used together, the down-regulation of Snail1 and pGSK-3β was more pronounced (figure R.13).

Therefore, although Akt seems to have an important effect on the levels of Snail1 and pGSK-3β, Erk also controls Snail1 stability.

These results propose that Notch stabilizes Snail1 through two different mechanisms, but only one is GSK-3β dependent. Because Akt2 is highly up-regulated in Notch conditions, it suggests that the isoform involved in GSK-3β phosphorylation is Akt2.

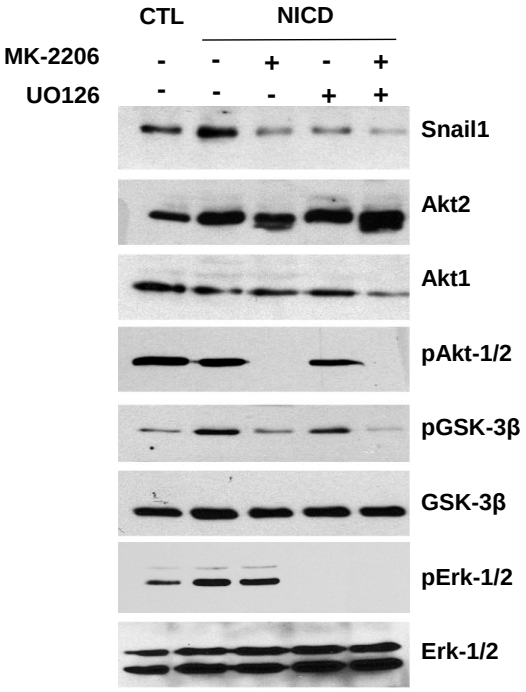

Figure R.13. Akt phosphorylates GSK-3β stabilizing Snail1 in Notch expressing cells. (A) Cells were treated with MK-2206 and UO126 at 10nM during 24 hours and the indicated proteins were analyzed by western blot. pAkt (Ser 473) and pErk-1/2 antibodies were used as control of the inhibition.

To assess Akt activation, we immunoprecipitated Akt1 and Akt2 and analyzed the phosphorylation by western blot. As expected, Akt2 in Notch expressing cells is phosphorylated at serine 473 and also at threonine 308. On the other hand Akt1 is phosphorylated in control cells but decreases dramatically when Notch is expressed (Figure R.14). This result demonstrated that the isoform activated in Notch expressing cells is Akt2.

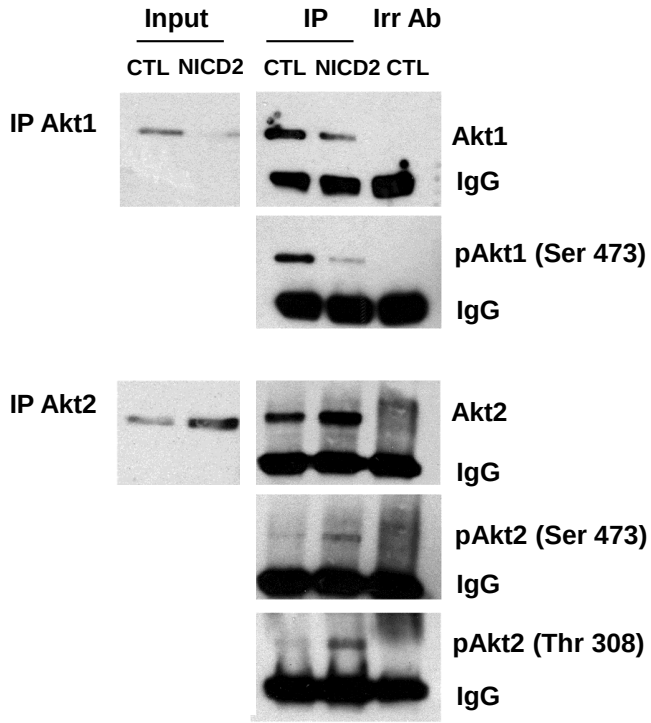

Figure R.14. Notch specifically induces Akt2 phosphorylation. Both Akt1 and Akt2 were immunoprecipitated in total extracts and pAkt at serine 473 was checked by western blot. pAkt at threonine 308 was also analyzed in the case of Akt2. Irrelevant rabbit antibody (Irr Ab) was used as unspecific binding.

To better study the relationship between Snail1 stability and Akt2 expression, Akt2 was down-regulated using specific short hairpins. PAE-CTL and PAE-NICD2 were infected with both shCT and shAkt2 and selected with puromycin. These shRNAs were specific because did not affect Akt1 expression (figure R.15.A-B). As we demonstrated in previous results, Snail1 was up-regulated upon Notch expression, and Akt2 depletion in Notch expressing cells diminished Snail1 levels. This decrease correlates with a down-regulation of pGSK-3β (Figure

R.15.B). Moreover, as a consequence of Snail1 down-modulation, VE-Cadherin was up-regulated in control cells and only slightly in Notch cells (Figure R15.B).

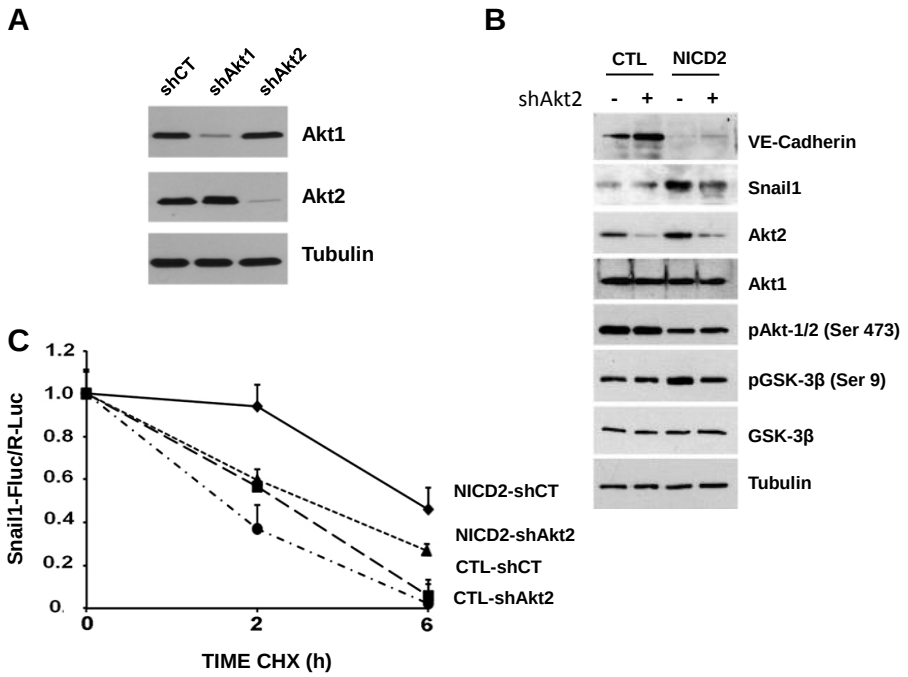

Figure R.15. Akt2 stabilizes Snail1 through inactivation of GSK-3β. (A) Control of specificity of the shAkt1 and shAkt2 in PAE cells. (B) PAE cells infected with both shCT and shAkt2 and total extracts were checked. (C) Snail1 fused to firefly-Luciferase (Snail1-F-Luc) and Renilla-Luciferase (R-Luc) were transiently transfected to PAE-CTL and PAE-NICD2 previously infected with shCT or shAkt2. 24 hours post-transfection, cells were treated with CHX (20 µg/ml) at indicated times. Luciferase signal was measured and normalized with Renilla. This graph represents the average of three different experiments.

To determine if the stability of Snail1 was Akt2 dependent, we studied the half-life of ectopic Snail1 in Akt2 deficient cells using Snail1-Firefly-Luciferase vector. This Snail1-FLuc fusion protein was previously described to behave like endogenous Snail1 protein [86]. This method allows a better quantification of protein levels that were normalized with Renilla-Luciferase. Similarly to the experiment from figure R.5, after transfection, cells were treated with CHX for the indicated times.

As shown in figure R.15.C, the degradation of Snail1-FLuc was accelerated in Akt2 depleted cells. With this data we confirm that up-regulation of Akt2 by Notch induces Snail1 stability through GSK-3β inactivation.

R.4 Notch transcriptionally activates Akt2 through TCF4/β-catenin

Akt2 is up-regulated in Notch active cells and correlates with an increase of pGSK-3β. To further confirm that Akt2 is transcriptionally induced by Notch, we used a 3.1Kbp fragment of the promoter of this gene fused to Luciferase, corresponding to -2898 to +220 with respect to the transcriptional start site [115]. This promoter was transfected to PAE-CTL together with increasing concentrations of NICD and luciferase activity was measured. The results showed a correlation between NICD and *Akt2* promoter activity (Figure R.16).

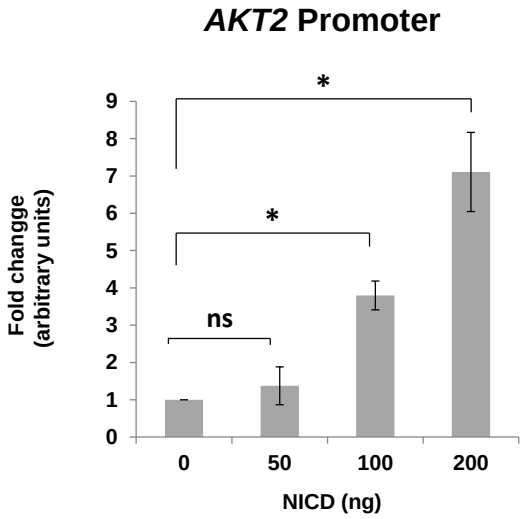

Figure R.16. Notch activates *Akt2* promoter in PAE cells. Indicated concentrations of NICD-Myc were transfected to PAE-CTL maintaining constant the amount of the 3.1 kbp *Akt2* promoter. Luciferase arbitrary units were normalized respect to TK-Renilla and expressed by fold change respect to non NICD-Myc expressing cells. The graph shows the average (n=3) ± SD. P-values were calculated using unpaired, two-tailed student's t-test (* P<0.05; "ns", not significance).

It has been published that *Akt2* promoter has several TCF-4 binding sites (Figure R.17) [116]. Since Notch activates β-catenin in several systems we hypothesized that *Akt2* promoter might be activated through TCF-4/β-catenin activity after Notch induction. To analyze this, reporter assays were done using TOP-FLASH reported plasmid after Notch expression.

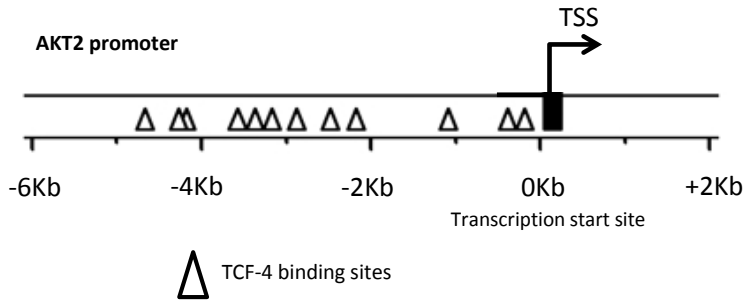

Figure R.17. *Akt2* promoter presents several TCF-4 binding sites [116]**.** *Akt2* Diagram of the promoter showing the location of Tcf-4/β-catenin binding sites with high degree of homology to the core consensus sequence (CTTTG or CAAAG).

To determine the activity of TCF-4/β-catenin in our system; PAE cells were transfected with TOP-FLASH reporter vector and luciferase activity was analyzed. Upon Notch expression its activity was up-regulated in a dose dependent manner. As a negative control the mutant FOP-FLASH was used (Figure R.18.A) [117].

To confirm that the activation of TCF-4/β-catenin was due to the Notch expression, the same experiment was carried out in HEK-293T cells. Upon Notch expression, TCF-4/β-catenin activity was increased almost

6 fold with respect to the control (Figure R.18.B), confirming the role of Notch in the induction of the TCF-4/β-catenin activity.

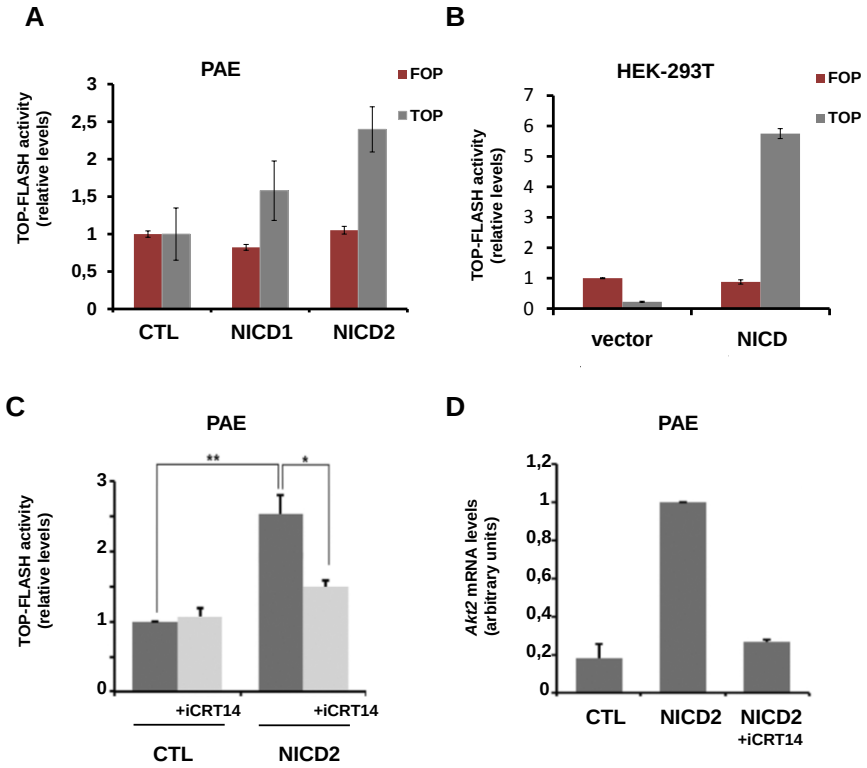

Figure R.18. Notch activates *Akt2* promoter through TCF-4/β-catenin activity. (A) TOP-FLASH activity was analyzed in PAE-CTL and in PAE stably expressing NICD cells. (B) TOP-FLASH activity was also analyzed in HEK-293-T transiently transfected with NICD-Myc. FOP-FLASH was used as a negative control (C) TOP-Flash activity was also compared between CTL and NICD2 clones after 48 hours of transfection. TCF4/β-Catenin inhibitor iCRT14 (25μM) was added 24 hours before the analysis. (D) *Akt2* mRNA levels were also checked in Notch cells after 24 hours of iCRT14 by RT-qPCR. All graphs show the average of 3 or 4 independent experiments ± SD. P-values were calculated using unpaired, two-tailed student's t-test (**P<0.01; *P<0.05).

To further demonstrate that Akt2 was activated through TCF-4/β-catenin, we used a potent inhibitor, iCRT14, which blocks the binding between TCF-4 and β-catenin [118]. In our cellular model, this inhibitor blocked the TCF-4/β-catenin activity induced by Notch (figure R.18.C). We also studied *Akt2* RNA levels by RT-qPCR in Notch cells treated with the inhibitor. Consistent with the previous results, the analysis showed that iCRT14 inhibited the increase in Akt2 mRNA caused by Notch (Figure R.18.D). We conclude that the interaction of TCF-4 and β-catenin was crucial in the transcriptional regulation of *Akt2* gene expression.

Furthermore, the effect of the inhibitor on protein levels was investigated. Since Akt2 is a very stable, at least three days of iCRT14 treatment was needed to see a down-regulation of Akt2 in total extracts (figure R.19.A). Akt2 protein was also investigated in different compartments. A down-regulation in the nuclear fraction was observed. As expected, low levels of Akt2 in the nuclear compartment were associated to a down-regulation of GSK-3β, and as a consequence to Snail1 destabilization (Figure R.19.B). To confirm that the inhibition of TCF-4/β-catenin promotes destabilization of Snail1 protein, we transfected exogenous Snail1-HA in HEK-293T cells with or without NICD-Myc. After iCRT14 treatment, Snail1-HA was up-regulated in Notch expressing cells; the inhibitor prevented this increase in ectopic Snail1-HA expression (figure R.19.C)

All these results confirmed that Notch transcriptionally activates Akt2 through the action of TCF-4 and β-catenin.

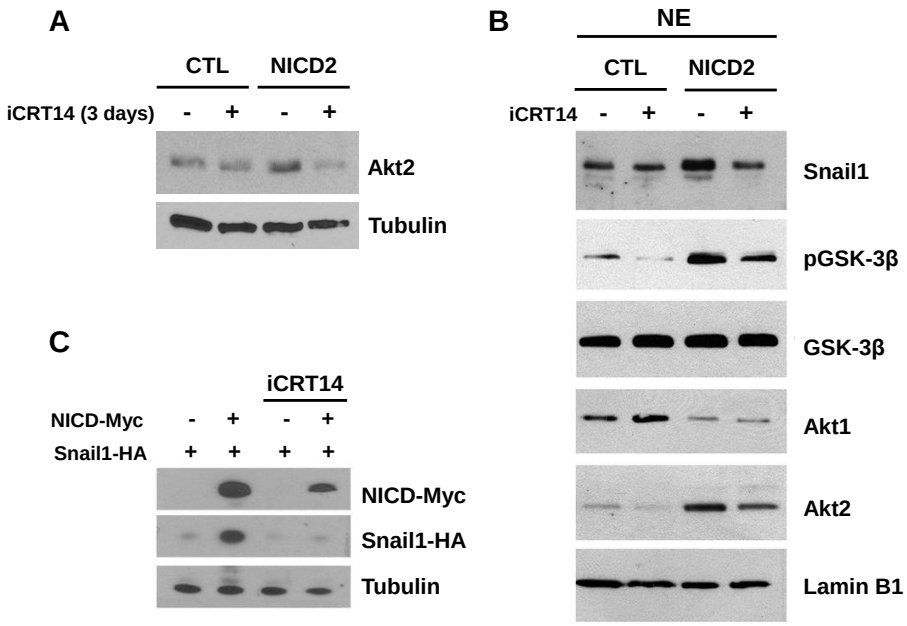

Figure R.19. Akt2 up-regulation depends on TCF-4/β-catenin activation. (A)Total extracts were analyzed after iCRT14 (25μM) treatment during three days. (B) Nuclear extracts were isolated and explored after 24 hours of iCRT14 treatment. Lamin B1 was used as a nuclear fraction control. (C) Snail1-HA and NICD-Myc were co-transfected in HEK-293T cells and treated with iCRT14 after 24 hours before the analysis.

R.5 Akt2 is essential for a complete EndMT

Akt2 is the isoform involved in the inactivation of GSK-3β when Notch is expressed, since Akt2 down-regulation decreased Snail1 stability. We wanted to investigate if Akt2 was relevant in endothelial cells for the acquisition of complete mesenchymal phenotype by the combined action of Notch and TGF-β1. Therefore, PAE-CTL and PAE-NICD2 were depleted in Akt2 and treated with TGF-β1.

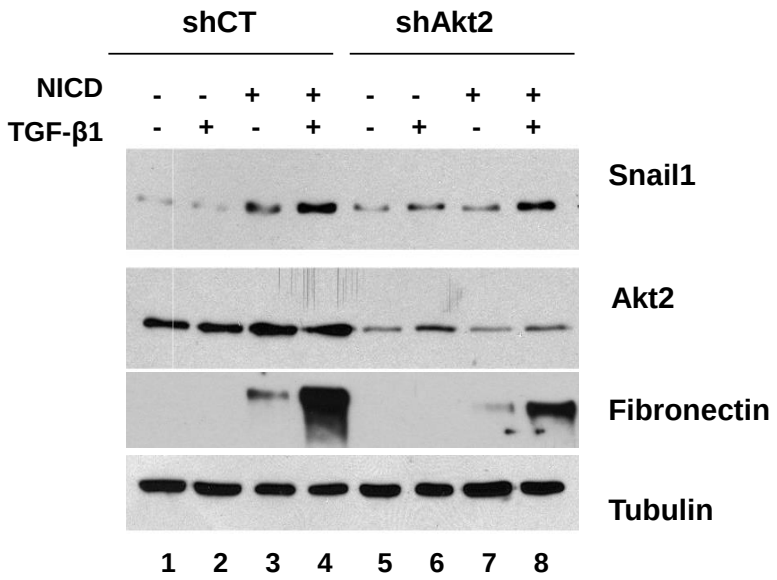

Figure R.20 Akt2 is needed in the cooperation between Notch and TGF-β1. PAE-CTL and PAE-NICD2 were infected with shCT and shAkt2 and selected with puromycin. Cells were treated with TGF-β1 during 24 hours. Indicated proteins were analyzed by western blot. Tubulin was used as a loading control.

Consistent with previous results, Notch and TGF-β1 cooperated in the induction of Snail1 and Fibronectin. When Akt2 was partially depleted with shAkt2 in Notch expressing cells, Snail1 and Fibronectin were down-regulated both in the absence or presence of TGF-β1 (compare lanes 3-7 and 4-8 in Figure R.20).

We validated the importance of Akt2 isoform in GSK-3β regulation in Murine Embryonic Fibroblasts, using cells wild type or knock out for Akt1 (Akt1 -/-) or knock out for Akt2 (Akt2-/-). Cells were treated with TGF-β1 that rapidly increased Snail1.

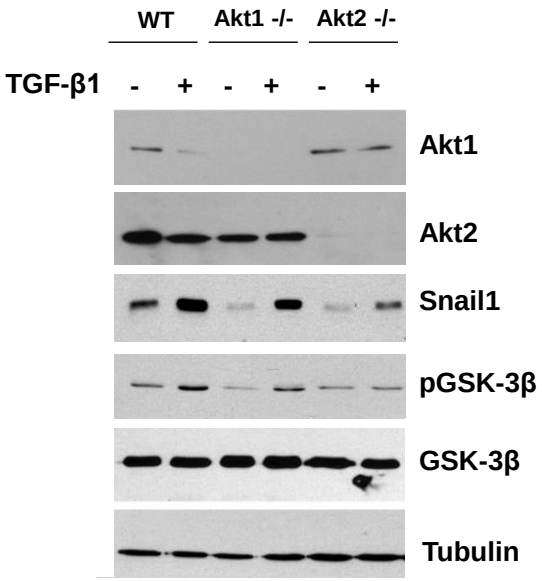

Figure R.21. Akt2 is necessary for the up-regulation of Snail1 upon TGF-β1 induction in MEFs cells. MEFs WT, Akt1-/- and Akt2-/- were treated for one hour with TGF-β1 (5ng/ml). Indicated proteins were analyzed by western blot. Tubulin was used as a loading control.

In MEFs-WT, TGF-β1 enhanced the levels of Snail1 concomitantly with an increase in pGSK-3β (figure R.21). Akt2 was required for this up-regulation since MEFs depleted in this isoform and not in Akt1 were severely affected in the response to TGF-β1; the stimulation by this cytokine of Snail1 protein and GSK-3β phosphorylation was reduced in these cells in contrast to control or Akt1-depleted MEFs (figure R.21). However, Snail1 and pGSK-3β basal levels are diminished in both Akt isoform depleted cells. Therefore, Akt2, and not Akt1, is involved in GSK-3β inactivation by TGF-β1 and Snail1 stabilization.

With all of these results, we suggest a Notch induced mechanism that up-regulates Akt2 and inactivates GSK-3β. This inactivation leads to Snail1 stabilization, necessary for a complete induction of mesenchymal genes such as Fibronectin.

R.6 Notch blocks apoptosis induced by oxidative stress

We have seen that Akt2 is important for EndMT and is required for a complete up-regulation of Snail1 and Fibronectin, necessaries for the acquisition of a complete mesenchymal phenotype. Once this transition is complete cells have some special characteristics such as resistance to apoptosis.

As it has been shown in our results, we suggest a specific role of Akt2 in the nucleus since it was up-regulated in this compartment. We wanted to investigate other Akt nuclear substrates, such as FoxO1. FoxO1 is member of the Forkhead family of transcriptional factors implicated in the induction of cell death [107].

FoxO1 protein was analyzed in our model of EndMT induced by Notch. Notch cells presented very low levels of FoxO1 protein (figure R.22.A) while mRNA was not modulated (figure R.22.B). Levels of phosphorylated FoxO1 slightly increased upon Notch induction. However, this modification is difficult to detect, because the rapid degradation of the protein after phosphorylation (Figure R.22.A) [107].

These preliminary results suggest that Notch down-regulation of FoxO1 may provide a mechanism that regulates cell death.

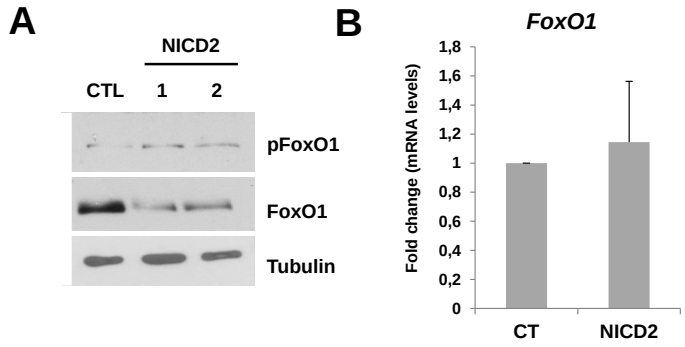

Figure R.22. Notch regulates FoxO1 protein levels. (A) Total and pFoxO1 were analyzed in PAE-CTL, PAE-NICD1 and in PAE-NICD2 by western blot. Tubulin was used as a loading control. (B) mRNA of PAE-CTL and PAE-NICD2 levels were also examined by RT-qPCR using specific primers. The graph shows the average ± SD of three independent experiments.

We decided to investigate the response of endothelial cells after an apoptotic stimulus and the role of Akt2 during this process. Oxydative stress triggered by hydrogen peroxide treatment is an apoptotic inductor in endothelial cells [119]. To first study this process in our cellular model we analyzed the signal of Annexin V which detect cells that have expressed phosphatidylserine (PS) on the cell surface, an event found in apoptosis. To measure Annexin V we used a fluorochrome conjugated Annexin V-APC as explained in M&M.

Cells were treated during 16 hours with H_2O_2 (200 µM). Annexin V-APC positive cells were detected by FACS analysis. Also, cells were treated with propidium iodide (PI) to distinguish necrotic cells from those that were in the early stages of apoptosis. In control cells, Annexin V-APC staining was up-regulated upon H_2O_2 (from 4.8% to 36.4%) whereas in Notch expressing cells the number of apoptotic

cells did not increase (from 4.5% to 7%) (Figure R.23), suggesting that Notch protects cells from apoptosis after oxidative stress.

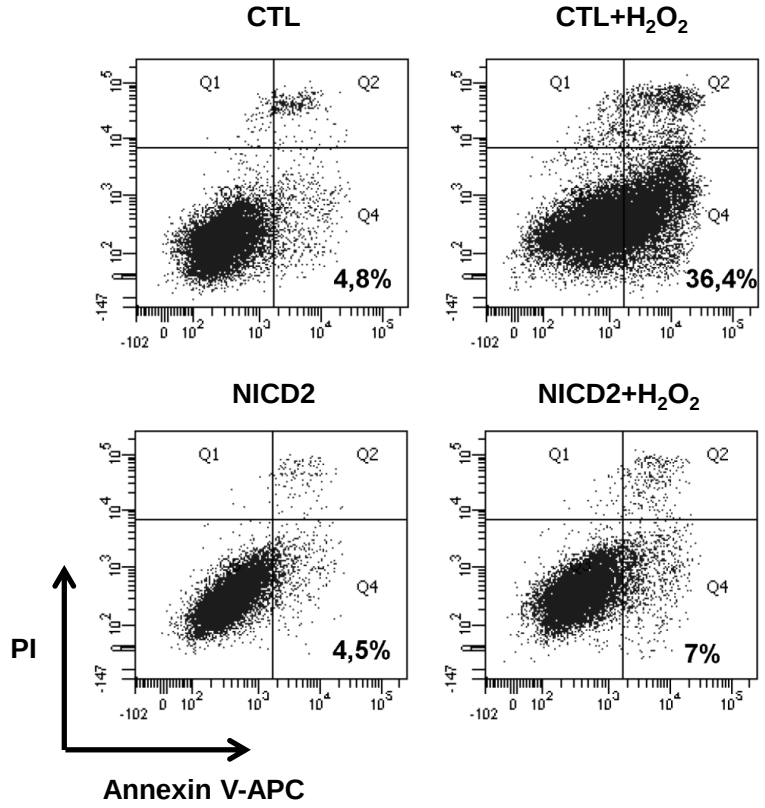

Figure R.23. Early stages of apoptosis were blocked upon H_2O_2 in Notch cells. Annexin V-APC staining was detected by FACS in PAE-CTL and PAE-NICD2 treated or untreated with H_2O_2 during 16 hours. Propidium iodide (PI) was used as a necrotic cell control.

Another marker of apoptosis is the determination of the active form of Caspase-3 (also called cleaved Caspase-3) which induces DNA fragmentation of DNA and cell death [119]. Levels of cleaved Caspase-3 were analyzed by western blot. As it is shown in figure

R.24.A, the expression of active Caspase-3 was up-regulated in control cells after 24 hours of treatment, contrary to Notch expressing cells, confirming the previous result. The expression of Akt2 and FoxO1 were not modulated by H_2O_2 treatment.

The experiment was done four times and quantified. The quantification shows significance stimulation by H_2O_2 in control cells but not in Notch cells after apoptosis induction (figure R.24.B).

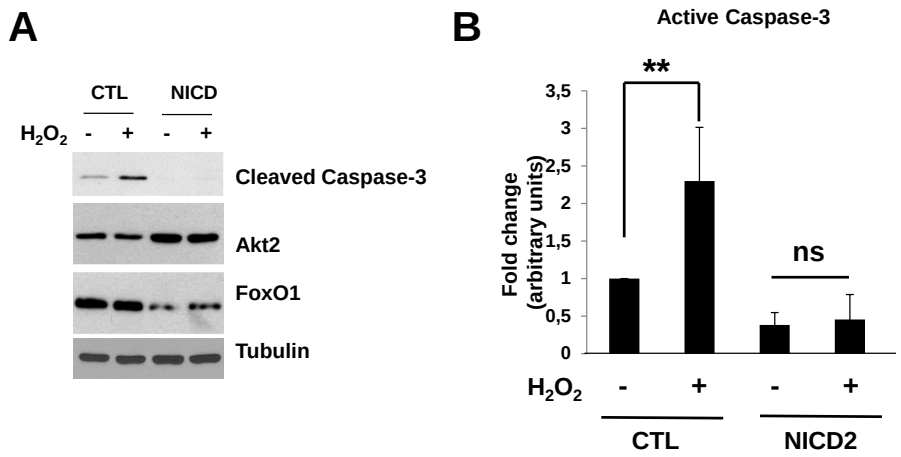

Figure R.24. Notch blocks oxidative stress apoptosis induced by H_2O_2. (A) Cleaved Caspase-3 was explored after 24 hours of H_2O_2 (200µM) treatment in control and in NICD expressing cells. (B) Densitometry analysis of Cleaved Caspase-3 normalized respect Tubulin. The graph shows the average (n=4) ± SD. P-values were calculated using unpaired, two-tailed student's t-test (** P<0.01; "ns" no significance).

These results indicate that Notch is impairing the induction of apoptosis, probably through the action of Akt2 in the nucleus.

R.7 Snail1 stability by Akt2 is necessary for apoptosis resistance induced by Notch

To elucidate the different role of Akt2 and Akt1 in apoptosis regulation, both kinases were depleted using specific shRNAs.

As shown in figure R.24.A levels of Caspase-3 were up-regulated in the presence of H_2O_2 in control cells whereas in Notch cells were not altered (compare lanes 2 and 4). The depletion of Akt2 in Notch expressing cells permitted the activation of the apoptotic pathway as shown by the increased in cleaved Caspase-3 (compare lanes 4 and 8). Snail1, as expected, was decreased in Akt2 depleted cells (figure R.25).

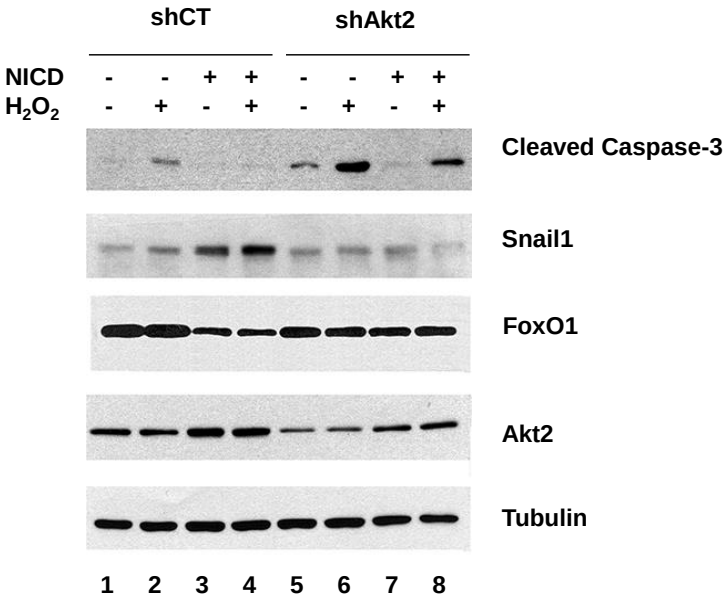

Figure R.25. Akt2 is essential for blocking apoptosis induced by H_2O_2. PAE-CTL and PAE-NICD2 were infected with shCT and shAkt2. They were treated with H_2O_2 (200µM) for 24 hours. Indicated proteins were analyzed by western blot. Tubulin was used as a control.

We also determined the levels of FoxO1 and, as previous results showed, Notch cells presented low levels of FoxO1. The down-regulation of Akt2 in control cells did not affect basal levels of FoxO1 (compare lanes 1-2 and 5-6); but partially recover the levels of the protein in Notch cells (compare lanes 3-4 and 7-8) (figure R.25).

The same experiment was performed using specific shRNA for Akt1, since did not affect Akt2 levels (figure R.15.A). Partial depletion of Akt1 did activate Caspase-3, not only in the presence of H_2O_2, but also without H_2O_2 in control cells (figure R.26; compare lanes 1-5 and 2-6). However, Akt1 depletion in Notch expressing cells was not sufficient to activate Caspase-3 (figure R.26; compare lanes 4 and 8).

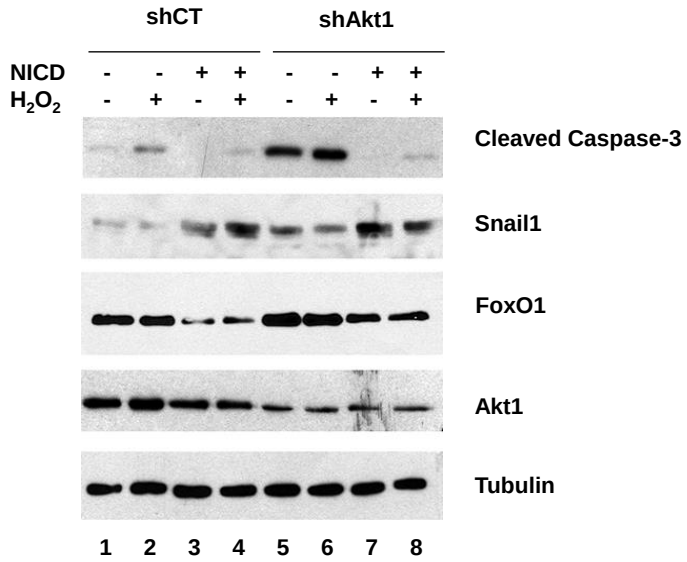

Figure R.26. Akt1 does not affect the anti-apoptotic effect of Notch. Infected PAE-CTL and PAE-NICD2 with shCT and ShAkt1 were treated with H_2O_2 (200μM) for 24 hours. Indicated proteins were analyzed by western blot. Tubulin was used as a control.

In contrast to Akt2, Akt1 depletion did not down-regulate the levels of Snail1 (figure R.26). Moreover, Akt1 attenuation increased basal levels of FoxO1 but only partially prevented its down-regulation by Notch (figure R.26). These results suggested that Akt2 induces resistance to apoptosis in response to H_2O_2.

We also wanted to investigate the role of Snail1 mediating apoptosis protection during this oxidative stress model in endothelial cells.

Therefore, we silenced Snail1 expression using specific siRNA. SiRNA were transfected for 72 hours, and 24 hours before lysis, cells were treated with H_2O_2 (200µM). As shown in figure R.27, Snail1 was completely depleted. Interestingly, Snail1 depletion permitted the up-regulation of active Caspase-3 after the oxidative stress stimuli (figure R.28; compare lanes 4 and 8). As expected, the down-regulation of Snail1 did not modulate Akt2 levels (figure R.27).

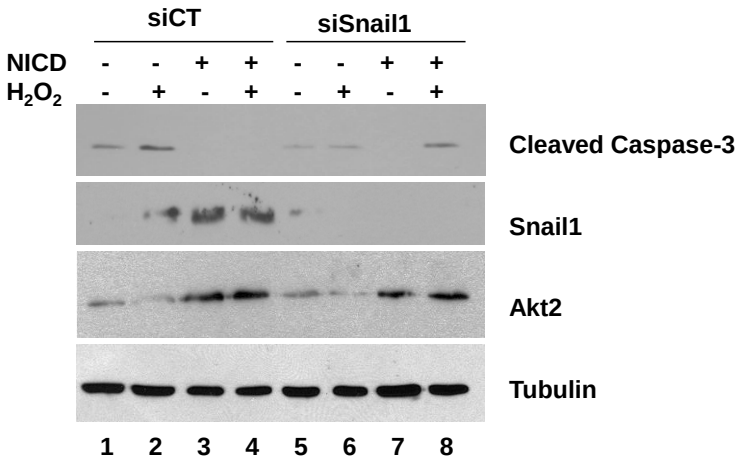

Figure R.27. Notch stabilizes Snail1 to inhibit apoptosis. PAE-CTL and PAE-NICD2 cells were transfected with siSNAIL1 and siCT RNA for 72 hours. 48 hours post-transfection cells were treated with H_2O_2 (200µM) for 24 hours. Active Caspase-3, Akt2, Snail1 were checked and tubulin was used as a control.

To confirm that this up-regulation of active Caspase-3 was translated into cell death, we performed an MTT assay to analyze cells viability after treatment. MTT signal was measured at 24 and 32 h after H_2O_2 treatment in PAE-CTL and in PAE-NICD2. At 24h cell death triggered by H_2O_2 is still not evident, but as shown in figure R.28.A, at 32 hours only 40% of control cells remained alive in comparison to the 80% in Notch cells. The same experiment was done in stably Akt2 depleted cells. Consistent with active Caspase-3 expression, Akt2 depletion in Notch cells conferred sensitivity to H_2O_2-induced apoptosis (figure R.28.B).

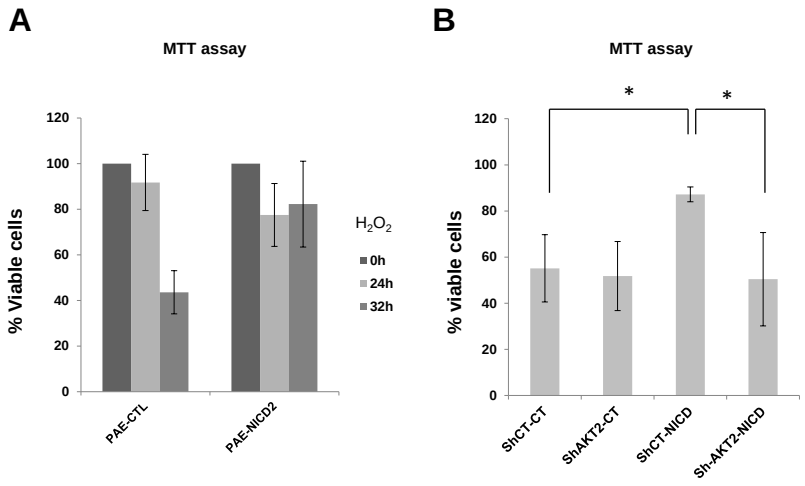

Figure R.28. Cell viability decreases upon H_2O_2 treatment in Akt2 deficient cells. (A) PAE-CTL and PAE-NICD2 cells were treated with H_2O_2 (200μM) for 24 and 32 hours and the reaction of MTT reduction to Formazan was measured at 590nm. The absorbance was quantified and represented as percentage of live cells respect to each cell line. (B) Similarly to figure A, cell viability was analyzed in PAE-CTL and PAE-NICD2 both stably infected with shCT and shAkt2. Cells were treated in the same conditions for 32 hours. The graph shows the average (n=3) ± SD. P-values were calculated using unpaired, two-tailed student's t-test (* P<0.05).

With all of this data, we know that Akt2 is essential for Snail1 stability during EndMT induced by Notch and for the resistance of apoptosis after oxidative stress.

To further investigate the role of Snail1, we performed an experiment where Snail1 was re-introduced in Akt2 depleted cells. To do that, we first infected PAE-CTL and PAE-NICD2 cells with shCT or shAkt2. After 72 hours of selection, cells were re-infected with pBabe-Snail1-HA or empty vector. As expected, Snail1-HA levels were lower in Akt2 depleted cells (compare lanes 3-4 with 9-10) (Figure R.29).

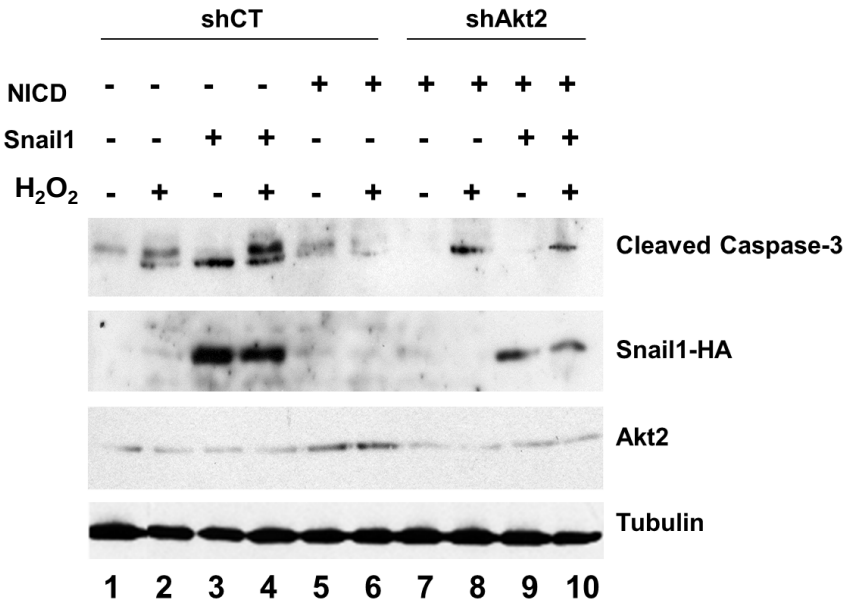

Figure R.29. Snail1 induces apoptosis resistance upon H_2O_2 induction. PAE-CTL and PAE-NICD2 cells were stably transfected with shCT and shAkt2, then selected with puromycin for 72 hours. After selection, cells were infected with pBABE-Snail1-HA or empty vector. Stable cell lines were treated with H_2O_2 for 24 hours and total extracts were analyzed by western blot. Indicated proteins were checked and Tubulin was used as a control

As previous results indicated, cells that express Notch showed high levels of Akt2 and no modulation of active caspase-3 (compare lanes 2 with 6 in figure R.29). Consistent with the previous data, down-regulation of Akt2 in these cells increased cleaved Caspase-3 by H_2O_2 (compare lanes 6 and 8 in figure R.29). Interestingly, when we re-introduced Snail1 in Notch-expressing, Akt2 deficient cells and treated them with H_2O_2 cleaved Caspase-3 was partially down-regulated (compare lane 8 and lane 10 in figure R.29).

Considering these results, we conclude that Akt2 and Snail1 mediate the protection against apoptosis induced by Notch.

R.8 Akt2 and Akt1 are different localized in the nucleus

To better understand the different role of Akt1 and Akt2 in the nucleus, we investigated their localization in this compartment by immunofluorescence. To amplify the nuclear signal we treated cells with CSK buffer [112], as indicated in Materials and Methods, to reduce cytoplasmic signal. With these conditions the expression of Akt1 was mainly detected in the nucleoplasm of PAE-CTL cells although it decreased when Notch was present (figure R.30; upper panel). By contrast, Akt2 was barely detected in control cells and was enhanced upon Notch expression (figure R.30).

Interestingly, nuclear Akt2 staining was concentrated around the nucleus, in the nuclear envelope, as shown by co-staining with Lamin B1 (Figure R.30; lower panel).

Taking these results in account, Akt2 seems to localize in the nucleus in a different sub-compartment comparing with Akt1 signal. Thus, the different nuclear role of Akt1 and Akt2 might depend on its different nuclear localization.

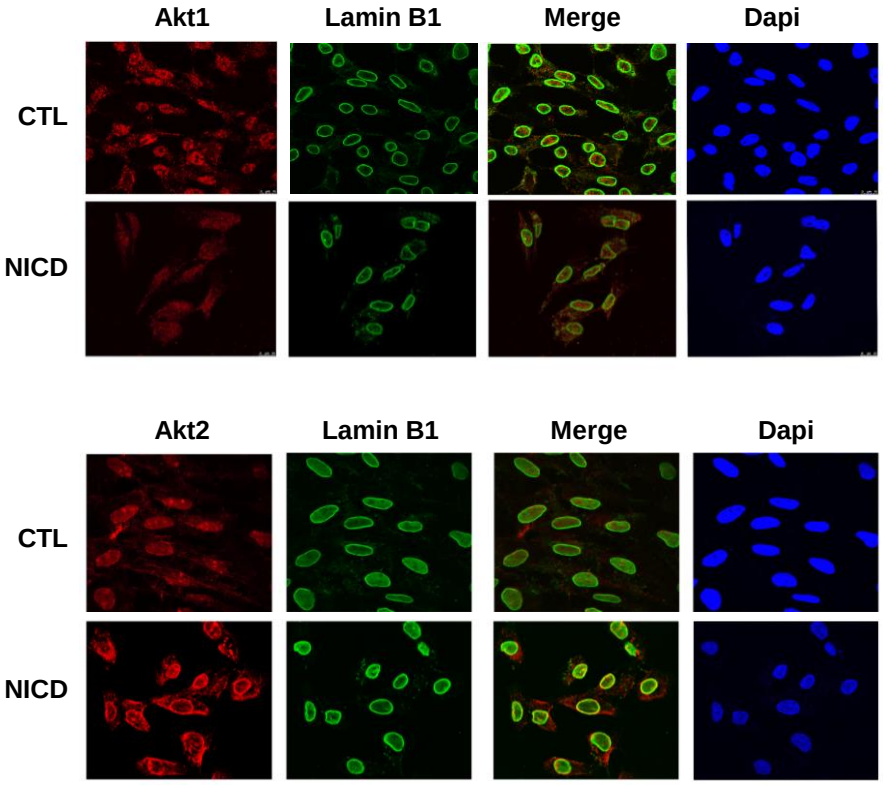

Figure R.30. Different nuclear localization of Akt1 and Akt2. Nuclear immunofluorescence staining using CSK protocol in PAE-CTL and PAE-NICD2. Co-staining of Akt1 or Akt2 (red) and Lamin B (green). Dapi was used for nuclear staining.

To have a better confocal quantification analysis of Akt2 and Lamin B1, we analyzed the fluorescence intensity in nuclear sections. Results shown in figure R.31 revealed that Akt2 was accumulated in the nuclear membrane upon NICD expression (figure R.31.B) and the signal decreased in the nucleoplasm. In contrast, in control cells, the little amount of nuclear Akt2 was mostly localized in the nucleoplasm (figure R.31.A).

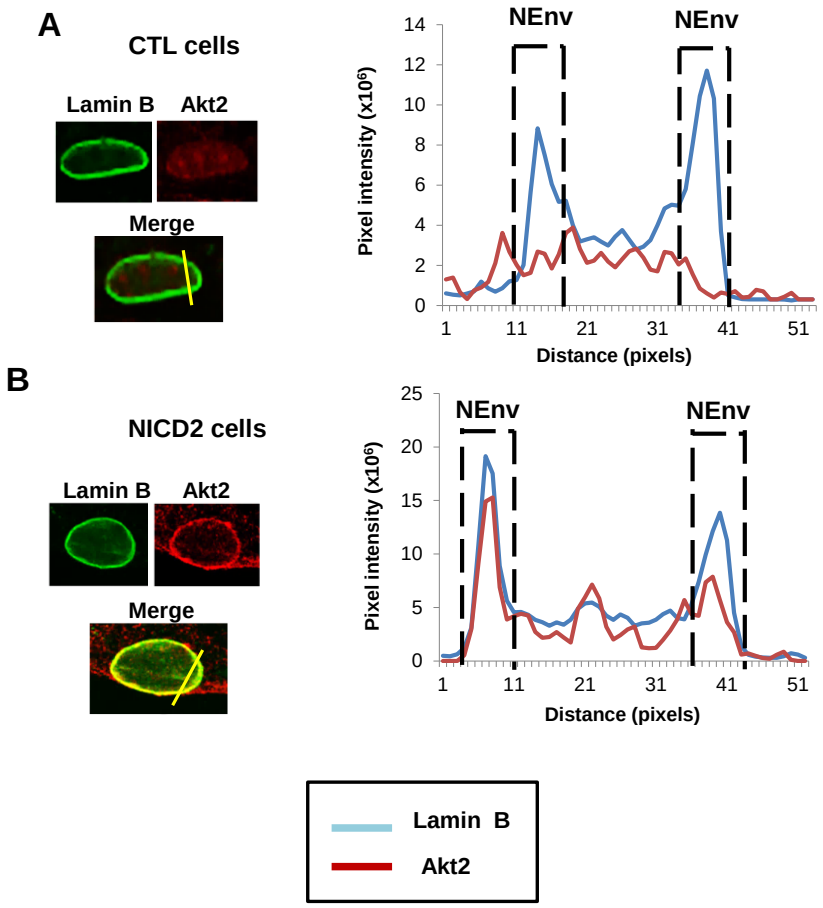

Figure R.31. Akt2 co-localizes with Lamin B in Notch expressing cells. (A-B) Representative graphs (right) showing the different line profile of the co-localization of Akt2 and Lamin B1 (left panel) in both PAE-CTL (A) and PAE-NICD2 (B). Each line profile represents the intensity of the signal versus pixel distance across an arbitrary line (yellow line, see photograph in the left panel). Blue line is Lamin B1 and red line is Akt2. The dashed line area represents the nuclear envelope fraction (Nenv).

The same analysis was done for Akt1 localization. Although Akt1 was present in the nucleus in control cells, it did not co-localize with the nuclear envelope component, Lamin B (figure R.32.A). As expected, in

Notch expressing cells, Akt1 was much less expressed in comparison with control cells (figure R.32.B).

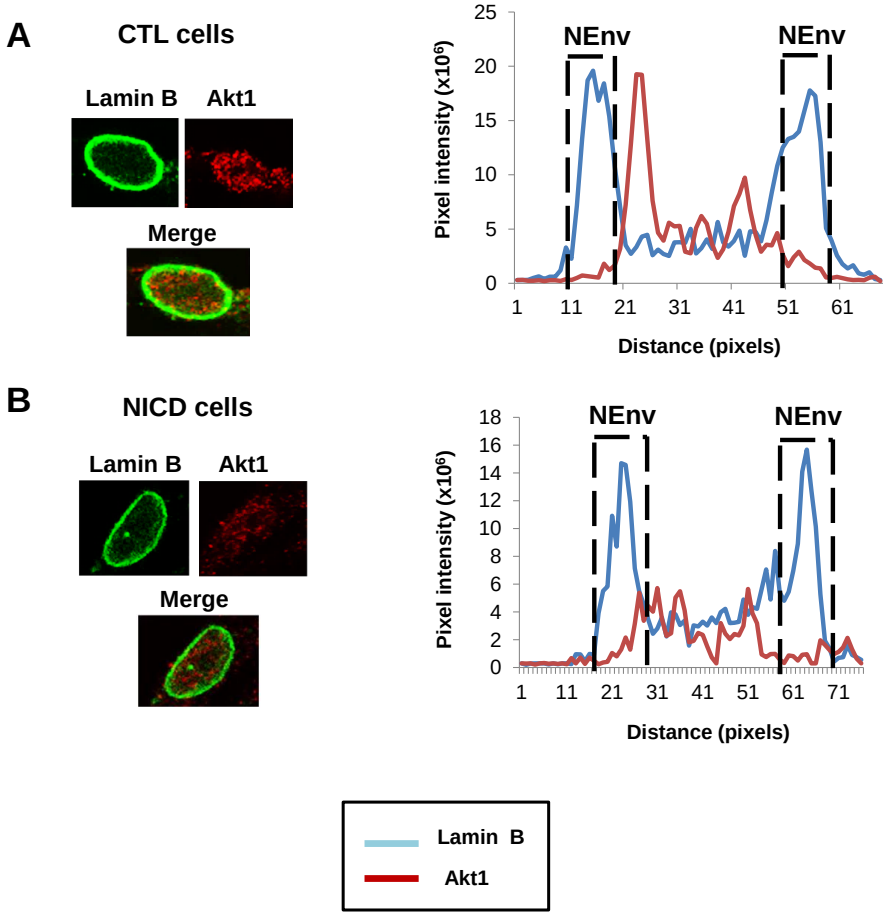

Figure R.32. Akt1 is not localized with Lamin B1 in both cell lines. (A-B) Representative graphs (right) showing the different line profile of the co-localization of Akt1 and Lamin B1 (left panel) in both PAE-CTL (A) and PAE-NICD2 (B). Each line profile represents the intensity of the signal versus pixel distance across an arbitrary line (yellow line, see photograph in the left panel). Blue line is Lamin B and red line is Akt1. The dashed line area represents the nuclear envelope fraction (Nenv).

In order to quantify the relative amount of each Akt isoform in both conditions, we measured the relative intensity of Akt1 and Akt2 present in the nuclear envelope. The relative value was quantified as nuclear envelope Akt versus total nuclear Akt. As it is shown in figure R.33, around 60% of Akt2 present in Notch cells is localized in the nuclear envelope compartment contrary to control cells. On the other hand Akt1 was mostly present in the nucleoplasm (around 80%), independently of its expression level (figure R.33).

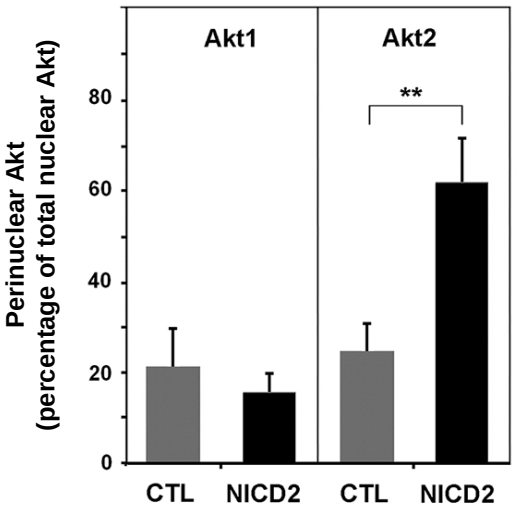

Figure R.33. Akt2 is mostly present in the nuclear envelope. Quantification of different immunofluorescences of Akt1 and Akt2 in the nuclear envelope (NEnv) compartment. At least 10 cells were analyzed of three independent experiments; perinuclear compartment were delineated by the Lamin B1 signal. Immunofluorescence co-localization and quantification were done by ImageJ software. The graph shows the average (n≥10) ± SD. P-values were calculated using unpaired, two-tailed student's t-test (** P<0.01)

To confirm the different nuclear localization of Akt2 and Akt1 in the nuclear envelope, specific nuclear sub-fractionation experiments were carried out. To do that, we isolated the nuclear fraction from PAE-CTL and PAE-NICD2. This fraction was purified and treated with DNase I in order to separate chromatin bound to nuclear envelope and their associated proteins, as indicated in M&M. Finally, the nuclear envelope was analyzed by western blot. The analysis showed a clear up-regulation of Akt2 by Notch in the nuclease resistant fraction that corresponded to the nuclear membrane. As expected, Akt2 was also detected in the nuclear digested fraction that corresponded with nucleoplasmic and chromatin associated Akt2 (figure R.34.A).

We also used a commercial kit for nuclear envelope isolation, which does not use digestion with DNase I. This specific sub-cellular fractionation revealed that Akt2, and not Akt1, co-purified with proteins only present in the nuclear membrane such as Lamin B1 and when Notch is induced (figure R.34.B). A significant part of pGSK-3β was also detected in this fraction. However, we did not detect Snail1 in the nuclear envelope, suggesting that it was a nucleoplasm substrate of GSK-3β (figure R.34.B).

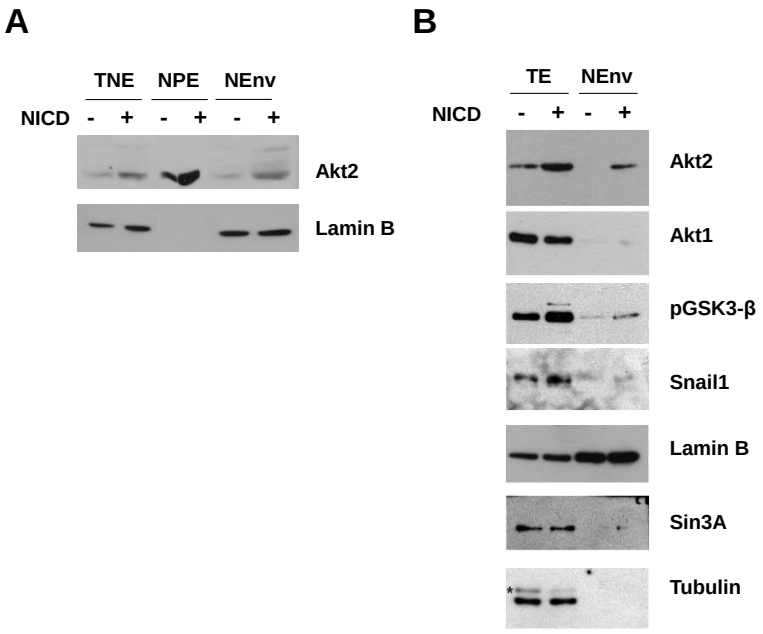

Figure R.34. Akt2 is co-purified with the nuclear envelope. (A) Akt2 levels of total nuclear, nucleoplasmic and nuclear envelope extracts (TE, NPE, NEnv, respectively) were analyzed by western blot. Lamin B1 was used as a Nuclear envelope control. (B) Total extracts and Nuclear membrane purification was done in control and in Notch cells. Indicated proteins were checked by western blot. Lamin B1 was used as a nuclear membrane control; Sin3A was used as a control for possible contaminations of chromatin in the nuclear envelope and Tubulin as a nuclear negative control.

Finally, in order to determine whether Akt2 activation was required to promote localization in the nuclear membrane, NICD cells were treated with the Akt inhibitor MK-2206. This inhibitor that completely blocks phosphorylation of Akt levels, as shown in previous experiments (figure R.13), also impairs Akt2 localization in the nuclear membrane as determined by immunofluorescence (figure R.35). On the contrary, treatment with the Erk inhibitor UO126 did not impair membrane localization (Figure R.35).

Notch expressing cells were also treated with a competitive Akt inhibitor CCT128930, which did not block phosphorylation. In fact, this inhibitor at low concentration, only inhibits the function of Akt2 [120]. As it is shown in figure R.35, Notch cells treated with the selective Akt2 competitive inhibitor did not affect Akt2 signal in the nuclear membrane.

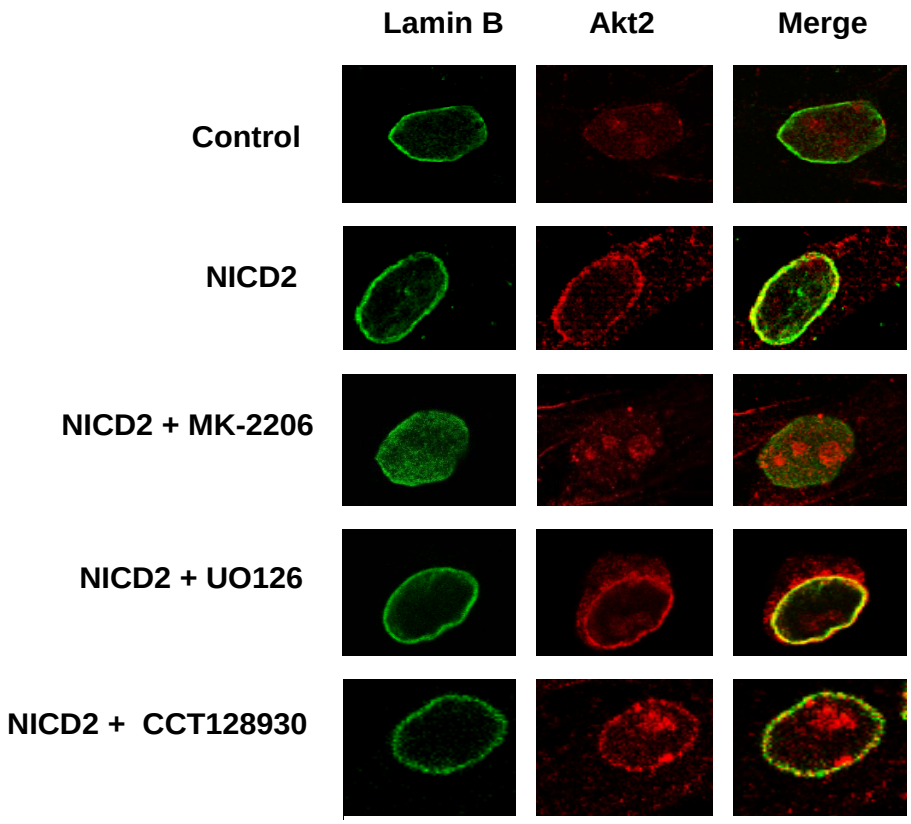

Figure R.35. The activation of Akt2 is necessary for its nuclear membrane localization. Akt2 and Lamin B were analysed in control cells (PAE-CTL), and also in non-treated Notch cells (PAE-NICD2) or treated with MK-2206 (10μM), UO-126 (10μM) or CCT-128930 (10μM) for 24 hours. To amplify nuclear staining cells were treated with CSK buffer. Merge indicates the co-localization. It's a representative single cell immunofluorescence. The analysis was done by confocal microscope.

This result suggests that Akt phosphorylation is required for nuclear transport. We also assessed which Akt2 domain was responsible for its nuclear localization. For this, we transfected different Akt2 mutants: Akt2 lacking the kinase domain (Akt2-ΔPK), without the pleckstrin domain (Akt2-ΔPH), only the plecktrin domain (Akt2-PH) or without the regulatory AGC-kinase C-terminal (Akt2-ΔAGC) to HEK-293T cells. All mutants were tagged with HA.

We sub-fractionated and analyzed the levels of both cytoplasmic and nuclear compartment by western blot. As shown in figure R.36 all mutants were present in both compartments, except Akt2-ΔPH which was completely nuclear. Therefore this domain was restricting Akt2 traffic to the nucleus.

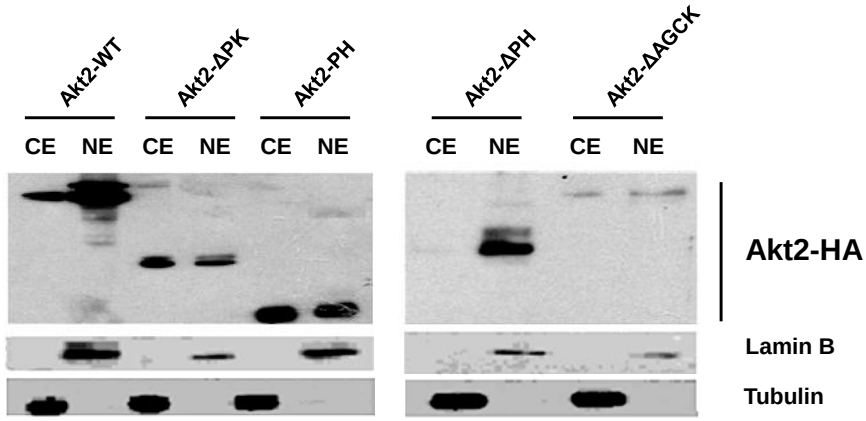

Figure R.36. Akt2 Pleckstrin domain is necessary for cytoplasmic retention. HEK-293T cells were transfected for 24 hours with different Akt2 mutants are: Akt2-WT; Akt2-ΔPK, deleted kinase domain; Akt2-PH, pleckstrin domain alone; Akt2-ΔPH, pleckstrin domain depletion; Akt2-ΔAGCK, which has mutated the regulatory domain. Cells were sub-fractionated and analyzed by western blot. Anti-HA tag was used to detect all transfected Akt2 mutants. Lamin B and Tubulin were used as a nuclear and cytoplasmic control, respectively.

Interestingly, as mentioned in the introduction, the pleckstrin domain is necessary for the kinase activation in the cytoplasmic membrane.

Altogether, these results suggest that active Akt2 is localized in the nuclear membrane of NICD cells, what might facilitate interaction and phosphorylation of nuclear substrates, such as GSK-3β or FoxO1, resulting in a Snail1 stabilization and protection against apoptosis to endothelial cells.

Discussion

In this thesis we have demonstrated that the expression of activated Notch in endothelial cells induces phenotypical changes of EndMT with a concomitant switch in gene expression characterized by the up-regulation of Snail1, Snail2, Fibronectin, α-SMA, N-Cadherin; and the down-regulation of the main endothelial marker VE-Cadherin. In addition, Notch cooperates with TGF-β in the acquisition of a complete mesenchymal phenotype by the hyper-induction of Fibronectin, Lef-1 and Snail1. Notch promotes the activation of β-catenin, the up-regulation of Akt2 with the subsequent inactivation of GSK-3β and nuclear accumulation and stabilization of Snail1 transcriptional factor. Furthermore, Notch expression promotes resistance to oxidative stress. We have seen that this protection requires both Akt2 and Snail1, but not Akt1. Moreover, Notch produces a switch in the expression of Akt1 and Akt2 isoforms and Akt2, in contrast to Akt1, is associated to the nuclear membrane when present in the nucleus.

D.1 Notch induces EndMT by down-regulating VE-Cadherin and cooperates with TGF-β in the activation of mesenchymal genes.

In this thesis we have used cells stably transfected with the activated form of Notch (NICD). We have demonstrated that this is a good model to study the EndMT since Notch induces an EMT, the down-regulation of the main endothelial gene VE-Cadherin and an increase of mesenchymal markers such as Snail1, Snail2, N-Cadherin, α-SMA and Fibronectin, at protein level (figure R.1).

The role of Snail1 in VE-Cadherin repression has been already investigated by other groups [18]. We have confirmed that Notch transcriptionally activates Snail1 and represses VE-Cadherin. However, after we silenced Snail1 we only observed a partial VE-Cadherin recovery in Notch expressing cells (figure R.2). This suggests that other induced repressors (such as Snail2, Twist, or Zeb) might be responsible for VE-Cadherin down-regulation. Accordingly, all Snail1, Snail2 and Twist transcriptional factors bind to VE-Cadherin E-boxes and repress its transcription [52]. Importantly, all these transcriptional factors are up-regulated by Notch [18][121][122]. In vivo, during the EndMT process required for cardiac cellularization, both Snail1 and Snail2 are needed for the completion of the process. However, Snail2 is first expressed at E9.5 concomitant to VE-Cadherin repression whereas Snail1 is expressed later at E10.5 [121]. This result suggests a more relevant role of Snail2 in the repression of VE-Cadherin.

We have also investigated if Notch expression is sufficient for the acquisition of a complete mesenchymal phenotype. Our experiments using TGF-β1 suggest that this cytokine cooperates with Notch to complete the induction of mesenchymal genes such as Snail1, Fibronectin and Lef-1 (figure R.3 and R.4). However, this cooperation

and the super-activation of Snail1 do not affect VE-cadherin. This was clearly observed in cells expressing moderate levels of Notch (NICD1) where TGF-β1 does not further down-regulate VE-cadherin (see figure R.3). Therefore, we conclude that Notch expression is sufficient to repress VE-Cadherin but not to promote a complete EndMT; cooperation with TGF-β in the expression of Snail1 is required for the up-regulation of Fibronectin and the acquisition of a full EndMT. The importance of both pathways, Notch and TGF-β, has been demonstrated during embryogenesis, tumor development and cardiac valve formation. A further element of cross-talk is provided by the fact that alterations in Notch affect TGF-β signaling components such as Snail1 in the AVC myocardium [18]). In addition, RBPJ mutants reduced the expression of TGF-β receptors in the endocardium impairing its signaling [123].

One important result was the observation that TGF-β1 induces Snail1 mRNA (Figure R.3) but not protein. This is surprising especially considering epithelial to mesenchymal models in which TGF-β1 is a potent Snail1 inducer [55]. Thus, in endothelial cells the cooperation between Notch and TGF-β1 is required for the up-regulation of Snail1 and the full activation of Fibronectin and Lef-1. This is in agreement with the role of Snail1 as a direct transcriptional activator of mesenchymal genes such as Fibronectin, Lef-1 or MMP-9 [75][74][73].

D.2 Notch stabilizes Snail1 inactivating GSK-3β

As mentioned in the introduction, Snail1 is a very unstable protein, and its half-life is regulated by different mechanisms. Snail1 degradation is slower when Notch is expressed (figures R.5 and R.6). These results were in agreement with a decreased Snail1 ubiquitination in Notch-expressing cells (figure R.7). Furthermore, we observed that β-TrCP1 did not degrade Snail1 in the presence of Notch (figure R.8). With all these results, we propose a mechanism by which Notch inactivates GSK-3β, blocking β-TrCP1-mediated Snail1 degradation.

Other kinases that control Snail1 stability mainly promoting its retention in the nucleus by phosphorylation, such as Lats-2, PAK-1, ATM and Erk2 [81][124][83]. It is likely that these phosphorylations create in Snail1 new docking sites for nuclear proteins precluding nuclear export and preventing the action of β-TrCP1 and other cytoplasmic Snail1 ubiquitin ligases [84]. For instance, the HSP90 chaperone interacts with Snail1 phosphorylated on S100 by the ATM kinase, stabilizing it [125]. Although our results suggest a predominant control on GSK-3β, we cannot discard an additional effect on Snail1 stability by Erk2 that is also activated by Notch [83]. We have not analyzed the role of other kinases, for instance, Lats-2 that is activated by TGF-β and stabilizes Snail1 in other cell systems [81]. However, it is unlikely that Lats-2 is relevant in our model since TGF-β1 does not up-regulate Snail1 stability in the absence of Notch.

A role for Notch stabilizing Snail1 protein has also been observed in hypoxia cell models through LOX activation [126]. However, a role for LOX on Snail1 stabilization has not been verified although a LOX analogue, LOXL2, attenuates GSK-3β dependent Snail1 degradation [66][127]. These authors suggest that it causes a conformational

change of Snail1 preventing the interaction with GSK-3β and increasing its stability [127].

Snail1 stability is also induced by de-phosphorylation by the small C-terminal domain phosphatase [128] or by Axin2 expression, since this chaperone promotes GSK-3β nuclear export [129]. We have discarded the effect of Axin2 because in cellular sub-fractionation experiments we have never observed a decrease in nuclear GSK-3β (figure R.12). Other results not shown in this thesis also demonstrated that Axin2 is not modulated by Notch. Finally, supporting our conclusions, BMP2 treatment of endothelial cells (BAEC) augments Snail1 mRNA in an NF-κB–dependent manner and stabilizes Snail1 protein by GSK-3β phosphorylation [130]. However, the authors do not clarify how GSK-3β is inactivated.

D.3 Notch up-regulates Akt2 inducing TCF-4/β-catenin activity

GSK-3β inactivation upon Notch expression occurs in parallel with an up-regulation of Akt2. Akt2 is a target gene of MyoD, Twist and TCF-4/β-catenin [115][116][131]. In our model Akt2 transcription is dependent on TCF-4 and β-catenin (figure R.18 and R.19), since the inhibition of the interaction using iCRT14 prevents the increase of Akt2 mRNA. It has been published that Akt1 down-modulation induces EMT and Akt2 up-regulation in mammary epithelial cells by a mechanism that requires Erk activation [93]. In our model, Notch decreases Akt1 and activates Erk, but the stable down-regulation of Akt1 does not increase Akt2. Furthermore, the inhibition of Erk-1/2 does not have an impact in Akt2 up-regulation by Notch. Therefore, in endothelial cells or MEFs the expression of Akt2 does not seem to be a consequence of the down-regulation of Akt1.

In addition to the up-regulation of Akt2 by Notch, our results show a decrease of Akt1 mRNA and protein. The mechanism underlying the down-regulation of Akt1 is not known. It is possible that as reported in other systems it might be dependent on Runx3 since this factor decreases Akt1 transcription by direct binding to this promoter [132] Moreover, Runx3 transcriptional factor is activated by Notch in other models [133]. This point is currently under investigation in our lab.

Notch and Wnt/β-catenin work together during EndMT in many cell types and different cellular contexts during development. For instance, in Drosophila and in vertebrate cells Notch induces transcriptional activation of β-catenin [134]. Furthermore, in colorectal cancer cells the activation of Notch stimulates TCF-4/β-catenin activity. However, the precise details of this mechanism are still unknown [135]. It has also been shown that Notch is downstream of Wnt signaling pathway in

colorectal cancer cells through β-catenin-mediated transcriptional activation of the Notch-ligand Jagged1 [136]. It is possible that Notch signaling modulates the Wnt pathway by affecting the capacity of TCF-4/β-catenin to bind to the promoter of target genes or to efficiently mediate transcription once it is bound. Actually, the interplay between both pathways is very tight and it has been proposed that both configure a unique signaling module [137]. Anyway, our results indicate that Notch modulates β-catenin to up-regulate Akt2.

D.4 Activated Akt2 but not Akt1 is localized in the nuclear envelope

The specific mechanism that links Akt2 and not Akt1 with EndMT is not known. The balance between Akt isoforms might be relevant for driving a differential phosphorylation of nuclear specific substrates [138][139]; thus, it might promote the regulation of specific Akt2 nuclear targets [140]. Akt2 is located both in the cytoplasm and the nucleus and the localization in this compartment requires the previous activation by phosphorylation (figure R.35), suggesting that these modifications release Akt2 from the interaction with some cytosolic chaperone that precludes its traffic to the nucleus. One important observation was the importance of the PH domain of Akt2 since depletion of this domain induces a complete nuclear localization (figure R.36). Probably PH domain is necessary for cytoplasmic membrane retention. Surprisingly, another observation was the specific localization of Akt2 at the nuclear membrane in Notch expressing cells, as observed by immunofluorescence since it co-stains with one of the major component of the nuclear envelope, Lamin B1 (see figure R.30 and R.31).This co-localization was never observed for Akt1.

Once Notch is expressed and Akt2 is in the nucleus, it is likely that an adaptor protein specific for Akt2 is expressed or exposed in the nuclear envelope upon Notch expression and is responsible for the specific binding. Also, it is possible that during EndMT the nuclear envelope changes its morphology [141], allowing the binding of the most abundant Akt isoform present in these cells that is Akt2. It has been described that PKA (cAMP-dependent protein kinase) is anchored to the nuclear lamina through the action of AKAPs (A-kinase anchoring proteins) giving specificity in signal transduction [142]. A similar nuclear scaffold proteins might also act on Akt2 facilitating its

action on GSK-3β and promoting the inactivation of this kinase and the subsequent stabilization of Snail1.

Other kinases have been localized to the nuclear envelope. Activated Erk-1/2 has been observed in the nuclear envelope in certain conditions. Upon mitogen stimulation, active Erk-1/2 binds to Lamin A/C and phosphorylates c-Fos, causing its release from the nuclear membrane. Hyper-phosphorylated c-Fos can then heterodimerize with AP-1 family members such as c-Jun, thus allowing the transcriptional activation of AP-1–responsive genes before de novo c-Fos synthesis [143].

We still do not know if the interaction of Akt2 with Lamin B or Lamin A/C is direct or it needs other proteins. Pull-down experiments that are not shown in this thesis indicate that Akt2 and Lamin A/C do not directly interact. Similarly, we have also not observed interaction between Akt2 and Lamin B by co-immunoprecipitation. Therefore, our hypothesis is that Akt2 anchoring to nuclear envelope requires additional molecules.

In summary, our results suggest that this specific localization in the nuclear envelope of Akt2 and not Akt1 is responsible for the distinct role between both isoforms. It is still a matter to study how Akt2 in Notch-expressing cells, and not Akt1 in not-treated cells, co-localizes with Lamins.

D.5 Notch blocks apoptosis through Akt2/Snail1 axis

Besides the role of Notch as EndMT inducer, we have studied its protective role upon oxidative stress. This effect has been previously reported for other apoptotic insults. For instance, constitutively active Notch4 inhibits endothelial cell apoptosis induced by lipopolysaccharide by a dual mechanism that requires JNK activation and Bcl-2 up-regulation [144]. On the contrary, impaired Notch4 activity is associated with endothelial cell apoptosis [145]. The molecular basis of apoptosis protection by Notch is not fully understood and may involve multiple players.

As a model of apoptosis we have used the addition of hydrogen peroxide mimicking the oxidative stress that occurs during atherosclerosis and hypertension. For example, high pressure-exposed arteries elicited substantial increases in vascular H_2O_2 generation [146]. In this context, we have demonstrated that Akt2 but not Akt1 is required for apoptosis-resistance triggered by Notch (figure R.25 and R.26). Furthermore, Snail1 stabilized by Akt2 was required to block cell death (figure R.27).

According with our results, it has been recently shown that aortas from Akt2-deficient mice displayed high apoptotic cell death that results in increased aortic aneurysm [147]. This Akt2-dependent protection is caused by elevated expression of matrix metalloproteinase-9 (MMP-9) and reduced expression of tissue inhibitor of metalloproteinase-1 (TIMP-1) due to decrease binding of FoxO1 to MMP-9 and TIMP-1 promoters [147]. We have not studied the expression of these downstream effectors, but our results also show a clear down-regulation of FoxO1.

The pro-apoptotic protein FoxO1is exported from the nucleus to the cytoplasm and degraded, after the phosphorylation of Akt [107]. As indicated above, FoxO1 protein is decreased upon Notch expression, and this shows a higher sensitivity to Akt2 than Akt1 down-modulation (figure R.25 and R.26). We suggest that in addition to GSK-3β inactivation, Akt2 localized in the nuclear lamina shows a greater activity on FoxO1. According with this, recent results indicate that forced nuclear localization of Akt in cardiac cells inhibits apoptosis [148] but whether this Akt is present in the nuclear lamina is still unclear. More experiments should be performed to better demonstrate this hypothesis.

Besides the FoxO1 down-modulation, Akt2 inactivates GSK-β3, which in turn induces Snail1 nuclear retention. The role of Snail family members protecting apoptosis is very well known. In particular, our group has shown that Snail1 down-regulates PTEN protecting from apoptosis [149]. Moreover, Snail1 also represses other genes related to this resistance such as p53, Bid or DFF40 [150]. Snail1 has also been reported to induce activation of Akt and Erk that confer resistance to apoptosis through up-regulation of Bcl-x_L, a member of Bcl-2 family of proteins that blocks stress-induced cell death [151]. In accordance, our group has also demonstrated that Snail1 interacts and increases Akt2 activity [112].

The Akt pathway may have other protective roles that have not been investigated in this thesis. For example, we cannot discard that the Akt might phosphorylate Caspase-9 inhibiting its pro-apoptotic activity [152]. Alternatively, other Akt nuclear targets regulating apoptosis, such as XIAP or B23/NPM, could have a role in our system [140][153][154]. In any case, our results explain how Snail1 is controlled by Notch in the regulation of EndMT and apoptosis.

D.6 Working model on Notch regulation of Snail1 and EndMT

To summarize this thesis we propose a model during EndMT induced by Notch:

1) In the absence of Notch, the induction of TGF-β1 stimulates Snail1 mRNA. However, this up-regulation of Snail1 mRNA is not able to induce EndMT. In addition, we hypothesize that β-catenin is degraded in the cytoplasm and cannot travel and interact with TCF-4 in the nucleus in these conditions.

2) Once Notch is activated, β-catenin is translocated to the nucleus and interacts with TCF-4. This interaction promotes the transcriptional activation of Akt2 isoform. On the other hand, Notch cooperates with TGF-β also on Snail1 transcription.

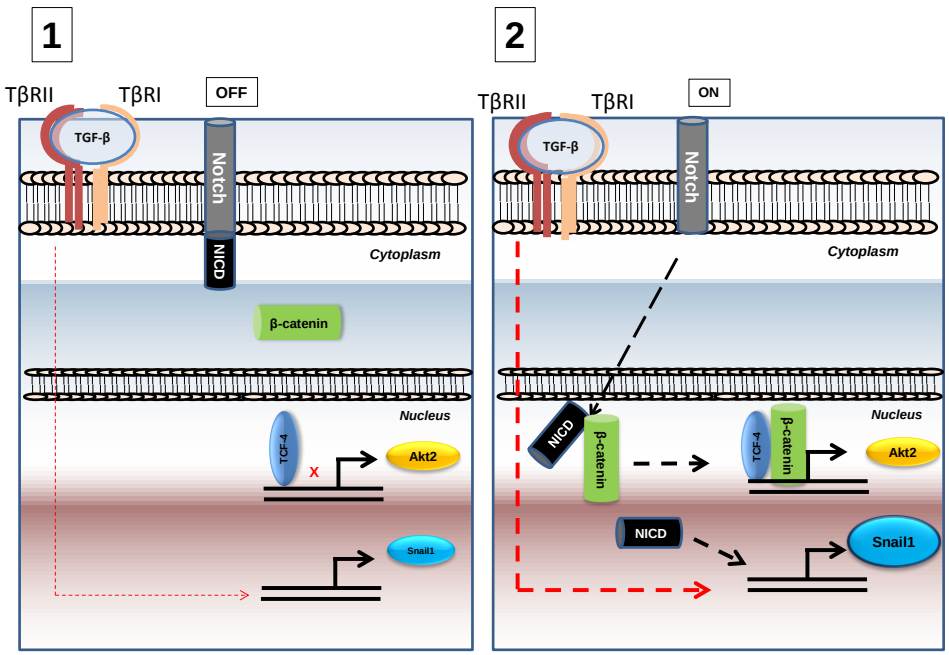

3) In control endothelial cells, Akt1 is nuclear but not present in the nuclear lamina and nuclear FoxO1 and GSK-3β substrates are not phosphorylated.

4) When Notch is expressed, Akt2 is induced, translocated to the nucleus and present in the nuclear envelope. This specific localization of Akt2 promotes the phosphorylation of FoxO1 and GSK-3β in the nucleus.

3 4

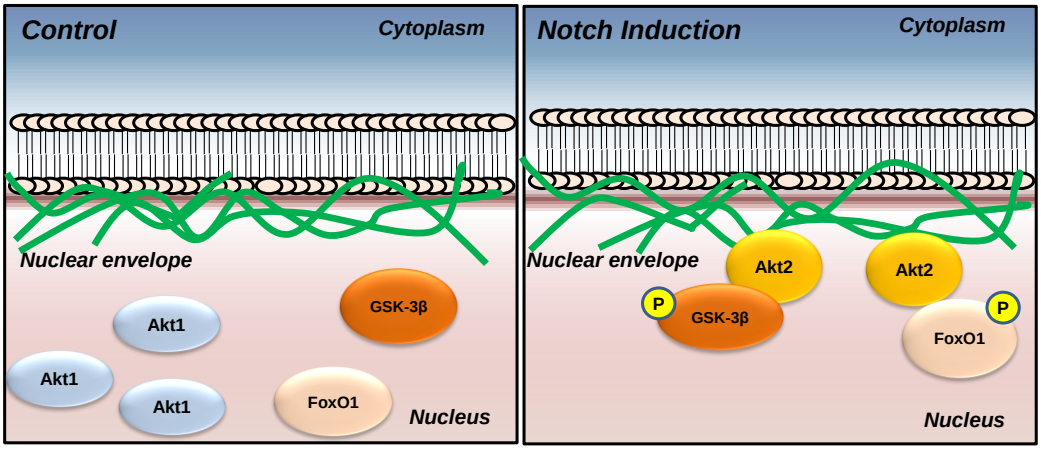

5) In control cells, active GSK-3β phosphorylates Snail1 in the nucleus inducing its nuclear export and degradation in the cytoplasm by the action of β-TrCP1 and Fbxl14 ubiquitin ligases (A). FoxO1 is nuclear and stable and facilitates apoptosis (B).

6) Conversely, in Notch active cells, GSK-3β is inactivated by the action of Akt2. This inactivation promotes Snail1 nuclear stabilization, allowing that Snail1 block apoptosis and induce mesenchymal markers such as Fibronectin and Lef-1 (A). Furthermore, Akt2 phosphorylates the pro-apoptotic transcriptional factor FoxO1, inducing the translocation to the cytoplasm and rapid degradation (B).

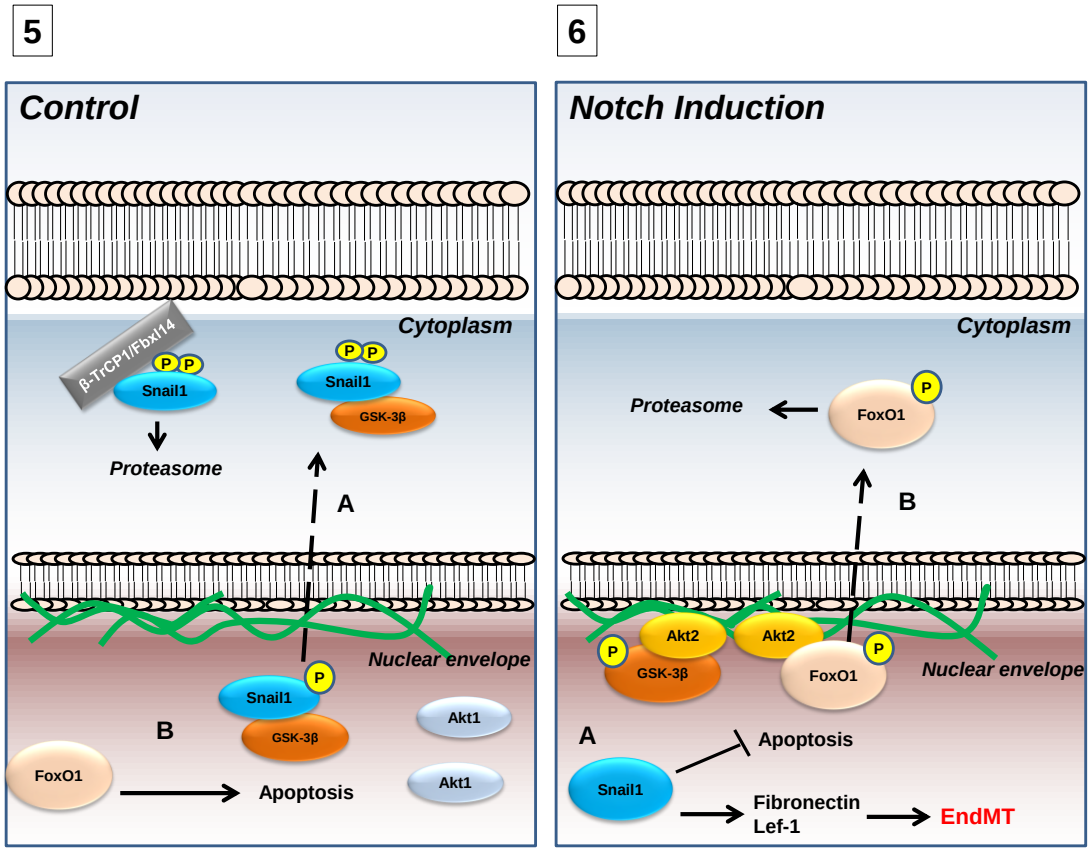

Conclusions

The following conclusions summarize the results presented in this PhD thesis:

1. Notch induces EndMT, a process characterized by the down-regulation of VE-Cadherin and up-regulation of mesenchymal markers such as Snail1/2, α-SMA, Lef-1, Fibronectin and N-Cadherin.

2. Notch and TGF-β cooperate in the up-regulation of mesenchymal genes such as Snail1, Fibronectin and Lef-1.

3. Notch up-regulates Akt2 through an increase of TCF-4/β-catenin activity.

4. Akt2 stabilizes Snail1 by GSK3-β inactivation. Due to GSK-3β inactivation, Snail1 is retained in the nucleus and β-TrCP1 cannot degrade it in the cytoplasm.

5. Activation of Akt2 is required for nuclear translocation. Nuclear Akt2 is localized in the nuclear envelope in Notch active cells increasing its activity on its substrates GSK-3β and FoxO1.

6. Notch expression in endothelial cells blocks apoptosis after oxidative stress through Akt2/Snail1 axis.

Materials & Methods

MM.1 Cell culture

All cells used in this thesis were grown in Dulbecco's modified Eagle's medium (DMEM, Invitrogen) supplemented with 4.5 g/L glucose (Life Technologies), 2mM glutamine, 56 U/ml penicillin, 56 µg/L streptomycin and 10% fetal bovine serum (FBS; all from GIBCO). Cells were maintained at 37ºC in a humid atmosphere containing 5% CO_2.

In this project we have used as a cellular model and endothelial cell line called PAE (Pig Aortic Endothelial). PAE cells were stably transfected with moderate or high levels of Notch (NICD1 and NICD2 respectively) and control cells having empty vector plus GFP. Cells were a generous gift of Dr. de la Pompa JL (Centro Nacional de Biotecnología, CSIC, Madrid, Spain). PAE cells were in maintenance with 1µg/ml G418 (neomycin) [18]. MEFs WT, KO for Akt1 or for Akt2 were a kind gift of D. M. Birnbaum (University of Pennsylvania) [155]. All the cell types used in this thesis are simplified in the next table (table MM.1).

Table MM.1. Cell lines used. Description of the main characteristics of the different cell lines used during this thesis.

Cell line	Origin	Characteristics
PAE-CTL	Pig Aortic Endothelial (endocardium E.9.5)	Elongated phenotype and grow until contact inhibition. Express GFP.
PAE-NICD1/NICD2	Pig Aortic Endothelial (endocardium E.9.5)	Lose endothelial phenotype, less elongated and lose contact inhibition
MEF-WT	Mouse Embryonic Fibroblast wild type	Mesenchymal morphology
MEF-Akt1 (-/-)	MEF Knock out for Akt1	Mesenchymal morphology
MEF-Akt2 (-/-)	MEF Knock out for Akt2	Mesenchymal morphology
HEK-293-T	Human embryonic Kidney	Contains the SV40 large T-antigen allowing episomal replication of transfected plasmids with SV40 origin of replication
RWP-1	Human pancreatic carcinoma	Epithelial morphology growing in colonies with well-formed intercellular junctions

MM.2 Cell treatments

To carry out various experiments cells were treated with different compounds for the indicated times at the concentration shown in table MM.2.

Table MM.2. Cell treatments. Detailed description of the cell treatments used in this work.

Compound	Function	Supplier	Concentration
TGF-β_1	EMT inducer	PeproTec	5 ng/ml
MG132 (Z-Leu-Leu-Leu-al)	Proteasome inhibitor	Sigma	10-50 μM
Cycloheximide (CHX)	Protein synthesis inhibitor	Sigma	20 μg/ml
Hydrogen peroxide (H_2O_2)	Oxidative stress inducer	Merk	200 μM
MK-2206	Allosteric Akt inhibitor	Deltaclon	10 μM
UO126	Allosteric Erk inhibitor	Cell Signaling	10 μM
iCRT14	TCF-4/β-catenin binding inhibitor	Tocris	25 μM
CCT128930	ATP-competitive and selective inhibitor of Akt2	Selleckchem	10 μM

MM.3 Cell transfection

For Snail1-HA degradation assays [85][84] in PAE cells, they were seeded in 60mm plates for 24 h or until 80% of confluence and transfected with 200ng of Snail1-HA using Lipofectamine-Plus reagent (Invitrogen) for 6h following manufacturer's instructions. Same conditions were used in RWP-1 cells overexpressing transiently NICD-Myc (1µg). After 24 h of transfection cells were harvested. When it was transfected the E3 ubiquitin ligase (Fbxl5-Myc, Fbxl14-HA, β-TrCP1-Flag) the ratio Snail-HA/Ligase was 1:5.

Alternatively, Snail1-F-Luc (Snail1-Firefly Luciferase fusion protein) and R-Luc (Renilla-Luciferase) were expressed with a pLEX-Snail-F-Luc and pMSCV-R-Luc vectors (a kind gift from Dr. Kang, Princeton University, USA) and used to measure Snail1 stability as previously described [86].

For HEK 293-T cells were also seeded in 60mm plates until 80% of confluence and transfected with polyethylenimine (PEI, Polyscience, Inc.). The transfection mix was composed of 200 ng of Snail1-HA and 1µg of NICD-Myc when indicated, 25µl of PEI (1 mg/ml) and up to 520µl with sterile NaCl (150mM). After 15 minutes at room temperature, mixture was added drop-wise to the cells containing 4 ml of cell culture medium. Cells were harvested after 24 h of transfection.

For siRNA transfection, iMax-RNA Lipofectamine was used following manufacturer's instructions. The amount of siRNA transfected was 70nM of the indicated siRNA. Cells were harvested after 72 h of siRNA transfection.

MM.4 Cell Infection

In this thesis we have used two different kinds of infection depending on the type of virus: Lentiviral or Retroviral infection.

MM.4.1 Lentiviral infection

Lentiviral expression in PAE cells was used to stably down-regulate genes using shRNAs cloned in pLKO.1-puro vector from Sigma. The different shRNAs used in this work were from the Mission shRNA library from Sigma. Each shRNA consists in a mix of 5 ShRNA.

For viral infection HEK-293-T cells were used in order to produce them. Cells were seeded in p100 mm plates with 10 ml of medium. They were transfected using PEI (1.5 ml of 150mM NaCl, DNA and 78µl of PEI (1 mg/ml) mixture incubated for 15 min at room temperature). Total DNA amount was 20µg composed by: 50% indicated shRNA, 10% was the pCMV-VsV-G (codes the viral envelope), 30% was the pMDLg/pRRE vector and 10% the pRSV rev vector. Note that the last two vectors were involved in the packaging of the virus.

The medium was removed 24 h later and replaced by 5.5 ml of fresh medium. After 24 h the supernatant was removed and filtrated through 45 µm membrane filters (Millipore). This last step was repited once again after 24 h. For several infections aliquots, the virus was concentrated using (Clonetech) following manufacturer's instructions.

MM.4.2 Retroviral infection

The procedure used is similar to that of lentiviral infection. In this case the vector used was pBabe-puro for overexpression of Snail1. The cells used for viral production were HEK-293 Phoenix Gag-Pol, which stably express the HIV-1 GAG and POL genes. Cells were seeded until 80% of confluence and transfected using PEI as previously described with a total of 10µg of DNA which 80% was the indicated pBabe vector and 20% was pCMV-VSV-G vector, coding for the viral envelope. The rest of the protocol was identical to that of lentiviral production but instead of lentiviral concentrator; it is used retroviral concentrator (Clonetech).

Once viruses are produced, they are infected to target cells. 24 h after infection target cells are selected using puromycin during 72 h. PAE cells were the target cells in all the experiments. The concentration of puromycin used was 2.5µg/ml. After selection, cells were expanded and used for experimental procedures.

MM.5 RNA analysis

MM.5.1 RNA extraction

To extract RNA, phenol-chloroform protocol was used. Cells were washed with cold PBS and lysed in 800 µl of TRIzol reagent (phenol, Invitrogent). The lysate was vortexed and added 200 µl of chloroform. It was mixed and incubated for 2 min at room temperature. The mixed was centrifuge at 13.200 rpm at 4ºC for 15 min. The clear supernatant was removed and mixed with 500 µl of isopropanol. It was incubated for 10 min at room temperature and the precipitation was pelleted at 13.200 rpm at 4ºC for 15 min. The pellet was washed with 1 ml of 75% ethanol and centrifuge at 7.500 rpm at 4ºC for 5 min. After ethanol evaporation in a 60ºC bath, the RNA pellet was resuspended in 20µ of water DEPC and dissolved at 60 ºC for 10 min prior to quantification. All the reagents used for RNA extraction were RNAase free. RNA was quantified using a NanoDrop™ Spectrophotometer (Thermo Scientific).

MM.5.2 Semi-Quantitative RT-PCR

For *VE-Cadherin, Snail1* and *HPRT* amplification 0.5µg of total RNA were retro-transcribed with SuperScript™ First-Strand Kit using Oligo-dT (Invitrogen) according to the manufacturer's instructions and cDNA was used in semi-quantitative RT-PCR. The primers used were *Snail1* (38 cycles), *VE-Cadherin* and *HPRT* (30 cycles) and their sequences used are shown in table MM.3.

MM.5.3 Quantitative Real Time PCR (qRT-PCR)

RNA was retrotranscribed using Oligo-dT and the Transcription First Strand cDNA Synthesis Kit (Roche) following manufacturer's instructions. Analyses were performed in triplicates with 100-150 ng of cDNA using the LightCycler 480 Real Time PCR System (Roche). The primers used for indicated genes are shown in Table MM.3.

Table MM.3. Primers used for mRNA analysis. Forward and reverse sequences of the different primers used in this study are listed.

Primer	Forward sequence	Reverse sequence	Specie
Snail1	5'CGAGTAGGAGAACTGGGGGA3'	5'CCAGGAGAGAGTCCCAGATG3'	PIG
AKT1	5'CTCAAGAACGACCCCCAAGCA3'	5'CCGTGAACTCCTGGTCGAAA3'	PIG
AKT2	5'ATTCACCGCCCAATCCATCA3'	5'CGAGTAGGAGAACTGGGGGA3'	PIG
FOXO1	5'GCAAATCGAGTTACGGAGGC3'	5'AATGTCATTATGGGGAGGAGAGT3'	PIG
Pumilio	5'CGGTCGTCCTGAGGATAAA3'	5'CGTACGTGAGGCGTGAGTAA3'	HUMAN
VE-Cadherin	5'CCTGACTGGAACCAGCACGCT3'	5'GTGTGTCGTATGGGGGGCCAC3'	PIG
Fibronectin	5'AGCAAGCCTGAGCCTGAAGAG3'	5'GCGATTTGCAATGGTACAGCT3'	MOUSE

MM.6 Protein analysis

Before analysis of protein extracts, quantification in duplicates using the DC Protein Assay kit (Lowry method; Bi-Rad) was performed. Prior to addition of the desired buffer for lysis cells were washed two or three times with cold PBS and scraped in the plate with the buffer. The volume of the lysis buffer for each plate depended on the number of cells.

MM6.1 Total cellular extracts

Total cell extracts were obtained using 2% SDS (sodium dodecyl sulfate) total lysis buffer.

The extract after scrapping was done at room temperature to avoid SDS precipitation. To homogenize the extract, it was syringed 3-5 times, centrifuged at maximum speed (13,200 rpm) for 10 minutes and boiled at 95ºC for 5 minutes.

Composition of 2% SDS Total Lysis buffer:

- 2% SDS
- 50mM Tris-HCL pH 7.5
- 10% glycerol

MM.6.2 Nuclear & cytoplasmic Sub-fractionated cell extracts

To obtain cell extracts with differentiated cytoplasmic and nuclear fractions cells were scrapped in cold Buffer A and the lysate pipetted up and down 4-5 times in order cell aggregates and incubated on ice up to 10 minutes. A volume equal to 1/30th of the first lysate of 10% Triton X-100 was added and the tube vortexed for 30 seconds. Centrifugation of each sample for 1 minute at 11,000 rpm was used to separate the cytoplasmic fraction (supernatant) which was stored at 4ºC in a new tube. The remaining pellet (nucleus) was washed twice in Buffer A to avoid cross-contamination of sub-cellular compartments and then it was lysate with total lysis buffer 2% SDS as previously explained. The nuclear fraction is composed by the nucleoplasmic and chromatin fraction [85].

Composition of Buffer A:

- 10 mM HEPES-KOH pH 7.8
- 1.5 mM MgCl2
- 10 mM KCl
- + Protease inhibitors

MM.6.3 Nuclear Membrane extracts

Nuclear membrane was isolated by two different protocols. First we used a nuclear fractionation protocol using DNase I and the second one using a commercial kit, which specifically separate all proteins associated to the nuclear envelope.

Nuclear extracts were isolated as described above and the nuclear pellets were lysate with Buffer NPE. The lysate was incubated in rotation with DNase I during 90 minutes at 4ºC in order to avoid chromatin contamination in the nuclear envelope fraction. Nuclear envelope fraction was sedimented by centrifugation at 10,000 x g for 30 minutes at 4ºC [156]. The supernatant, which was the nucleoplasmic extract (NPE), was separated into another tube. The pellet, which was the nuclear envelope fraction (NEnv) was then lysate with 2% SDS total lysis buffer.

Buffer NPE

- 10 mM Tris·HCl pH 7.4
- 10 mM NaH_2PO_4/Na_2HPO_4
- + DNAase
- + proteases inhibitor

When the commercial kit was used, the manufacturer's instructions were followed. The kit we used was Minute™ Nuclear Envelope Protein Extraction Kit (from Invent Technologies, Inc).

MM.6.4 Western Blot

Protein was analyzed by SDS polyacrylamide gel electrophoresis (SDS-PAGE) by loading the samples previously mixed with 5x Loading buffer and boiled at 95ºC for 5 minutes. Gels had a 7.5-15% polyacrylamide concentration. The Mini-Protean System (Bio-Rad) was used to run gels in TGS buffer that were then transferred to Protran nitrocellulose membranes (Whatman) during 60 minutes using transfer buffer at 4ºC.

After the transferred, membranes were stained with Ponceau S in order to know that proteins were loaded correctly. The Ponceau S solution was then removed and washed with distilled water.

Membranes were blocked in 5% skimmed milk or 3% BSA (phospho-proteins antibodies) in TBS-T for 45-60 minutes and incubated with the interested antibody for 1 hour at room temperature or overnight at 4ºC. In the table MM.4 are summarized al the antibodies used. After three 10 minutes washes with TBS-T Horseradish peroxidase (HRP)-combined secondary antibody (Dako) was diluted in 5% skimmed and the membrane was incubated for 1 more hour at room temperature. Prior to continue, three more washes with TBS-T were done. Membranes were developed using Luminata Western HRP Substrates (Millipore) and exposed on Agfa-Curix or Hyperfilms ECL (Amersham) for those proteins that were difficult to detect.

5x Loading buffer

- 250 mM Tris·HCl pH 6.8
- 10% SDS
- 0.02% Bromophenol blue
- 50% glycerol
- 20% β-mercaptoethanol

TBS-T

- 25 mM Tris·HCl pH 7.5
- 137 mM NaCl
- 0.1% Tween-20

TGS buffer

- 25 mM Tris·OH pH 8.3
- 192 mM glycine
- 5% SDS

Transfer buffer

- 50 mM Tris·OH
- 386 mM glycine
- 0.1% SDS
- 20% methanol

Ponceau S stain

- 0.5% Ponceau S
- 1% acetic acid

MM.6.5 Immunofluorescence

Around 30,000-50,000 cells were seeded on sterile coverslips in 24-well plates. Culture media was removed and the plate was washed with cold PBS. Cells were fixed with paraformaldehyde at 4% during 15 minutes at room temperature. After washing three times with PBS, cells were permeabilized with 0.3%-Tritón X-100 for 10 minutes at room temperature. After three more washes, cells were blocked with PBS-3% BSA for 1 hour. After blocking, coverslips were incubated with the indicated antibody diluted in blocking buffer for 1 hour at room temperature. In the case of Snail1 hybridoma, the incubation was overnight at 4ºC (for the dilution used, see the table MM.4). Prior to proceed to secondary antibody incubation, cells were washed three times more with PBS. Finally, coverslips were incubated with purified Alexa-Fluor 488, Alexa-Fluor 555 or Alexa-Fluor647-conjugated anti-

mouse, rabbit or goat IgGs (depending on the primary antibody and the combination needed; all from Invitrogen) in BSA or blocking buffer for 1 hour at room temperature.

MM.6.6 CSK buffer treatment.

When nuclear amplification signal was needed, prior to fix cells in the coverslips, they were treated for 5 minutes with CSK-0.5% Tritón X-100 buffer. After 5 minutes cells were washed with CSK buffer in order to remove all Tritón X-100. The rest of the immunofluorescence protocol was as explained previously.

CSK Buffer:

- 10 mM HEPES-KOH pH 7.8
- 100 mM KCl
- 3 mM $MgCl_2$
- 300 mM Sucrose
- + Protease inhibitors

MM.6.7 Quantification analysis

Quantification analysis of localization of the different Akt isoforms in the nucleus was done using ImageJ software. At least 10 cells from three different confocal images were analyzed. The analysis we did was to quantify the fluorescence intensity of the signal versus pixel distance across an arbitrary line. Then, Perinuclear compartment were delineated by the Lamin B1 signal and the relative value of Ak present in the nuclear lamina area was expressed versus total nuclear Akt.

Table MM.4. Antibodies used and their applications. (WB: western blot; IP: immunoprecipitation; IF: immunofluorescence).

Antibody	Species	Provider	Dilution
Tubulin	Mouse	Sigma	1:10000
Lamin B1	Goat	Santa Cruz	WB: 1:2000 IF: 1:50
Sin-3A	Rabbit	Santa Cruz	1:1000
total Akt	Rabbit	Cell Signaling	1:1000
Akt1	Rabbit	Cell Signaling	WB: 1:1000 IF/IP: 1:50
Akt2	Rabbit	Cell Signaling	WB: 1:1000 IF/IP: 1:50
pAkt S473	Rabbit	Cell Signaling	1:1000 (BSA)
pAkt T308	Rabbit	Cell Signaling	1:1000 (BSA)
β-TrCP1	Rabbit	Santa Cruz	1:200
total GSK-3β	Mouse	BD Transduction Laboratories	1:1000
pGSK-3β S9	Rabbit	Cell Signaling	1:1000
total Erk-1/2	Mouse	Zymed	1:1000
pERK-1/2 44/42	Rabbit	Cell Signaling	1:1000
Snail1	Mouse	Hybridoma F9	WB: 1:10 IF: 1:1
Fibronectin	Rabbit	Dako	1:10000
Lef-1	Goat	Santa Cruz	1:200
Slug	Goat	Santa Cruz	1:200
α-SMA	Goat	Abcam	1:4000
N-Cadherin	Mouse	BD Transduction Laboratories	1:1000
VE-Cadherin	Goat	Santa Cruz	1:500
FoxO1	Rabbit	Cell Signaling	1:1000
pFoxO1 S256	Rabbit	Cell Signaling	1:1000
HA	Rat	Roche	WB: 1:2000 IP: 1:50
Myc	Mouse	Hybridoma 9E10	1:200
Cleaved Caspase 3	Rabbit	Cell Signaling	1:1000

MM.7 Luciferase Reporter Assay

Cells were transfected with TOP-FLASH plasmid, a synthetic promoter sensitive to the activity of the TCF-4/β-catenin complex that contains three copies of the TCF-4 binding site upstream of a Firefly luciferase reporter gene. A mutant form of this promoter (FOP plasmid) was used as a negative control.

For this kind of experiments, 30,000-40,000 cells were seeded in 24 wells plate and each condition were transfected for triplicate. The amounts for each well were 50 ng for TOP/FOP-FLASH and 5 ng for Renilla-TK. In the case of HEK-293-T cells transfected with Notch, the amount of NICD-Myc was 500ng. For Akt2 promoter activity studies, 200 ng of pGL3-Akt2 promoter (-2898 to +220) was transfected (kind gift of Dr J.Q. Cheng; Moffitt Cancer Center, Tampa, FL).Empty vector was transfected as control. After 48 hours of transfection, cells were washed twice with cold PBS. Luciferase was analyzed using Dual Luciferase Reporter Assay System Kit (from Promega) in a FB 12 luminometer (Berthold Detection System).

Activity of the product of the Renilla luciferase gene under the control of a constitutive thymidine kinase promoter (Promega) was used to normalize transfection efficiency. Assays were always performed in triplicate. Graphs were represented with the average of three independent experiments ± SD (standard deviation).

MM.8 Apoptosis assays

MM.8.1 Annexin V

The Annexin V-APC conjugated (ImmunoTools) assay was used as an early apoptotic indicator through the detection of phosphatydylserine in the plasma membrane. Cells were treated with hydrogen peroxide (200μM) during 16 hours, trypsinized and 500.000 cells were then resuspended in 70μL of binding buffer (2.7mM CaCl2 in PBS) with 5μL of Annexin V that were incubated at RT for 15 minutes in the dark. Prior to flow cytometry analysis, 10μL of 10μg/ml propidium iodide were added to each sample in order to detect late apoptotic/necrotic cells. Samples were analyzed using the LSR II flow cytometer (Beckton Dickinson) at the CRG/UPF FACS Unit. The percentages of cells in each quadrant were analyzed using FACS-Diva Software (Becton Dickinson).

MM.8.2 MTT assay

To analyze cell viability MTT assays were performed. 10,000 cells were seeded in 96 wells plate. After 24 hours, cells were treated with H_2O_2 for indicated times. Then, 0.5 mg/mL of 3-(4,5-dimethylthiazol-2-yl)-2,5-diphenyltetrazolium bromide (MTT; Sigma) was added and incubated for 3 hours at 37°C. MTT was removed and cells were solubilize with DMSO:isopropanol (1:4). After 15 minutes the absorbance at 590 was determined.

MM.9. Immunoprecipitation of endogenous Akt isoforms

PAE cells were seeded in 150mm plates. Cells were collected with IP buffer. The lysates were syringed five times, vortex for 5 seconds, rotate at 4ºC for 15-30 minutes and centrifuged at 13,200 rpm for 10 minutes. The supernatant was placed in a new tube and one tenth of the volume stored as input.

The lysate was pre-cleared for 2 hours with magnetic protein A beads. The antibody for the IP was added to the lysate and rotated overnight at 4ºC. After incubation, magnetic beads were added to the lysate during 1-2 hours at 4ºC. The supernatant was removed and beads were eluted and boiled for 2 minutes at 95ºC. Finally, a western blot was carried out to identify the phosphorylation of each Akt isoform immunoprecipitated.

IP (RIPA) Buffer :

- 50mM Tris-HCl pH=7.5
- 150mM NaCl
- 1% Triton X-100
- 1% NaDoc
- 1mM EDTA
- + Protease inhibitors

MM.10. Ubiquitination assay

In order to analyzed the ubiquitination pattern of the proteins a ubiquitination assay was carried out. PAE cells were seeded in 100mm plates and transfected with Snail-HA and Ubiquitin-His (1:4). After 24 hours cells were treated during 4 hours with MG-132 at 10μM. Then, cells were lysate with Buffer I and rotate for 30 minutes at 4ºC. A fifth part was separate for the input. After sample sonication, they were incubated for 30 minutes at 4ºC with Ni-agarose beads for 2-3 hours. After incubation, beads were washed twice with buffer I. Beads were again washed with buffer II (twice) and with buffer III (three times). Finally, beads were washed once with PBS in order to equilibrate the pH and salt concentration. Once the PBS was removed, beads were elute with sample buffer 2x and boiled for 3 minutes at 95ºC. For inputs preparation, the lysate was precipitated with Trichloroacetic acid (TCA) and the pellet was washed with acetone. To investigate the ubiquitination pattern a western blot was performed and blotted again Snail-HA [84].

Buffer I:

- 6M Guanidin-HCl
- 0.1M Na_2HPO_4/NaH_2PO_4 pH=8
- 0.01M Tris-HCl pH=8
- 0.2% Triton X-100
- 5mM Imidazole
- 10mM β-Mercaptoethanol
- + Protease inhibitors

Buffer II:

- 8M Urea
- 0.1M Na_2HPO_4/NaH_2PO_4 pH=8
- 0.01M Tris-HCl pH=8
- 0.2% Triton X-100
- 5mM Imidazole
- 10mM β-Mercaptoethanol
- + Protease inhibitors

Buffer III:

- 8M Urea
- 0.1M Na_2HPO_4/NaH_2PO_4 pH=6.3
- 0.01M Tris-HCl pH=6.3
- 0.2% Triton X-100
- 5mM Imidazole
- 10mM β-Mercaptoethanol
- + Protease inhibitors

BIBLIOGRAPHY

[1] G. Greenburg and E. D. Hay, “Epithelia Suspended in Collagen Gels Can Lose Polarity and Express Characteristics of Migrating Mesenchymal Cells,” vol. 95, no. October, pp. 333–339, 1982.

[2] J. P. Thiery, H. Acloque, R. Y. J. Huang, and M. A. Nieto, “Epithelial-mesenchymal transitions in development and disease.,” *Cell*, vol. 139, no. 5, pp. 871–90, Nov. 2009.

[3] D. Medici and R. Kalluri, “Endothelial-mesenchymal transition and its contribution to the emergence of stem cell phenotype.,” *Semin. Cancer Biol.*, vol. 22, no. 5–6, pp. 379–84, Oct. 2012.

[4] S. Potenta, E. Zeisberg, and R. Kalluri, “The role of endothelial-to-mesenchymal transition in cancer progression.,” *Br. J. Cancer*, vol. 99, no. 9, pp. 1375–9, Nov. 2008.

[5] W. Yu, Z. Liu, S. An, J. Zhao, L. Xiao, Y. Gou, Y. Lin, and J. Wang, “The Endothelial-Mesenchymal Transition (EndMT) and Tissue Regeneration,” pp. 196–204, 2014.

[6] L. M. Eisenberg and R. R. Markwald, “Molecular Regulation of Atrioventricular Valvuloseptal Morphogenesis,” *Circ. Res.*, vol. 77, no. 1, pp. 1–6, Jul. 1995.

[7] E. J. Armstrong and J. Bischoff, “Heart valve development: endothelial cell signaling and differentiation.,” *Circ. Res.*, vol. 95, no. 5, pp. 459–70, Sep. 2004.

[8] J. Garcia, M. J. Sandi, P. Cordelier, B. Binétruy, J. Pouysségur, J. L. Iovanna, and R. Tournaire, “Tie1 deficiency induces endothelial-mesenchymal transition.,” *EMBO Rep.*, vol. 13, no. 5, pp. 431–9, May 2012.

[9] J. Folkman, “Angiogenesis: an organizing principle for drug discovery?,” vol. 6, no. April, pp. 273–286, 2007.

[10] E. M. Zeisberg, O. Tarnavski, M. Zeisberg, A. L. Dorfman, J. R. McMullen, E. Gustafsson, A. Chandraker, X. Yuan, W. T. Pu, A. B. Roberts, E. G. Neilson, M. H. Sayegh, S. Izumo, and R. Kalluri, “Endothelial-to-mesenchymal transition contributes to cardiac fibrosis.,” *Nat. Med.*, vol. 13, no. 8, pp. 952–61, Aug. 2007.

[11] R. Kalluri and M. Zeisberg, “Fibroblasts in cancer.,” *Nat. Rev. Cancer*, vol. 6, no. 5, pp. 392–401, May 2006.

[12] K. Niessen and A. Karsan, “Notch signaling in the developing cardiovascular system,” *AJP Cell Physiol.*, vol. 293, pp. C1–C11, 2007.

[13] S. J. Bray, “Notch signalling: a simple pathway becomes complex.,” *Nat. Rev. Mol. Cell Biol.*, vol. 7, no. 9, pp. 678–89, Sep. 2006.

[14] B. a Osborne and L. M. Minter, “Notch signalling during peripheral T-cell activation and differentiation.,” *Nat. Rev. Immunol.*, vol. 7, no. 1, pp. 64–75, Jan. 2007.

[15] T. Kume, “Novel insights into the differential functions of Notch ligands in vascular formation.,” *J. Angiogenes. Res.*, vol. 1, p. 8, Jan. 2009.

[16] B. D’Souza, a Miyamoto, and G. Weinmaster, “The many facets of Notch ligands.,” *Oncogene*, vol. 27, no. 38, pp. 5148–67, Sep. 2008.

[17] A. Pintar, A. De Biasio, M. Popovic, N. Ivanova, and S. Pongor, “The intracellular region of Notch ligands: does the tail make the difference?,” *Biol. Direct*, vol. 2, p. 19, Jan. 2007.

[18] L. a Timmerman, J. Grego-Bessa, A. Raya, E. Bertrán, J. M. Pérez-Pomares, J. Díez, S. Aranda, S. Palomo, F. McCormick, J. C. Izpisúa-Belmonte, and J. L. de la Pompa, “Notch promotes epithelial-mesenchymal transition during cardiac development and oncogenic transformation.,” *Genes Dev.*, vol. 18, no. 1, pp. 99–115, Jan. 2004.

[19] Anne Joutel and E. Tournier-lasserve, “Notch signalling pathway and human diseases,” *Cell Dev. Biol.*, vol. 9, pp. 619–625, 1998.

[20] U.-M. Fiúza and A. Martinez Arias, “Cell and molecular biology of Notch.,” *J. Endocrinol.*, vol. 194, no. 3, pp. 459–74, Sep. 2007.

[21] A. Zolkiewska, “ADAM Proteases: Ligand Processing and Modulation of the Notch Pathway,” *cell Mol Life*, vol. 65, no. 13, pp. 2056–2068, 2009.

[22] R. Kopan and M. X. G. Ilagan, “The Canonical Notch Signaling Pathway: Unfolding the Activation Mechanism,” *Cell*, vol. 137, no. 2, pp. 216–233, 2010.

[23] A. Herve Nwabo Kamdje and M. Krampera, “Notch signaling in acute lymphoblastic leukemia : any role for stromal microenvironment ?,” *Blood*, vol. 118, no. 25, pp. 6506–6515, 2015.

[24] J. L. de la Pompa and J. Epstein, “Coordinating tissue interactions: Notch signaling in cardiac development and disease,” *Dev Cell*, vol. 22, no. 2, pp. 244–254, 2013.

[25] K. G. Guruharsha, M. W. Kankel, and S. Artavanis-Tsakonas, “The Notch signalling system: recent insights into the complexity of a conserved pathway.,” *Nat. Rev. Genet.*, vol. 13, no. 9, pp. 654–66, Sep. 2012.

[26] J. N. Anastas and R. T. Moon, “WNT signalling pathways as therapeutic targets in cancer.,” *Nat. Rev. Cancer*, vol. 13, no. 1, pp. 11–26, Jan. 2013.

[27] Y. Komiya and R. Habas, “Wnt signal transduction pathways,” *Organogesis*, vol. 4, no. 2, pp. 68–75, 2008.

[28] S. Ikeda, S. Kishida, H. Yamamoto, H. Murai, S. Koyama, and A. Kikuchi, “Axin , a negative regulator of the Wnt signaling pathway , forms a complex with GSK-3 β and β -catenin and promotes GSK-3 β -dependent phosphorylation of β -catenin,” *EMBO J.*, vol. 17, no. 5, pp. 1371–1384, 1998.

[29] M. Hart, J. Concordet, I. Lassot, I. Albert, R. L. Santos, H. Durand, C. Perret, B. Rubinfeld, F. Margottin, R. Benarous, and P. Polakis, “The F-box protein β -TrCP associates with phosphorylated β -catenin and regulates its activity in the cell,” *Curr. Biol.*, vol. 9, no. 4, pp. 207–211, 1999.

[30] J. Behrens, J. P. von Kries, M. Kühl, L. Bruhn, D. Wedlich, R. Grosschedl, and W. Birchmeier, “Functional interaction of beta-catenin with the transcription factor LEF-1,” *Lett. to Nat.*, vol. 382, pp. 638–642, 1996.

[31] E. Tzahor1, “Wnt/b-Catenin Signaling and Cardiogenesis: Timing Does Matter,” *Dev. Cell*, vol. 13, pp. 10–13, 2007.

[32] B. S. Gillers, A. Chiplunkar, H. Aly, T. Valenta, K. Basler, V. M. Christoffels, I. R. Efimov, B. J. Boukens, and S. Rentschler, “Canonical wnt signaling regulates atrioventricular junction programming and electrophysiological properties.,” *Circ. Res.*, vol. 116, no. 3, pp. 398–406, Jan. 2015.

[33] O. Aisagbonhi, M. Rai, S. Ryzhov, N. Atria, I. Feoktistov, and A. K. Hatzopoulos, “Experimental myocardial infarction triggers canonical Wnt signaling and endothelial-to-mesenchymal transition.,” *Dis. Model. Mech.*, vol. 4, no. 4, pp. 469–83, Jul. 2011.

[34] S. P. De Langhe, F. G. Sala, P.-M. Del Moral, T. J. Fairbanks, K. M. Yamada, D. Warburton, R. C. Burns, and S. Bellusci, “Dickkopf-1 (DKK1) reveals that fibronectin is a major target of Wnt signaling in branching morphogenesis of the mouse embryonic lung.,” *Dev. Biol.*, vol. 277, no. 2, pp. 316–31, Jan. 2005.

[35] D. GRADL, M. Kühl, and D. Wedlich, “The Wnt / Wg Signal Transducer β -Catenin Controls Fibronectin Expression,” *Mol. Cell. Biol.*, vol. 19, no. 8, pp. 5576–5587, 1999.

[36] L. R. Howe, O. Watanabe, J. Leonard, and A. M. C. Brown, “Twist Is Up-Regulated in Response to Wnt1 and Inhibits Mouse Mammary,” *Cancer Res.*, vol. 63, pp. 1906–1913, 2003.

[37] J. I. Yook, X.-Y. Li, I. Ota, E. R. Fearon, and S. J. Weiss, “Wnt-dependent regulation of the E-cadherin repressor snail.,” *J. Biol. Chem.*, vol. 280, no. 12, pp. 11740–8, Mar. 2005.

[38] P. Andersen, H. Uosaki, L. T. Shenje, and C. Kwon, “Non-canonical Notch signaling: emerging role and mechanism.,” *Trends Cell Biol.*, vol. 22, no. 5, pp. 257–65, May 2012.

[39] Y. Yoshimatsu and T. Watabe, “Roles of TGF-β signals in endothelial-mesenchymal transition during cardiac fibrosis.,” *Int. J. Inflam.*, vol. 2011, pp. 1–8, Jan. 2011.

[40] A. Moustakas and C.-H. Heldin, “Signaling networks guiding epithelial-mesenchymal transitions during embryogenesis and cancer progression.,” *Cancer Sci.*, vol. 98, no. 10, pp. 1512–20, Oct. 2007.

[41] F. Huang and Y.-G. Chen, “Regulation of TGF-β receptor activity.,” *Cell Biosci.*, vol. 2, no. 1, p. 9, Jan. 2012.

[42] S. Sridurongrit, J. Larsson, R. Schwartz, P. Ruiz-Lozano, and V. Kaartinen, “Signaling via the Tgf-β type I receptor Alk5 in heart development,” *Dev. Biol.*, vol. 322, no. 1, pp. 208–218, 2009.

[43] T. a Townsend, J. L. Wrana, G. E. Davis, and J. V Barnett, “Transforming growth factor-beta-stimulated endocardial cell transformation is dependent on Par6c regulation of RhoA.,” *J. Biol. Chem.*, vol. 283, no. 20, pp. 13834–41, May 2008.

[44] S. Yoo, C. H. Ko, P. L. Lowrey, E. D. Buhr, E. Song, S. Chang, O. J. Yoo, S. Yamazaki, C. Lee, and J. S. Takahashi, “A noncanonical E-box enhancer drives mouse Period2 circadian oscillations in vivo,” vol. 102, no. 7, pp. 3–8, 2005.

[45] X. Zhang, S. P. Patel, J. J. McCarthy, A. G. Rabchevsky, D. J. Goldhamer, and K. a Esser, “A non-canonical E-box within the MyoD core enhancer is necessary for circadian expression in skeletal muscle.,” *Nucleic Acids Res.*, vol. 40, no. 8, pp. 3419–30, Apr. 2012.

[46] E. Batlle, E. Sancho, C. Francí, D. Domínguez, M. Monfar, J. Baulida, and A. G. De Herreros, “The transcription factor Snail is a repressor of E-cadherin gene expression in epithelial tumour cells,” vol. 2, no. February, 2000.

[47] A. Cano, M. A. Pérez-moreno, I. Rodrigo, A. Locascio, M. J. Blanco, M. G. Barrio, F. Portillo, and M. A. Nieto, “The transcription factor Snail controls epithelial – mesenchymal transitions by repressing E-cadherin expression,” vol. 2, no. February, 2000.

[48] V. Bolos, H. Peinado, M. A. Pérez-moreno, M. F. Fraga, M. Esteller, and A. Cano, “The transcription factor Slug represses E-cadherin expression and induces epithelial to mesenchymal transitions: a comparison with Snail and E47 repressors,” *J. Cell Sci.*, vol. 116, no. 3, pp. 499–511, Dec. 2002.

[49] A. Eger, K. Aigner, S. Sonderegger, B. Dampier, S. Oehler, M. Schreiber, G. Berx, A. Cano, H. Beug, and R. Foisner, “DeltaEF1 is a transcriptional repressor of E-cadherin and regulates epithelial plasticity in breast cancer cells.,” *Oncogene*, vol. 24, no. 14, pp. 2375–85, Mar. 2005.

[50] J. Comijn, G. Berx, P. Vermassen, K. Verschueren, L. Van Grunsven, E. Bruyneel, M. Mareel, D. Huylebroeck, and F. Van Roy, “The Two-Handed E Box Binding Zinc Finger Protein SIP1 Downregulates E-Cadherin and Induces Invasion,” *Mol. Cell*, vol. 7, pp. 1267–1278, 2001.

[51] J. Yang, S. A. Mani, J. L. Donaher, S. Ramaswamy, R. A. Itzykson, C. Come, P. Savagner, I. Gitelman, A. Richardson, and R. A. Weinberg, “Twist , a Master Regulator of Morphogenesis , Plays an Essential Role in Tumor Metastasis,” *Cell*, vol. 117, pp. 927–939, 2004.

[52] D. Lopez, G. Niu, P. Huber, and W. B. Carter, “Tumor-induced upregulation of Twist, Snail, and Slug represses the activity of the human VE-cadherin promoter.,” *Arch. Biochem. Biophys.*, vol. 482, no. 1–2, pp. 77–82, Feb. 2009.

[53] C. Vandewalle, F. Van Roy, and G. Berx, “The role of the ZEB family of transcription factors in development and disease.,” *Cell. Mol. life Sci.*, vol. 66, no. 5, pp. 773–87, Mar. 2009.

[54] E. Sánchez-Tilló, L. Fanlo, S. M.-M. Siles, A. Moros4, G. Chiva-Blanch5, R. Estruch5, A. Martinez, B. Gyorffy, G. Roue´, and A. Postigo*, “The EMT activator ZEB1 promotes tumor growth and determines differential response to chemotherapy in mantle cell lymphoma,” *Cell Death Differ.*, 2014.

[55] N. Dave, S. Guaita-Esteruelas, S. Gutarra, A. Frias, M. Beltran, S. Peiró, and A. G. de Herreros, “Functional cooperation between Snail1 and twist in the regulation of ZEB1 expression during epithelial to mesenchymal transition,” *J. Biol. …*, vol. 286, no. 14, pp. 12024–12032, Apr. 2011.

[56] M. Beltran, I. Puig, C. Peña, J. M. García, A. B. Álvarez, R. Peña, F. Bonilla, and A. G. de Herreros, “A natural antisense transcript regulates Zeb2/Sip1 gene expression during Snail1-induced epithelial–mesenchymal transition,” *Genes Dev.*, vol. 22, pp. 756–769, 2008.

[57] Q. Qin, Y. Xu, T. He, C. Qin, and J. Xu, “Normal and disease-related biological functions of Twist1 and underlying molecular mechanisms.,” *Cell Res.*, vol. 22, no. 1, pp. 90–106, Jan. 2012.

[58] M.-H. Yang and K.-J. Wu, “TWIST activation by hypoxia inducible factor-1 (HIF-1): Implications in metastasis and development,” *Cell Cycle*, vol. 7, no. 14, pp. 2090–2096, Oct. 2014.

[59] A. Barrallo-Gimeno and M. A. Nieto, “The Snail genes as inducers of cell movement and survival: implications in development and cancer.,” *Development*, vol. 132, no. 14, pp. 3151–61, Jul. 2005.

[60] V. Díaz, R. Viñas-Castells, and a García de Herreros, “Regulation of the protein stability of EMT transcription factors.,” *Cell Adh. Migr.*, vol. 8, no. 4, pp. 418–28, Jul. 2014.

[61] M. A. Nieto, “The snail superfamily of zinc-finger transcription factors.,” *Nat. Rev. Mol. Cell Biol.*, vol. 3, no. 3, pp. 155–66, Mar. 2002.

[62] M. Sefton, S. Sánchez, and M. A. Nieto, “Conserved and divergent roles for members of the Snail family of transcription factors in the chick and mouse embryo,” vol. 3121, pp. 3111–3121, 1998.

[63] H. Peinado, E. Ballestar, M. Esteller, and A. Cano, “Snail Mediates E-Cadherin Repression by the Recruitment of the Sin3A / Histone Deacetylase 1 (HDAC1)/ HDAC2 Complex,” *Mol. Cell. Biol.*, vol. 24, no. 1, pp. 306–319, 2004.

[64] N. Herranz, D. Pasini, V. M. Díaz, C. Francí, A. Gutierrez, N. Dave, M. Escrivà, I. Hernandez-Muñoz, L. Di Croce, K. Helin, A. García de Herreros, and S. Peiró, “Polycomb complex 2 is required for E-cadherin repression by the Snail1 transcription factor.,” *Mol. Cell. Biol.*, vol. 28, no. 15, pp. 4772–81, Aug. 2008.

[65] Y. Lin, Y. Wu, J. Li, C. Dong, X. Ye, Y.-I. Chi, B. M. Evers, and B. P. Zhou, “The SNAG domain of Snail1 functions as a molecular hook for recruiting lysine-specific demethylase 1.,” *EMBO J.*, vol. 29, no. 11, pp. 1803–16, Jun. 2010.

[66] H. Peinado, M. Del Carmen Iglesias-de la Cruz, D. Olmeda, K. Csiszar, K. S. K. Fong, S. Vega, M. A. Nieto, A. Cano, and F. Portillo, “A molecular role for lysyl oxidase-like 2 enzyme in snail regulation and tumor progression.,” *EMBO J.*, vol. 24, no. 19, pp. 3446–58, Oct. 2005.

[67] A. Millanes-Romero, N. Herranz, V. Perrera, A. Iturbide, J. Loubat-Casanovas, J. Gil, T. Jenuwein, A. García de Herreros, and S. Peiró, “Regulation of heterochromatin transcription by Snail1/LOXL2 during epithelial-to-mesenchymal transition.,” *Mol. Cell*, vol. 52, no. 5, pp. 746–57, Dec. 2013.

[68] D. Domínguez, A. Virgo, S. Guaita, J. Grueso, I. Puig, J. Baulida, C. Francí, and A. Garcia de Herreros, “Phosphorylation Regulates the Subcellular Location and Activity of the Snail Transcriptional Repressor,” *Mol. Cell. Biol.*, vol. 23, no. 14, pp. 5078–5089, 2003.

[69] J.-M. Mingot, S. Vega, B. Maestro, J. M. Sanz, and M. A. Nieto, “Characterization of Snail nuclear import pathways as representatives of C2H2 zinc finger transcription factors.,” *J. Cell Sci.*, vol. 122, no. Pt 9, pp. 1452–60, May 2009.

[70] H. Yamasaki, T. Sekimoto, T. Ohkubo, T. Douchi, Y. Nagata, M. Ozawa, and Y. Yoneda, “Zinc finger domain of Snail functions as a nuclear localization signal for importin β-mediated nuclear import pathway,” *Genes to Cells*, vol. 10, no. 5, pp. 455–464, Mar. 2005.

[71] J. Ikenouchi, M. Matsuda, M. Furuse, and S. Tsukita, “Regulation of tight junctions during the epithelium-mesenchyme transition: direct repression of the gene expression of claudins/occludin by Snail.,” *J. Cell Sci.*, vol. 116, no. Pt 10, pp. 1959–67, May 2003.

[72] H. G. Palmer, M. J. Larriba, J. M. Garcia, P. Ordonez-Moran, C. Pena, S. Peiro, I. Puig, R. Rodriguez, R. de la Fuente, A. Bernad, M. Pollan, F. Bonilla, C. Gamallo, A. G. de Herreros, and A. Munoz, “The transcription factor SNAIL represses vitamin D receptor expression and responsiveness in human colon cancer,” *Nat Med*, vol. 10, no. 9, pp. 917–919, Sep. 2004.

[73] S. Guaita, I. Puig, C. Franci, M. Garrido, D. Dominguez, E. Batlle, E. Sancho, S. Dedhar, A. G. De Herreros, and J. Baulida, “Snail induction of epithelial to mesenchymal transition in tumor cells is accompanied by MUC1 repression and ZEB1 expression.,” *J. Biol. Chem.*, vol. 277, no. 42, pp. 39209–16, Oct. 2002.

[74] M. Jordà, D. Olmeda, A. Vinyals, E. Valero, E. Cubillo, A. Llorens, A. Cano, and A. Fabra, “Upregulation of MMP-9 in MDCK epithelial cell line in response to expression of the Snail transcription factor.,” *J. Cell Sci.*, vol. 118, no. Pt 15, pp. 3371–85, Aug. 2005.

[75] J. Stanisavljevic, M. Porta-de-la-Riva, R. Batlle, A. G. de Herreros, and J. Baulida, “The p65 subunit of NF-κB and PARP1 assist Snail1 in activating fibronectin transcription.,” *J. Cell Sci.*, vol. 124, no. Pt 24, pp. 4161–71, Dec. 2011.

[76] L. D. M. Derycke and M. E. Bracke, “N-cadherin in the spotlight of cell-cell adhesion , differentiation , embryogenesis , invasion and signalling,” *Int. J. Dev. Biol.*, vol. 48, pp. 463–476, 2004.

[77] H. Oda, S. Tsukita, and M. Takeichi, “Dynamic Behavior of the Cadherin-Based Cell – Cell Adhesion System during Drosophila Gastrulation,” *Dev. Biol.*, vol. 203, pp. 435–450, 1998.

[78] C.-H. Heldin, M. Vanlandewijck, and A. Moustakas, “Regulation of EMT by TGFβ in cancer.,” *FEBS Lett.*, vol. 586, no. 14, pp. 1959–70, Jul. 2012.

[79] M. J. Barberà, I. Puig, D. Domínguez, S. Julien-Grille, S. Guaita-Esteruelas, S. Peiró, J. Baulida, C. Francí, S. Dedhar, L. Larue, and A. García de Herreros, “Regulation of Snail transcription during epithelial to mesenchymal transition of tumor cells.,” *Oncogene*, vol. 23, no. 44, pp. 7345–54, Sep. 2004.

[80] A. Garcia de Herreros, S. Peiro, M. Nassour, and P. Savagner, “Snail family regulation and epithelial mesenchymal transitions in breast,” *J Mammary Gland Biol Neoplasia*, vol. 15, no. 2, pp. 135–147, 2010.

[81] K. Zhang, N. Yabuta, J. M. Mingot, M. A. Nieto, E. Rodriguez-Aznar, H. Nojima, R. J. Owen, and G. D. Longmore, “Lats2 kinase potentiates Snail1 activity by promoting nuclear retention upon phosphorylation,” *The EMBO Journal*, vol. 31, no. 1. pp. 29–43, 2011.

[82] R. J. Boohaker, X. Cui, M. Stackhouse, and B. Xu, “ATM-mediated Snail Serine 100 phosphorylation regulates cellular radiosensitivity.,” *Radiother. Oncol.*, vol. 108, no. 3, pp. 403–8, Sep. 2013.

[83] K. Zhang, C. a Corsa, S. M. Ponik, J. L. Prior, D. Piwnica-Worms, K. W. Eliceiri, P. J. Keely, and G. D. Longmore, “The collagen receptor discoidin domain receptor 2 stabilizes SNAIL1 to facilitate breast cancer metastasis.,” *Nat. Cell Biol.*, vol. 15, no. 6, pp. 677–87, Jun. 2013.

[84] R. Viñas-Castells, M. Beltran, G. Valls, I. Gómez, J. M. García, B. Montserrat-Sentís, J. Baulida, F. Bonilla, A. G. de Herreros, and V. M. Díaz, “The hypoxia-controlled FBXL14 ubiquitin ligase targets SNAIL1 for proteasome degradation.,” *J. Biol. Chem.*, vol. 285, no. 6, pp. 3794–805, Feb. 2010.

[85] R. Viñas-Castells, Á. Frías, E. Robles-Lanuza, K. Zhang, G. D. Longmore, A. García de Herreros, and V. M. Díaz, “Nuclear ubiquitination by FBXL5 modulates Snail1 DNA binding and stability.,” *Nucleic Acids Res.*, vol. 42, no. 2, pp. 1079–94, Jan. 2014.

[86] H. Zheng, M. Shen, Y.-L. Zha, W. Li, Y. Wei, M. A. Blanco, G. Ren, T. Zhou, P. Storz, H.-Y. Wang, and Y. Kang, “PKD1 phosphorylation-dependent degradation of SNAIL by SCF-FBXO11 regulates epithelial-mesenchymal transition and metastasis.,” *Cancer Cell*, vol. 26, no. 3, pp. 358–73, Sep. 2014.

[87] J.-Y. Shih and P.-C. Yang, “The EMT regulator slug and lung carcinogenesis.,” *Carcinogenesis*, vol. 32, no. 9, pp. 1299–304, Sep. 2011.

[88] Z.-Q. Wu, X.-Y. Li, C. Y. Hu, M. Ford, C. G. Kleer, and S. J. Weiss, “Canonical Wnt signaling regulates Slug activity and links epithelial-mesenchymal transition with epigenetic Breast Cancer 1, Early Onset (BRCA1) repression.,” *Proc. Natl. Acad. Sci. U. S. A.*, vol. 109, no. 41, pp. 16654–9, Oct. 2012.

[89] S.-H. Kao, W.-L. Wang, C.-Y. Chen, Y.-L. Chang, Y.-Y. Wu, Y.-T. Wang, S.-P. Wang, a I. Nesvizhskii, Y.-J. Chen, T.-M. Hong, and P.-C. Yang, “GSK3β controls epithelial-mesenchymal transition and tumor metastasis by CHIP-mediated degradation of Slug.,” *Oncogene*, vol. 33, no. 24, pp. 3172–82, Jun. 2014.

[90] D. A. . Cross, D. R. Alessi, P. Cohen, M. Andjelkovich, and B. A. Hemmings, “Inhibition of glycogen synthase Kinase-3 by insulin mediated by protein Kinase B,” *Lett. to NatureNature*, vol. 378, no. 21/28, pp. 785–789, 1995.

[91] Q. Ding, W. Xia, J.-C. Liu, J.-Y. Yang, D.-F. Lee, J. Xia, G. Bartholomeusz, Y. Li, Y. Pan, Z. Li, R. C. Bargou, J. Qin, C.-C. Lai, F.-J. Tsai, C.-H. Tsai, and M.-C. Hung, “Erk associates with and primes GSK-3beta for its inactivation resulting in upregulation of beta-catenin.,” *Mol. Cell*, vol. 19, no. 2, pp. 159–70, Jul. 2005.

[92] T. F. Franke, “PI3K/Akt: getting it right matters,” *Oncogene*, vol. 27, no. 50, pp. 6473–6488, Oct. 2008.

[93] H. Y. Irie, R. V Pearline, D. Grueneberg, M. Hsia, P. Ravichandran, N. Kothari, S. Natesan, and J. S. Brugge, “Distinct roles of Akt1 and Akt2 in regulating cell migration and epithelial-mesenchymal transition.,” *J. Cell Biol.*, vol. 171, no. 6, pp. 1023–34, Dec. 2005.

[94] S. J. Grille, A. Bellacosa, J. Upson, A. J. Klein-szanto, F. Van Roy, W. Lee-kwon, M. Donowitz, P. N. Tsichlis, and L. Larue, “The Protein Kinase Akt Induces Epithelial Mesenchymal Transition and Promotes Enhanced Motility and Invasiveness of Squamous Cell Carcinoma Lines,” *Cancer Res.*, vol. 63, pp. 2172–2178, 2003.

[95] H. Cho, J. L. Thorvaldsen, Q. Chu, F. Feng, and M. J. Birnbaum, “Akt1/PKBalpha is required for normal growth but dispensable for maintenance of glucose homeostasis in mice.,” *J. Biol. Chem.*, vol. 276, no. 42, pp. 38349–52, Oct. 2001.

[96] A. C. D, H. Cho, J. Mu, J. K. Kim, J. L. Thorvaldsen, Q. Chu, E. B. C. Iii, K. H. Kaestner, M. S. Bartolomei, G. I. Shulman, and M. J. Birnbaum, “Insulin Resistance and a Diabetes Mellitus – Like Syndrome in Mice Lacking the Protein Kinase Akt2 (PKB),” *Science (80-.).*, vol. 292, pp. 1728–1732, 2001.

[97] R. M. Easton, H. Cho, K. Roovers, D. W. Shineman, M. Mizrahi, M. S. Forman, V. M. Lee, M. Szabolcs, R. De Jong, T. Oltersdorf, T. Ludwig, A. Efstratiadis, and M. J. Birnbaum, “Role for Akt3 / Protein Kinase B-gamma in Attainment of Normal Brain Size,” *Mol. Cell. Biol.*, vol. 25, no. 5, pp. 1869–1878, 2005.

[98] B. Ananthanarayanan, M. Fosbrink, M. Rahdar, and J. Zhang, “Live-cell molecular analysis of Akt activation reveals roles for activation loop phosphorylation.,” *J. Biol. Chem.*, vol. 282, no. 50, pp. 36634–41, Dec. 2007.

[99] J. R. Testa and A. Bellacosa, “AKT plays a central role in tumorigenesis,” *PNAS*, vol. 98, no. 20, pp. 10983–10985, 2001.

[100] A. Bellacosa and L. Larue, “PI3K/AKT Pathway and the Epithelial–Mesenchymal Transition,” *Cancer Genome and Tumor Microenviroment*, pp. 11–33, 2010.

[101] B. P. Zhou, J. Deng, W. Xia, J. Xu, Y. M. Li, M. Gunduz, and M.-C. Hung, “Dual regulation of Snail by GSK-3beta-mediated phosphorylation in control of epithelial-mesenchymal transition.,” *Nat. Cell Biol.*, vol. 6, no. 10, pp. 931–40, Oct. 2004.

[102] D. Kim, S. Kim, H. Koh, S. Yoon, and C. Jongkyeong, “Akt / PKB promotes cancer cell invasion via increased motility and metalloproteinase production,” *FASEB*, vol. 15, pp. 1953–1962, 2001.

[103] L. Marek, M. Subbareddy, E. Bettina, and K. Schulze-Osthoff, “Switching Akt : from survival signaling to deadly response,” *Bioessays*, vol. 31, no. 5, pp. 492–495, 2010.

[104] S. Elmore, “Apoptosis: A review of Programmed Cell death,” *Toxicol Pathol*, vol. 35, no. 4, pp. 495–516, 2007.

[105] M. E. Carter, “Quick guide FOXO transcription factors,” *Curr. Biol.*, vol. 17, no. 4, pp. 113–114.

[106] M. Hanada, J. Feng, and B. a Hemmings, “Structure, regulation and function of PKB/AKT--a major therapeutic target.,” *Biochim. Biophys. Acta*, vol. 1697, no. 1–2, pp. 3–16, Mar. 2004.

[107] B. M. T. Burgering, “Decisions on life and death : FOXO Forkhead transcription factors are in command when PKB / Akt is off duty,” *J. Leukoc. Biol.*, vol. 73, pp. 689–701, 2003.

[108] B. T. Nave, D. M. Ouwens, D. J. Withers, D. R. Alessi, and P. R. Shepherd, “Mammalian target of rapamycin is a direct target for protein kinase B: identification of a convergence point for opposing effects of insulin and amino-acid deficiency on protein translation,” *Biochem. Soc.*, vol. 334, pp. 427–431, 1999.

[109] K. Inoki, Y. Li, T. Zhu, J. Wu, and K.-L. Guan, “TSC2 is phosphorylated and inhibited by Akt and suppresses mTOR signalling.,” *Nat. Cell Biol.*, vol. 4, no. 9, pp. 648–57, Sep. 2002.

[110] B. D. Manning, A. R. Tee, M. N. Logsdon, J. Blenis, and L. C. Cantley, “Identification of the Tuberous Sclerosis Complex-2 Tumor Suppressor Gene Product Tuberin as a Target of the Phosphoinositide 3-Kinase / Akt Pathway,” *Mol. Cell*, vol. 10, pp. 151–162, 2002.

[111] M. J. Arboleda, J. F. Lyons, F. F. Kabbinavar, M. R. Bray, B. E. Snow, R. Ayala, M. Danino, B. Y. Karlan, and D. J. Slamon, “Overexpression of AKT2 / Protein Kinase B-beta Leads to Up-Regulation of beta-1 Integrins , Increased Invasion , and Metastasis of Human Breast and Ovarian Cancer Cells,” *Cancer Res.*, vol. 63, pp. 196–206, 2003.

[112] P. Villagrasa, V. M. Díaz, R. Viñas-Castells, S. Peiró, B. Del Valle-Pérez, N. Dave, a Rodríguez-Asiain, J. I. Casal, J. M. Lizcano, M. Duñach, and a García de Herreros, “Akt2 interacts with Snail1 in the E-cadherin promoter.,” *Oncogene*, vol. 31, no. 36, pp. 4022–33, Sep. 2012.

[113] H. Hirai, H. Sootome, Y. Nakatsuru, K. Miyama, S. Taguchi, K. Tsujioka, Y. Ueno, H. Hatch, P. K. Majumder, B.-S. Pan, and H. Kotani, “MK-2206, an allosteric Akt inhibitor, enhances antitumor efficacy by standard chemotherapeutic agents or molecular targeted drugs in vitro and in vivo.,” *Mol. Cancer Ther.*, vol. 9, no. 7, pp. 1956–67, Jul. 2010.

[114] S. Chow, H. Patel, and D. W. Hedley, “Measurement of MAP Kinase Activation by Flow Cytometry Using Phospho-Specific Antibodies to MEK and ERK : Potential for Pharmacodynamic Monitoring of Signal Transduction Inhibitors,” *Cytometry*, vol. 46, no. January, pp. 72–78, 2001.

[115] G. Z. Cheng, J. Chan, Q. Wang, W. Zhang, C. D. Sun, and L.-H. Wang, “Twist transcriptionally up-regulates AKT2 in breast cancer cells leading to increased migration, invasion, and resistance to paclitaxel.,” *Cancer Res.*, vol. 67, no. 5, pp. 1979–87, Mar. 2007.

[116] J. Zhang, K. Huang, Z. Shi, J. Zou, Y. Wang, Z. Jia, A. Zhang, L. Han, X. Yue, N. Liu, T. Jiang, Y. You, P. Pu, and C. Kang, “High b-catenin / Tcf-4 activity confers glioma progression via direct regulation of AKT2 gene expression,” *Neuro. Oncol.*, vol. 13, no. 6, pp. 600–609, 2011.

[117] M. Van De Wetering, R. Cavallo, D. Dooijes, M. Van Beest, J. Van Es, J. Loureiro, A. Ypma, D. Hursh, T. Jones, A. Bejsovec, M. Peifer, M. Mortin, and H. Clevers, “Armadillo Coactivates Transcription Driven by the Product of the Drosophila Segment Polarity Gene dTCF,” *Cell*, vol. 88, pp. 789–799, 1997.

[118] B. Bilir, O. Kucuk, and C. S. Moreno, “Wnt signaling blockage inhibits cell proliferation and migration, and induces apoptosis in triple-negative breast cancer cells.,” *J. Transl. Med.*, vol. 11, no. 1, p. 280, Jan. 2013.

[119] C.-L. Liu, L.-X. Xie, M. Li, S. S. K. Durairajan, S. Goto, and J.-D. Huang, “Salvianolic acid B inhibits hydrogen peroxide-induced endothelial cell apoptosis through regulating PI3K/Akt signaling.,” *PLoS One*, vol. 2, no. 12, p. e1321, Jan. 2007.

[120] T. a Yap, M. I. Walton, L.-J. K. Hunter, M. Valenti, A. de Haven Brandon, P. D. Eve, R. Ruddle, S. P. Heaton, A. Henley, L. Pickard, G. Vijayaraghavan, J. J. Caldwell, N. T. Thompson, W. Aherne, F. I. Raynaud, S. a Eccles, P. Workman, I. Collins, and M. D. Garrett, “Preclinical pharmacology, antitumor activity, and development of pharmacodynamic markers for the novel, potent AKT inhibitor CCT128930.,” *Mol. Cancer Ther.*, vol. 10, no. 2, pp. 360–71, Feb. 2011.

[121] K. Niessen, Y. Fu, L. Chang, P. a Hoodless, D. McFadden, and A. Karsan, “Slug is a direct Notch target required for initiation of cardiac cushion cellularization.,” *J. Cell Biol.*, vol. 182, no. 2, pp. 315–25, Jul. 2008.

[122] K.-W. Hsu, R.-H. Hsieh, K.-H. Huang, A. Fen-Yau Li, C.-W. Chi, T.-Y. Wang, M.-J. Tseng, K.-J. Wu, and T.-S. Yeh, “Activation of the Notch1/STAT3/Twist signaling axis promotes gastric cancer progression.,” *Carcinogenesis*, vol. 33, no. 8, pp. 1459–67, Aug. 2012.

[123] V. C. Garside, A. C. Chang, A. Karsan, and P. a Hoodless, “Co-ordinating Notch, BMP, and TGF-β signaling during heart valve development.,” *Cell. Mol. Life Sci.*, vol. 70, no. 16, pp. 2899–917, Aug. 2013.

[124] Z. Yang, S. Rayala, D. Nguyen, R. K. Vadlamudi, S. Chen, and R. Kumar, “Pak1 Phosphorylation of Snail , a Master Regulator of Epithelial-to-Mesenchyme Transition , Modulates Snail ’ s Subcellular Localization and Functions,” *Am. Assoc. Cancer*, vol. 65, no. 8, pp. 3179–3185, 2005.

[125] M. Sun, X. Guo, X. Qian, H. Wang, C. Yang, K. L. Brinkman, M. Serrano-gonzalez, R. S. Jope, B. Zhou, D. A. Engler, M. Zhan, S. T. C. Wong, L. Fu, and B. Xu, “Activation of the ATM-Snail pathway promotes breast cancer metastasis,” *J. Mol. Cell Biol.*, vol. 4, pp. 304–315, 2012.

[126] C. Sahlgren, M. V Gustafsson, S. Jin, L. Poellinger, and U. Lendahl, “Notch signaling mediates hypoxia-induced tumor cell migration and invasion,” *PNAS*, vol. 105, no. 17, pp. 6392–97, 2008.

[127] H. Peinado, F. Portillo, and A. Cano, “Switching On-Off Snail: LOXL2 Versus GSK3-beta,” *Cell Cycle*, vol. 4, no. 12, pp. 1749–1752, Oct. 2014.

[128] Y. Wu, B. M. Evers, and B. P. Zhou, “Small C-terminal domain phosphatase enhances snail activity through dephosphorylation.,” *J. Biol. Chem.*, vol. 284, no. 1, pp. 640–8, Jan. 2009.

[129] J. I. YOOK, X.-Y. LI, I. OTA, C. HU, H. S. KIM, N. H. KIM, S. Y. CHA, J. K. RYU, Y. J. CHOI, J. KIM, E. R. FEARON, and S. J. WEISS, “A Wnt-Axin2-GSK3β cascade regulates Snail 1 activity in breast cancer cells,” *Nat. Cell Biol.*, vol. 8, no. 12, pp. 1398–1406.

[130] L. Luna-zurita, B. Prados, J. Grego-bessa, G. Luxán, G. Monte, A. Benguría, R. H. Adams, J. M. Pérez-pomares, J. Luis, and D. Pompa, “Integration of a Notch-dependent mesenchymal gene program and Bmp2-driven cell invasiveness regulates murine cardiac valve formation,” *J. Clin. Invest.*, vol. 120, no. 10, pp. 3493–3507, 2010.

[131] T. N. and J. Q. Satoshi Kaneko, Richard I. Feldman, Lu Yu, Zhenguo Wu, Tatiana Gritsko, Sue A. Shelley, Santo V. Nicosia and Cheng, “Positive Feedback Regulation Between Akt2 and MyoD During Muscle Differentiation: Cloning of Akt2 Promoter,” *J. Biol. Chem.*, vol. 277, no. 26, pp. 23230–5, 2002.

[132] F.-C. Lin, Y.-P. Liu, C.-H. Lai, Y.-S. Shan, H.-C. Cheng, P.-I. Hsu, C.-H. Lee, Y.-C. Lee, H.-Y. Wang, C.-H. Wang, J. Q. Cheng, M. Hsiao, and P.-J. Lu, “RUNX3-mediated transcriptional inhibition of Akt suppresses tumorigenesis of human gastric cancer cells.,” *Oncogene*, vol. 31, no. 39, pp. 4302–16, Sep. 2012.

[133] Y. Fu, A. C. Y. Chang, M. Fournier, L. Chang, K. Niessen, and A. Karsan, “RUNX3 maintains the mesenchymal phenotype after termination of the Notch signal.,” *J. Biol. Chem.*, vol. 286, no. 13, pp. 11803–13, Apr. 2011.

[134] P. Hayward, K. Brennan, P. Sanders, T. Balayo, R. DasGupta, N. Perrimon, and A. Martinez Arias, “Notch modulates Wnt signalling by associating with Armadillo/beta-catenin and regulating its transcriptional activity.,” *Development*, vol. 132, no. 8, pp. 1819–30, Apr. 2005.

[135] J. Pannequin, C. Bonnans, N. Delaunay, J. Ryan, J.-F. Bourgaux, D. Joubert, and F. Hollande, “The wnt target jagged-1 mediates the activation of notch signaling by progastrin in human colorectal cancer cells.,” *Cancer Res.*, vol. 69, no. 15, pp. 6065–73, Aug. 2009.

[136] A. Villanueva, A. Obrador-hevia, V. Ferna, F. Torres, M. Dun, X. Sanjuan, A. Grilli, N. Lo, S. Gonzalez, T. Gridley, G. Capella, A. Bigas, and L. Espinosa, “Jagged1 is the pathological link between Wnt and Notch pathways in colorectal cancer,” vol. 106, no. 15, pp. 6315–6320, 2009.

[137] S. Muñoz Descalzo and A. Martinez Arias, “The structure of Wntch signalling and the resolution of transition states in development.,” *Semin. Cell Dev. Biol.*, vol. 23, no. 4, pp. 443–9, Jun. 2012.

[138] C. Girardi, P. James, S. Zanin, L. a Pinna, and M. Ruzzene, “Differential phosphorylation of Akt1 and Akt2 by protein kinase CK2 may account for isoform specific functions.,” *Biochim. Biophys. Acta*, vol. 1843, no. 9, pp. 1865–74, Sep. 2014.

[139] M. Y. Lee, A. K. Luciano, E. Ackah, J. Rodriguez-Vita, T. a Bancroft, A. Eichmann, M. Simons, T. R. Kyriakides, M. Morales-Ruiz, and W. C. Sessa, “Endothelial Akt1 mediates angiogenesis by phosphorylating multiple angiogenic substrates.,” *Proc. Natl. Acad. Sci. U. S. A.*, vol. 111, no. 35, pp. 12865–70, Sep. 2014.

[140] S. B. Lee, T. L. X. Nguyen, J. W. Choi, K. Lee, S. Cho, Z. Liu, K. Ye, S. Sik, and J. Ahn, “Nuclear Akt interacts with B23 / NPM and protects it from proteolytic cleavage , enhancing cell survival,” *PNAS*, vol. 105, no. 43, pp. 16584–89, 2008.

[141] K.-H. Chow, R. E. Factor, and K. S. Ullman, “The nuclear envelope environment and its cancer connections.,” *Nat. Rev. Cancer*, vol. 12, no. 3, pp. 196–209, Mar. 2012.

[142] R. L. Steen, S. B. Martins, K. Taskén, and P. Collas, “Recruitment of Protein Phosphatase 1 to the Nuclear Envelope by A-Kinase Anchoring Protein AKAP149 Is a Prerequisite for Nuclear Lamina Assembly,” *J. Cell Biol.*, vol. 150, no. 6, pp. 1251–1261, 2000.

[143] J. M. González, A. Navarro-puche, B. Casar, P. Crespo, and V. Andres, “Fast regulation of AP-1 activity through interaction of lamin A/C, ERK1/2, and c-Fos at the nuclear envelope,” *J. Cell Biol.*, vol. 183, no. 4, pp. 653–666, 2008.

[144] F. MacKenzie, P. Duriez, F. Wong, M. Noseda, and A. Karsan, “Notch4 inhibits endothelial apoptosis via RBP-Jkappa-dependent and -independent pathways.,” *J. Biol. Chem.*, vol. 279, no. 12, pp. 11657–63, Mar. 2004.

[145] T. Quillard, S. Coupel, F. Coulon, J. Fitau, M. Chatelais, M. C. Cuturi, E. Chiffoleau, and B. Charreau, “Impaired Notch4 activity elicits endothelial cell activation and apoptosis: implication for transplant arteriosclerosis.,” *Arterioscler. Thromb. Vasc. Biol.*, vol. 28, no. 12, pp. 2258–65, Dec. 2008.

[146] A. Csiszar, K. E. Smith, A. Koller, G. Kaley, J. G. Edwards, and Z. Ungvari, “Regulation of bone morphogenetic protein-2 expression in endothelial cells: role of nuclear factor-kappaB activation by tumor necrosis factor-alpha, H2O2, and high intravascular pressure.,” *Circulation*, vol. 111, no. 18, pp. 2364–72, May 2005.

[147] Y. H. Shen, L. Zhang, P. Ren, M. T. Nguyen, S. Zou, D. Wu, X. L. Wang, J. S. Coselli, and S. a LeMaire, “AKT2 confers protection against aortic aneurysms and dissections.,” *Circ. Res.*, vol. 112, no. 4, pp. 618–32, Feb. 2013.

[148] I. Shiraishi, J. Melendez, Y. Ahn, M. Skavdahl, E. Murphy, S. Welch, E. Schaefer, K. Walsh, A. Rosenzweig, D. Torella, D. Nurzynska, J. Kajstura, A. Leri, P. Anversa, and M. a Sussman, “Nuclear targeting of Akt enhances kinase activity and survival of cardiomyocytes.,” *Circ. Res.*, vol. 94, no. 7, pp. 884–91, Apr. 2004.

[149] M. Escrivà, S. Peiró, N. Herranz, P. Villagrasa, N. Dave, B. Montserrat-Sentís, S. a Murray, C. Francí, T. Gridley, I. Virtanen, and A. García de Herreros, “Repression of PTEN phosphatase by Snail1 transcriptional factor during gamma radiation-induced apoptosis.,” *Mol. Cell. Biol.*, vol. 28, no. 5, pp. 1528–40, Mar. 2008.

[150] M. Kajita, K. N. Mcclinic, and P. A. Wade, “Aberrant Expression of the Transcription Factors Snail and Slug Alters the Response to Genotoxic Stress,” vol. 24, no. 17, pp. 7559–7566, 2004.

[151] S. Vega, A. V Morales, O. H. Ocaña, F. Valdés, I. Fabregat, and M. A. Nieto, “Snail blocks the cell cycle and confers resistance to cell death,” pp. 1131–1143, 2004.

[152] H. Zhou, X. Li, J. Meinkoth, and R. N. Pittman, “Akt Regulates Cell Survival and Apoptosis at a Postmitochondrial Level,” vol. 151, no. 3, pp. 483–494, 2000.

[153] W.-H. Liu, H.-W. Hsiao, W.-I. Tsou, and M.-Z. Lai, “Notch inhibits apoptosis by direct interference with XIAP ubiquitination and degradation.,” *EMBO J.*, vol. 26, no. 6, pp. 1660–9, Mar. 2007.

[154] H. C. Dan, M. Sun, S. Kaneko, R. I. Feldman, S. V Nicosia, H.-G. Wang, B. K. Tsang, and J. Q. Cheng, “Akt phosphorylation and stabilization of X-linked inhibitor of apoptosis protein (XIAP).,” *J. Biol. Chem.*, vol. 279, no. 7, pp. 5405–12, Feb. 2004.

[155] G.-L. Zhou, D. F. Tucker, S. S. Bae, K. Bhatheja, M. J. Birnbaum, and J. Field, “Opposing roles for Akt1 and Akt2 in Rac/Pak signaling and cell migration.,” *J. Biol. Chem.*, vol. 281, no. 47, pp. 36443–53, Nov. 2006.

[156] H. Otto, F. Hucho, M. Dreger, L. Bengtsson, and T. Scho, “Nuclear envelope proteomics : Novel integral membrane proteins of the inner nuclear membrane,” *PNAS*, vol. 98, no. 21, pp. 11943–48, 2001.

RESEARCH ARTICLES

The work related with this thesis was under revision for publication in Molecular Cell Biology.

Frias A, et al. *A switch in Akt isoforms is required for Notch-induced Snail1 expression and protection from cell death*

Other results not presented in this thesis were included in these two articles:

Vinas-Castells R, Frias A, Robles-Lanuza E, Zhang K, Longmore GD, Garcia de Herreros A, Diaz VM. 2014. Nuclear ubiquitination by FBXL5 modulates Snail1 DNA binding and stability. Nucleic Acids Res **42:**1079-1094.

Dave N, Guaita-Esteruelas S, Gutarra S, Frias A, Beltran M, Peiro S, de Herreros AG. 2011. Functional cooperation between Snail1 and twist in the regulation of ZEB1 expression during epithelial to mesenchymal transition. J Biol Chem **286:**12024-12032.

ANKNOWLEDGMENTS

Aquesta tesis no hagués estat possible sense el suport incondicional dels meus directors de tesis Antonio García de Herreros y Víctor Díaz. Han estat en tot moment al meu costat i m'han aportat molts coneixements en una matèria la qual en tenia ben pocs degut als meus estudis universitaris en Ciències Químiques.

Agrair també a tot el laboratori per la seva companyia en aquests anys i tot el que he après d'ells. Òbviament a tots els qui fan possible el funcionament del departament del programa de càncer del IMIM i totes les institucions com el CRG i la UPF que m'han ajudat al utilitzar certes instal·lacions com la de microscopia confocal i citometria.

Vull donar també les gràcies a les beques que han contribuït en el finançament de la meva tesis doctoral, que són la Marató de Tv3 i la beca de col·laboració de la Pompeu Fabra, la qual m'ha permès donar pràctiques als futurs biòlegs i metges de la universitat UPF. Per últim a l'ajut econòmic del IMIM per imprimir totes les tesis doctorals necessàries.